2015-8

Cold Plasma Treatment of Biodegradable films and smart packaging

Shashi Pankaj
Technological University Dublin, shashi.pankaj@tudublin.ie

COLD PLASMA TREATMENT OF BIODEGRADABLE FILMS AND SMART PACKAGING

Shashi Kishor Pankaj

A thesis submitted to Dublin Institute of Technology, in accordance with the requirements for degree of Doctor of Philosophy

Supervisors:

Dr. P. J. Cullen

Dr. Paula Bourke

Dublin Institute of Technology

School of Food Science and Environmental Health

August 2015

Abstract

Cold plasma is an emerging technology offering many potential applications for food packaging. While it was originally developed to increase the surface energy of polymers, enhancing their adhesion and printability, it has recently emerged as a powerful tool for surface sterilisation of both food and food packaging materials. The food packaging industry is still dominated by petroleum derived polymers but in the past few decades there has been significant interest in the development of environment friendly, biodegradable green polymers. In this study, the interaction and effects of cold plasma with biopolymer based packaging materials (polylactic acid, zein, sodium caseinate, starch, chitosan and gelatin) and its potential for active and intelligent packaging was investigated.

DBD (Dielectric Barrier Discharge) plasma increased the surface roughness of all the treated polymers films. DBD plasma treatments did not induce significant changes in the thermal profile of the polymers, but significant increases in the initial degradation temperature and maximum degradation temperature was observed for poly(lactic acid) and starch. DBD plasma also increased the equilibrium moisture content of both protein films: zein and sodium caseinate, but no significant increases in the water vapour and oxygen permeability was noticed for any of the films. An increase in overall migration was observed in PLA for various food simulants however they were below the EU regulatory limits. Plasma treatment increased the polar component of the total surface energy of all the polymers. The increase in the O/C atomic ratio shows the formation of new oxygen-containing polar groups on the film surface of the plasma treated films. Plasma treatments of both zein and sodium caseinate film lead to a change in the

protein conformation which was confirmed by X-ray diffraction and Fourier transform infrared spectroscopy.

Plasma treatment of antimicrobial films (zein and chitosan) also increased their surface roughness. A significant increase in the diffusion coefficient was observed which lead to an accelerated release of the active compound into the food simulant.

Phosphorescent optochemical oxygen sensors (Optech™ and PP based) were also evaluated for compatibility with DBD in-package plasma treatment under different gaseous environments. Both sensors worked well under the modified atmospheric condition (devoid of any oxygen) during plasma treatment. However, the PP based sensor was found to be largely degraded after plasma treatment when packed under atmospheric air. Optech™ sensors were found to be compatible with the plasma treatment under both gaseous environment tested, although, a re-calibration was required for sensor accuracy.

Declaration

I certify that this thesis which I now submit for examination for the award of Doctor of Philosophy, is entirely my own work and has not been taken from the work of others, save and to the extent that such work has been cited and acknowledged within the text of my work.

This thesis was prepared according to the regulations for postgraduate study by research of the Dublin Institute of Technology and has not been submitted in whole or in part for another award in any other third level institution.

The work reported on in this thesis conforms to the principles and requirements of the DIT's guidelines for ethics in research.

DIT has permission to keep, lend or copy this thesis in whole or in part, on condition that any such use of the material of the thesis be duly acknowledged.

Shashi Kishor Pankaj Date: 31.08.2015

Acknowledgement

I wish to express my sincere thanks to my supervisors, Dr. P.J. Cullen and Dr. Paula Bourke for providing me the opportunity to join the Bioplasma research group and for their continuous guidance and encouragement throughout my research work. I would also like to extend my sincere thanks to Dr. Carmen Bueno-Ferrer for sharing her experience and valuable insights during my research.

I would also like to thank Dr. Carl O'Sullivan, Fintan Moran, Dr. B. K. Tiwari, Dr. A. Jiménez, Dr. Dmitri Pakovsky, Dr. Kevin Keener and Dr. Luke O'Neil for their guidance and help throughout my work. I am very grateful to all the students and staff of DIT for all of their assistance.

I would also like to thank my friends and colleagues especially Misra, Shekhar, Yash, Chaitu, Lu, Dana, Caitlin, Apurva, Kompal, Daniela and Raquel for all the laughs we have shared, the distraction was indispensible.

Finally, I would like to thank my parents, sister and fiancée for their constant encouragement and support throughout my work without which none of this would have been possible.

Table of Contents

List of Figures

List of Tables

List of Abbreviations

ACP	Atmospheric cold plasma
AFM	Atomic force microscopy
APGD	Atmospheric pressure glow discharge
DBD	Dielectric barrier discharge
DSC	Differential scanning calorimeter
FHC	Fused hollow cathode
FTIR	Fourier transmission Infra-red
HDPE	High density polyethylene
HPLC	High pressure liquid chromatography
LDPE	Low density polyethylene
MAP	Modified atmospheric packaging
NTP	Non thermal plasma
OTR	Oxygen transmission rate
PE	Polyethylene
PET	Polyethylene terephthalate
PLA	Poly(lactic acid)
PP	Polypropylene
PtBP	Platinum (II) benzo-porphyrin
RMSE	Root mean square error

SFE	Surface free energy
TGA	Thermo gravimetric analysis
WVTR	Water vapour transmission rate
XPS	X-ray photoelectron spectroscopy
XRD	X-ray diffraction

Chapter 1 Introduction

Atmospheric Cold Plasma (ACP) has gained significant attention for the decontamination of fresh fruits and vegetables. Dielectric barrier discharge is one of the common methods for cold plasma generation which offers versatility in its mode of operation and system configuration. The Bioplasma group at Dublin Institute of Technology are working on the novel approach of in-package plasma decontamination of foods and biomaterials which relies on use of the polymeric package itself as a dielectric and means for containing the generated plasma afterglow. The approach has been proposed for numerous packaging materials such as LDPE, HDPE, polystyrene (PS), Tyvek® etc (Keener et al., 2012). All these works have demonstrated significant reductions in the microbial populations on food products. Moreover, this approach is amenable to scale-up to continuous industrial processing and could prevent post-packaging contamination (Misra et al., 2011).

Biodegradable polymers from renewable resources have shown significant potential in packaging applications due to their environmental benefits. Whilst biodegradable packaging materials have limitations pertaining to properties and cost, the fact that certain chemicals used for synthetic packaging are endocrine disrupters and lead to greenhouse gases, the demand for eco-friendly wrappings has increased (Isobe, 2003, Zhang and Mittal, 2010). Since, DBD plasma is known to modify the properties of conventional polymers like polyethylene, polypropylene, poly(ethylene terephthalate) and polystyrene, it was necessary to evaluate the compatibility of biodegradable polymers with DBD plasma treatment (Borcia et al., 2004, Leroux et al., 2008, Ren et al., 2008, Kun et al., 2008, Upadhyay et al., 2004). There is limited information available on the effects of plasma on biodegradable polymers

and none at higher voltage levels. For a complete assessment of the technology it is essential to quantify and understand possible changes to the packaging material, induced by the cold plasma. For example, any adverse change in the permeability of water vapour and gas or migration kinetics of additives, monomers, oligomers and low molecular weight volatile compounds from the packaging material will limit the package utility.

This forms the impetus for the present work of characterising and assessing the effects of cold plasma on different food packaging systems. An outline of the work carried out has been shown in Figure 1.

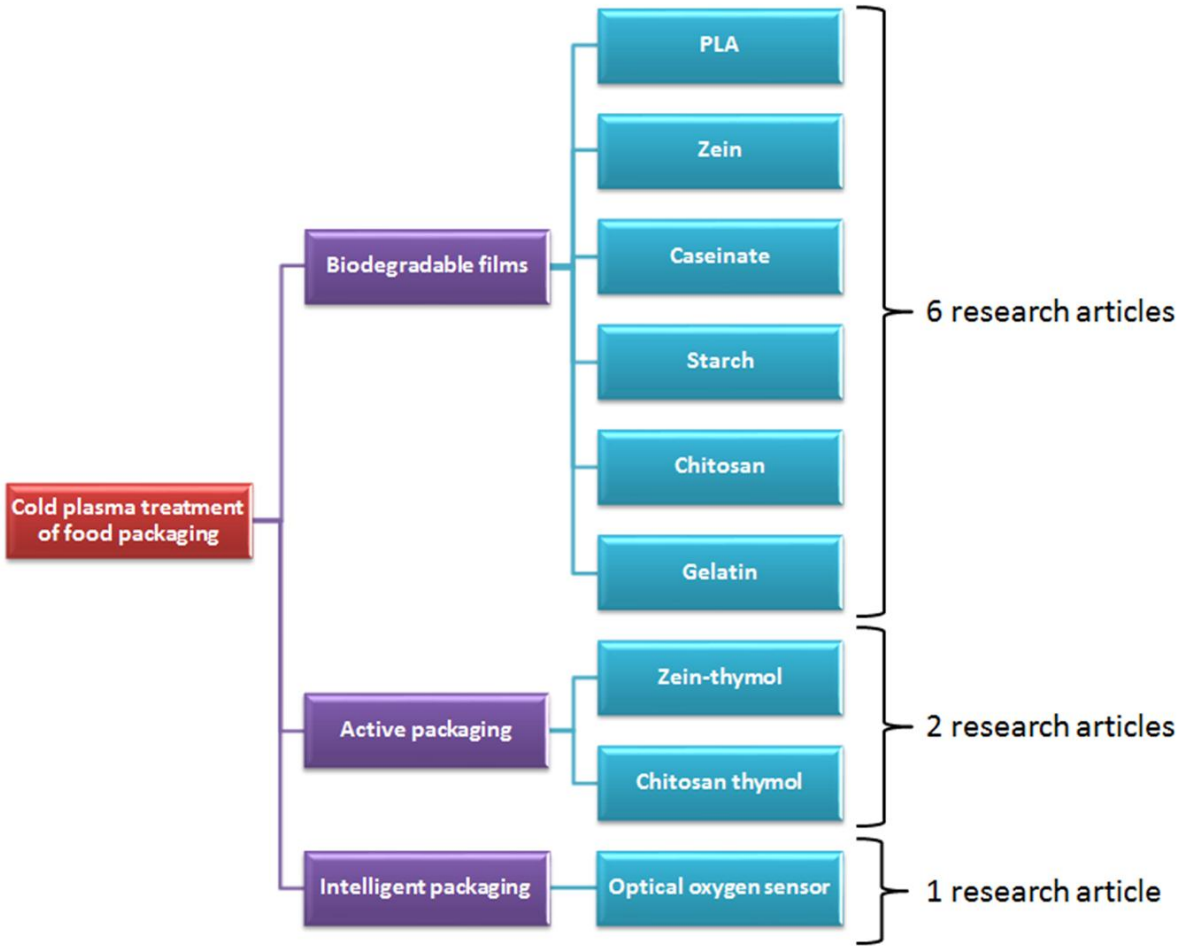

Figure 1. Outline of the thesis and publications

As evident from the thesis outline, this work has been carried out in three following major sections which have been discussed in detail in the later chapters:

(a) Characterising the effects of DBD plasma on different types of biodegradable polymers,

(b) Characterising the effects of DBD plasma on active packaging systems (antimicrobial packaging), and

(c) Characterising the effects of DBD plasma on intelligent packaging systems (oxygen sensors).

Chapter 2 Review of literature

2.1. Introduction

For the past few decades the trend of replacing traditional materials such as glass, metals and paper with polymeric materials has been continually growing in various industries, including the food industry. This is justified by the fact that physical and chemical characteristics of polymers are at par with conventional materials and are relatively cheaper. In addition, polymeric packaging materials provide greater flexibility, transparency and adequate chemical inertness, with low specific weights. However, in most cases polymeric surfaces are hydrophobic in nature and often characterised by a low surface energy (Médard et al., 2002, Vesel and Mozetic, 2012). This implies that these do not possess specific surface properties demanded for various applications. Moreover, the production of multi-layer structured food packaging polymers is economically demanding. In order to obtain polymers with the desired properties, in most instances various surface treatments are employed.

Surface treatments of packaging can serve various purposes including surface functionalisation, surface cleaning or etching, and surface deposition. Surface functionalisation refers to the introduction of specific functional groups onto the surface layer of a polymer. Surface functionalisation of polymers is usually carried out to improve its wettability, sealability, printability, dye up-take, resistance to glazing, or adhesion to other polymers or materials, without compromising the desired bulk properties of the polymer (Chou and Chang, 1994, Ozdemir et al., 1999a). Surface functionalisation has additionally been used to enhance the barrier characteristics of food packaging polymers and to impart antimicrobial properties (Ozdemir et al., 1999b). Surface treatments can also be employed to

clean or etch polymer surfaces by removing unwanted materials and contaminants from polymer surface layers. Additionally surface treatments can be used for the deposition of thin layers of coatings on the polymer surface or for sterilisation.

Surface modification of polymers can be performed either by chemical or physical methods. Physical methods have gained preference over chemical techniques, considering the greater precision, ease of process control, and environment friendliness of the approach. Classical physicochemical methods for modifying polymer surfaces include flame and corona treatment, UV, gamma-ray, ion-beam techniques, low-pressure plasma and laser treatment (Adler et al., 1999). Flame and corona treatments are not very successful for polymers due to the rather short time scale of the improved properties.

Cold plasma (CP) induces several chemical and physical processes within the plasma volume and on the plasma-polymer interface, which modify the surface properties. This has been exploited in surface functionalisation to impart selective and tunable surface energies to the packaging polymer to promote adhesion or sometimes anti-adhesion (Poncin-Epaillard et al., 1999), improve printability, sealability, impart anti-mist properties and improve the polymer's resistance to mechanical failure. Using plasma deposition of barrier layers, the barrier properties of the packaging materials towards gases (oxygen, carbon-dioxide) and chemical solvents can be improved (Schneider et al., 2009). Gas plasma reactions also establish efficient inactivation of micro-organisms (bacterial cells, spores, yeasts and molds) adhering to the polymer surfaces within short treatment times. Packaging materials such as plastic bottles, lids and films can be rapidly sterilized using cold plasma, without adversely affecting their bulk properties or leaving any residues (Muranyi et al., 2007).

This chapter reviews the state of the art applications of cold plasma technology for modification of polymers of importance to food packaging, following a brief discussion on the physics and chemistry of cold plasmas. The polymers considered include polyethylene, polypropylene and polyethylene-terephthalate, which together account for more than 80% of food packaging polymers (Plastics-the-Facts, 2012). The review also identifies research gaps and lays direction for future research work.

2.2. Plasma Physics and Chemistry

The term "plasma" refers to a quasi-neutral ionised gas, primarily composed of photons, ions and free electrons as well as atoms in their fundamental or excited states with a net neutral charge. Plasma discharges are widely used for processing and are indispensible for many technological applications (Milosavljević et al., 2007). Through their wide variety of operational conditions, plasma sources offer a significant freedom in the generation of radiation and the creation of chemical compositions. As a result, the field of technological and industrial plasma applications is expanding rapidly. Several plasma applications have been identified in the literature: High-efficiency light sources (a rich plasma UV source for surface sterilisation), Material processing, such as deposition, cleaning and surface modification (Law, 2012), Spectrochemical analysis (analytical chemistry- plasma spectral emission can be used for element detection with very low detection limits) (Milosavljević et al., 2011) and waste treatment (e.g. detoxification - use of thermal plasma torches, cascaded arc plasmas, or microwave plasmas for the production of negative ions).

The ions and electrons from the plasma are generated at an electrode by means of a radiofrequency (RF), microwave (MW) or dielectric barrier discharge power source, and a biasing power source is applied to another (packaging holding) electrode to create a

significant ion bombardment (remove-clean-deposit) component during plasma treatment (Breen et al., 2011). The plasma process is a simultaneous deposition/removing process in which loosely "deposited species," over planar or topographical surfaces are sputtered off by reactive ions and radicals during deposition.

Plasma is an effective, economical, environmentally safe method for cleaning. The vacuum ultraviolet (VUV) energy is very effective in breaking most organic bonds (i.e., C-H, C-C, C=C, C-O, and C-N) of surface contaminants. This helps to break apart high molecular weight contaminants (Donegan, 2013). A second cleaning action is carried out by the oxygen species created in the plasma (O_2^+, O_2^-, O_3, O, O^+, O^-, ionized ozone, metastably-excited oxygen, and free electrons). These species react with organic contaminants to form H_2O, CO, CO_2, and lower molecular weight hydrocarbons. The resulting surface is ultra-clean/sterilized. The plasma activated atoms and ions behave like molecular ‘sandblasting’ and can break down organic contaminants.

Most of the cleaning process by-products are small quantities of gasses such as carbon dioxide, and water vapour with trace amounts of carbon monoxide and other hydrocarbons (Prysiazhnyi et al., 2012). Whether or not the organic removal is complete can be assessed with contact angle measurements. When an organic contaminant is present, the contact angle of water with the surface will be high. After the removal of the contaminant, the contact angle will be reduced to that characteristic of the pure substrate. Plasma cleaning requires optimization of a number of interrelated variables, most notably gas species, pressure, time treatment, nature of substrate, and power. Thus, a series of experiments designed to optimize processing conditions should be carried out. The net result is a high degree of day-to-day repeatability and higher yields.

Different treatment systems are currently being studied for applications in food packaging (Kowalonek et al., 2010). A capacity coupled plasma (CCP) source is one of the most common types of technological plasma sources (Milosavljevic et al., 2008). It consists of two metal electrodes separated by a small distance, placed in a chamber. The gas pressure in the chamber can be lower than atmosphere or it can be atmospheric. A typical CCP system is driven by a single RF power supply, typically at 13.56 MHz. One of two electrodes is connected to the power supply, and the other one is grounded. As this configuration is similar in principle to a capacitor in an electric circuit, the plasma formed in this configuration is called a capacitively coupled plasma. CCPs have wide applications from the deposition, sputtering and cleaning (Ryan et al., 2011).

An inductive coupled plasma (ICP) is a type of plasma source in which the energy is supplied by electrical currents which are produced by electromagnetic induction, that is, by time-varying magnetic fields (Milosavljevic et al., 2007). There are two types of ICP geometries: planar and cylindrical. In a planar geometry, the electrode is a coil of flat metal wound like a spiral. In a cylindrical geometry, it is like a helical spring. When a time-varying electric current is passed through the coil, it creates a time varying magnetic field around it, which in turn induces azimuthal electric currents in the rarefied gas, leading to gas break down and formation of plasma. The benefit of ICP discharges is that they are relatively free of contamination because the electrodes are completely outside the reaction chamber. In a CCP, in contrast, the electrodes are often placed inside the reactor and are thus exposed to the plasma and subsequent reactive chemical species (Bauer et al., 2013).

Electron cyclotron resonance (ECR) plasma source has a microwave input at 2.45 GHz and a magnetron generates the plasma (Milosavljević, 2013). Electrons trajectory is spiral

vertically along magnetic field lines. The magnetic field strength is 875 Gauss with a dome shaped contour. The electrode which holds the food packaging could be a RF power supplied and is used to generate direct current (DC) bias independently of plasma ionization. Electrons travel, in ECR, far enough to gain sufficient energy to strike gas molecules and cause ionization. Electron density (ion flux) is over an order of magnitude higher than for CCP or ICP plasma tools, and therefore could be more efficient for surface treatments of packaging, i.e. surface functionalisation, surface cleaning, etching, and/or surface deposition.

Dielectric barrier discharge is the electrical discharge between two electrodes separated by an insulating dielectric barrier (O'Connor et al., 2011). The process uses high voltage alternating current, often at lower RF frequencies, but recently even at microwave levels. DBD devices can be made in many configurations, typically planar, using parallel plates separated by a dielectric or cylindrical, using coaxial plates with a dielectric tube between them. In a common coaxial configuration, the dielectric is shaped in the same form as common fluorescent tubing. It is filled at atmospheric pressure with either a rare gas or rare gas-halide mix, with the glass walls acting as the dielectric barrier. Due to the atmospheric pressure level, such processes require high energy levels to be sustained. Common dielectric materials include glass, quartz, ceramics and polymers (Liang et al., 2011).

2.3. Modification of food packaging polymers

2.3.1. Polyethylene (PE)

Structurally PE is one of the simplest polymers used in food packaging. PE of varying densities, characterised by different water vapor and gas permeability, tensile strength, heat sealing and other properties are commercially available. This provides great freedom to food

manufacturers to choose the package type optimum for their needs (Pankaj et al., 2011). However, the low surface energy of PE, on the other hand, has driven most research in cold plasma surface modifications of PE. Surface characterisation of PE on CO_2, H_2O and CO_2/H_2O plasma has been reported by Médard, Soutif and Poncin-Epaillard (2002) and the proposed mechanism of CO_2 plasma is described in Figure 2 below (Medard et al., 2002). Table 1 summarises the key findings from important studies conducted on PE using cold plasma.

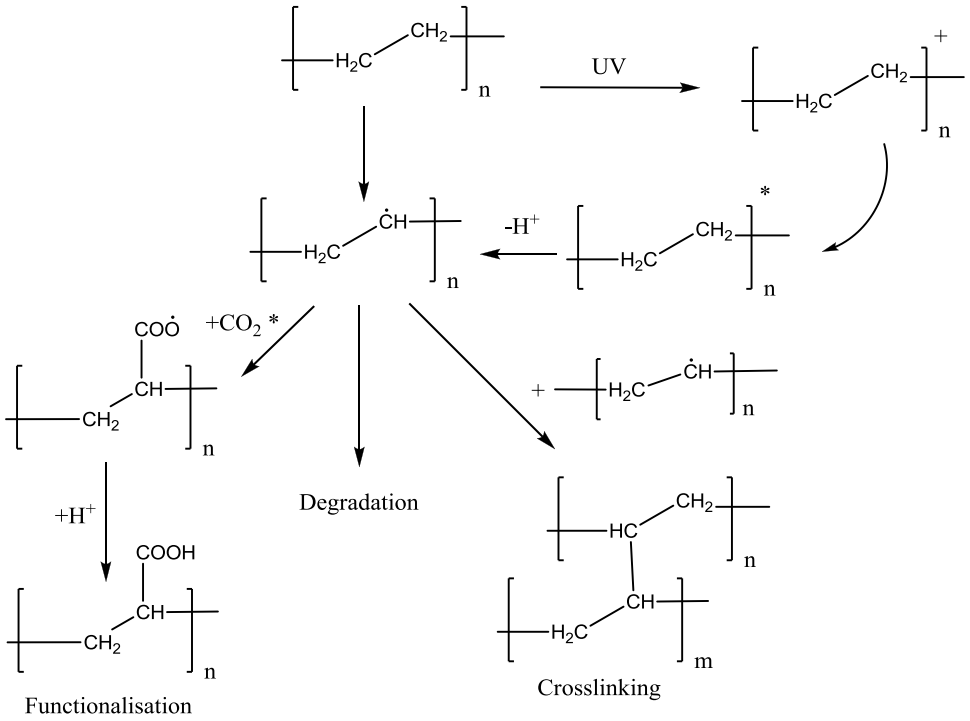

Figure 2**.** Mechanisms of degradation, cross-linking and functionalisation occurring on polyethylene treated by CO_2 cold plasma. Adapted from Medard, Soutif, and Poncin-Epaillard (2002) with permission.

Table 1. Summary of findings for cold plasma processing of polyethylene (PE).

Polymeric packaging material	Plasma source	Treatment conditions	Key findings	References
LDPE film	RF discharge (13.56 MHz, 100W)	Ar plasma (15-90s, 25-100W, 15ml/min)	Contact angle (↓), Crystallinity (↓), Roughness (↑)	Ataeefard, Moradian, Mirabedini, Ebrahimi, and Asiaban (2009)
LDPE film	RF discharge (13.56 MHz, 100W)	O_2 plasma (15-90s, 25-100W, 15ml/min)	Contact angle (↓), Crystallinity (↓), Roughness (↑)	Ataeefard, et al. (2009)
HDPE film	RF discharge (13.56MHz)	Ar:O_2=9:1 (150W, 30sccm, 0.01 torr)	Contact angle (↓)	Banik, et al. (2002)
HDPE film	RF discharge (13.56MHz)	Ar:O_2=1:9 (150W, 30sccm, 0.01 torr)	Contact angle (↓)	Banik, et al. (2002)
LDPE film	RF discharge (13.56MHz,)	O_2 plasma (150W, 0.02torr)	Contact angle (↓)	Bronco, Bertoldo, Taburoni, Cepek and Sancrotti (2004)
LDPE film	RF discharge (13.56MHz,)	N_2 plasma (150W, 0.02torr)	Contact angle (↓)	Bronco, et al. (2004)
LDPE film	RF discharge (8W, 50 mTorr)	Ar (2sccm), Ar:O_2(1:1sccm), Ar:H_2O(1:1sccm) plasma	Contact angle (↓)	Gilliam and Yu (2006)
PE film	Microwave plasma (2860MHz)	Air plasma (140mA, 0.04mbar, 15-60s)	Contact angle (↓)	Kamińska, Kaczmarek and Kowalonek (2002)
LDPE film	RF discharge (2kV, 0.1mA, 13.56MHz)	O_2 , N_2 and Air plasma (60s, 26Pa)	Surface energy(↑)	Novák, et al. (2007)

2.3.2. Polypropylene (PP)

PP is a versatile polymer used in food packaging. Its low density, low cost, high melting point, good heat sealabilty and chemically inert nature have made it an obvious choice as a packaging material for different food products (Pankaj et al., 2011). The low surface tension of PP poses problems in printing, coating and lamination, thereby requiring some additional surface treatment to increase its surface energy. PP is a saturated hydrocarbon polymer with a carbon backbone containing hydrogen and methyl ($-CH_3$) groups arranged in an alternating fashion. The reactivity of the hydrogen groups for surface reactions in PP depends on the nature of the C atom to which they are attached and in general it varies as $H_{tert} > H_{sec} > H_{pri}$ where H_{tert} refers to H atom bonded to three C atoms, H_{sec} refers to H atom bonded to two C atoms and H_{pri} which is bonded to only one C. Extensive work on modelling the modification of PP films in atmospheric pressure plasma discharges has been carried out by Dorai and Kushner (2003) and Wang and He (2006). The reaction mechanism for PP treatment by air plasmas has been described by Akishev, et al. (2008), as summarised in Figure 3, the degradation of polypropylene upon plasma treatment is mainly due to branch scissions, formation of low molecular weight organic molecules (LMWOM) and the degradation order is as follows: $N_2 < He < Air \lll O_2$ (Poncin-Epaillard et al., 1999). Salient results of selected studies in cold plasma processing of PP and biaxially oriented PP (BOPP) have been summarised in Table 2.

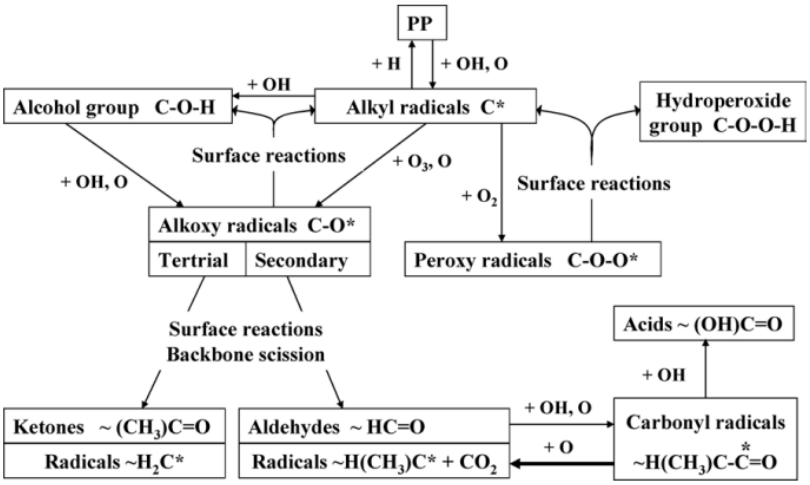

Figure 3. Diagram illustrating the reaction mechanism for the PP treatment by air plasma. The process resulting in etching of PP surface is shown by the thick arrow. Adapted from Akishev, et al. (2008) with permission.

Table 2. Important findings regarding cold plasma processing of polypropylene (PP).

Polymeric packaging material	Plasma Source	Treatment conditions	Key findings	References
PP film	AC discharge (50 Hz, 2 electrodes, 1000 Pa)	Air plasma (30kV, 20dm^3/hr, 120s)	Contact angle (↓), Adhesion (↑)	Carrino, Moroni, and Polini (2002)
PP film	Jet plasma DC discharge (35W, diffusive-filamentary mode)	Air plasma (20m/s, 6W/cm^2)	Contact angle (↓)	Akishev, et al. (2008)
PP film	Jet plasma DC discharge (35W, diffusive-filamentary mode)	Nitrogen plasma (15m/s, 3-5W/cm^2)	Contact angle (↓)	Akishev, et al. (2008)
Isotactic PP film	Microwave plasma (433 MHz, 0-250W)	CO_2 plasma (60 W, 20 sccm, 0.75 mbar)	Degradation yield (↑), Roughness (↑), Total surface energy (↑)	Bertrand and Poncin-Epaillard (2003)
PP film	Air corona	Air plasma (30kHz, 1.7J/cm^2)	Contact angle (↓), Ink Adhesion (↑)	Dixon nd J. Meenan (2012), Strobel, Strobel, Lyons, Dunatov, and Perron (1991)
PP film	RF plasma (13.56 MHz, 150W)	CH_4-O_2 plasma[80:20] (100cm^3/min, 31-32Pa)	Contact angle (↓), Increase in weight, Oxygen content(↑), Nitrogen content(~), Roughness(↑)	Garcia, Fenollar, Lopez, Sanchis, & Balart (2008), López, Sanchis, García, Fenollar, and Balart (2009)
PP film	RF plasma (13.56 MHz, 155W)	Ar plasma (20sccm, 23.33Pa, 8min)	Contact angle (↓), Roughness(↑)	Gomathi and Neogi (2009)
BOPP film	Air corona	Air plasma (1kHz)	Contact angle (↓), Roughness(↑)	Guimond, Radu, Czeremuszkin, Carlsson, and Wertheimer (2002)

BOPP film	APGD	N_2 plasma (1-6kHz)	Contact angle (↓), Roughness(↑)	Guimond, et al (2002)
BOPP film	RF plasma (13.56 MHz, 10-50W)	Ar plasma (15ml/min, 0.35bar, 0-300s)	Contact angle (↓), Roughness(↑)	Mirabedini, Arabi, Salem, and Asiaban (2007)
BOPP film	RF plasma (13.56 MHz, 10-50W)	O_2 plasma (15ml/min, 0.35bar, 0-300s)	Contact angle (↓), Roughness(↑)	Mirabedini, et al. (2007)
PP film	Glow discharge (DC) (400V,10W, 25mA)	Air plasma (0.2mbar, 2-20min)	Contact angle (↓), Adhesion work(↑), Polarity(↑),Degradation yield (↑),Oxygen content(↑), Roughness(↑)	Navaneetha Pandiyaraj, Selvarajan, Deshmukh, and Gao (2008)
PP film	Diode plasma discharge (3.1, 8.3W)	Ar plasma (10Pa, 0-240s)	Contact angle (↓), Oxygen content(↑), Roughness(~)	Slepička, et al.(2010)
PP film	DC plasma (1-30kV)	O_2 plasma (5-120s, 0.5-2kPa)	Contact angle (↓)	Sorrentino, Carrino, and Napolitano (2007)
PP film	DBD plasma (3-20kV,25-50kHz)	Air plasma (upto 6.7J/cm^2)	Contact angle (↓), O/C ratio(↑and then saturates)	Sorrentino, Carrino, and Napolitano (2004)
PP film	Microwave plasma (2860MHz)	Air plasma (140mA, 0.04mbar, 15-135s)	Contact angle (↓)	Kamińska, et al. (2002)
PP film	DBD plasma (15kV,300-1000W,30kHz)	Air plasma (1.2-60kJ/m^2)	Contact angle (↓), (↓), O/C ratio (↑and then saturates), Roughness (↑)	Leroux, Campagne, Perwuelz, and Gengembre (2008)

2.3.3. Poly(ethylene terephthalate) (PET)

PET has many desirable properties, including good strength, rigidity, high strength-to-weight ratio, transparency, thermal stability, gas barrier property, chemical resistance and formability which make it a packaging material of choice for a wide range of food products (Pankaj et al., 2011). However, PET, like other synthetic polymers has low surface energy, which necessitates surface modification for good adhesion, printing and dyeing properties. The crystallinity of PET film is an important factor which decides the changes in surface energy upon CP treatments (Jacobs et al., 2011). Surface characterisation studies for plasma treated PET film using oxygen, carbon dioxide, nitrogen and helium plasma have been reported by Almazan-Almazan, et al. (2005), (2006), Inagaki, Narushim, Tuchida, and Miyazaki (2004). Table 3 summarises the key findings of various studies conducted on PET using cold plasma.

Table 3. Important findings in the area of cold plasma processing of PET.

Polymeric packaging material	Plasma Source	Treatment conditions	Key findings	References
PET film	Jet plasma DC discharge (35W, diffusive-filamentary mode)	Air plasma (20m/s, 6W/cm^2)	Contact angle (↓)	Akishev, et al. (2008)
PET film	Jet plasma DC discharge (35W, diffusive-filamentary mode)	Nitrogen plasma (15m/s, 3-5W/cm^2)	Contact angle (↓)	Akishev, et al. (2008)
PET film	Microwave plasma (200W)	CO_2 plasma (4 and15min, 1.33 mbar)	Surface energy (↑), Roughness(↑)	Almazan-Almazan, et al. (2005)
PET film	Microwave	O_2 plasma (4	Surface energy (↑),	Almazan-

	plasma (200W)	and15min, 1.33 mbar)	Roughness(↑)	Almazan, et al. (2005)
PET fiber	RF plasma (13.56 MHz, 50W)	O_2 plasma (40Pa, 5-100s)	Contact angle (↓), Average tensile strength (↑)	Cioffi, Voorwald, and Mota (2003)
PET film	DBD plasma (3-20kV, 40-80kHz)	Air plasma (9.6, 14, 21.9W/cm^2)	Contact angle (↓), O/C ratio(↑)	Cui, Upadhyay, Anderson, Meenan, and Brown (2007)
PET film	RF plasma (150-300W, 15kV, 30kHz)	Air plasma (43.4, 73.4, 105.4J/cm^2)	Reflectivity(↑), Roughness(↑)	Esena, Zanini, and Riccardi (2007)
PET film (biaxially oriented)	Jet plasma (285V, 6A, 16kHz)	Air plasma (0.16-0.81m/s)	Contact angle (↓)	Gotoh, Yasukawa, and Taniguchi (2011)
PET film	Microwave plasma (2860MHz)	Air plasma (140mA, 0.04mbar, 15-135s)	Contact angle (↓)	Kamińska, et al. (2002)
PET film	Glow discharge (DC) (400V,10W, 25mA)	Air plasma (0.2mbar, 2-20min)	Contact angle (↓), Adhesion work(↑), Polarity(↑), Degradation yield (↑), Oxygen content(↑), Roughness(↑)	Navaneetha Pandiyaraj, et al. (2008)
PET film	Corona discharge (0.14-1kW)	Air plasma (5-25m/min)	Contact angle (↓), Oxygen content(~),	O'Hare, et al. (2002)
PET film	Glow discharge (400V)	Air plasma (0.2mbar, 2-25min)	Contact angle (↓), Degradation yield (↑), Roughness(↑), Crystallinity(↑), Oxygen content(↑)	Pandiyaraj, Selvarajan, Deshmukh, and Bousmina (2008)

2.4. Ageing Effect

Cold plasma modification of packaging surfaces is not stable for extended periods. Because of the minimisation of the free surface enthalpy, dynamic processes are observed on all

functionalized surfaces which fade initially achieved modification effect (Adler et al., 1999). The loss of beneficial attributes derived from CP processing of polymers over time is often called “ageing”. For example, a loss in hydrophilicity is observed for CP treated polymeric films when stored. This is referred as hydrophobic recovery. Such effects are attributed primarily to inward-diffusion, agglomeration or sublimation of low molecular weight organic materials, the reorientation or reptation of polymer chains, whereby covalently bonded polar groups become “buried” beneath the outer surface; and migration of additives from the bulk towards the surface (Guimond et al., 2002, Strobel et al., 1991, Garcia et al., 2008, Poncin-Epaillard et al., 1999). Ageing effects are dominant when power input to plasma and process times are low. For the afore mentioned example, this signifies insignificant changes in the surface roughness, i.e. less etching (Mirabedini et al., 2007, Carrino et al., 2004). Conversely, where intermediate to high doses of plasma discharges are employed, a further post-processing decrease in the contact angle occurs (Upadhyay et al., 2004, Kamińska et al., 2002). Selection of suitable operating gas mixtures for plasma, such as use of an organic gas (CH_4) with a highly reactive gas (O_2) can considerably reduce the ageing process with respect to hydrophobic recovery (Garcia et al., 2008). The mechanism of ageing and approaches to delay the hydrophobic recovery is a subject of active research. Table 4 provides a summary of the research works conducted to study the ageing effects in cold plasma treated polymeric surfaces. The ageing behaviour of plasma treated polymers depends on different parameters, such as the ageing medium, temperature, crystallinity, humidity, etc. (Vesel and Mozetic, 2012).

Table **4. Important findings regarding the ageing effects in cold plasma treated polymeric surfaces.**

Polymeric packaging material	Plasma Source	Treatment conditions	Storage period	Observations	References
BOPP film	RF plasma (13.56 MHz, 10-50W)	Ar and O_2 plasma (15ml/min, 0.35bar, 0-300s)	30 days	Aging effect on samples treated for a longer time is less than samples treated for shorter time	Mirabedini, et al. (2007)
BOPP film	Air corona and APGD	Air and N_2plasma (1kHz; 1-6kHz)	3 months	Similar aging kinetics for both treatments	Guimond, et al.(2002)
PP film	RF plasma (13.56 MHz, 150W)	CH_4-O_2 plasma[80:20] ($100cm^3$/min, 31-32Pa)	3 weeks	Reduction in wettability is low than other gas plasma, Storage temperature and RH are critical for hydrophobic recovery process	Garcia, et al. (2008)
PP film	AC discharge (50 Hz, 2 electrodes, 1000 Pa)	Air plasma (30kV, $20dm^3$/hr, 120s)	10 days	Wettability decrease not significant in first few hours treatment, but is relevant after one or more days, Wettability decay is not influenced by cold plasma parameters like tension, treatment time and air flow rate	Carrino, et al. (2004)
PP film	Diode plasma discharge (3.1, 8.3W)	Ar plasma (10Pa, 0-240s)	7 days	Independent to plasma discharge power, full surface relaxation and contact angle restoration to saturated value was observed after about 70 h of aging	Slepička, et al. (2010)

PP film	DC plasma (1-30kV)	O_2 plasma (5-120s, 0.5-2kPa)	30 days	Decrease of 5% wettability in one day after the treatment while it achieves 18% after 30 days	Sorrentino, et al. (2007)
PP film	DBD plasma (3-20kV,25-50kHz)	Air plasma (upto 6.7J/cm^2)	30 days	Lower doses: slight recovery of contact angle; Intermediate and high doses: Decrease in contact angle	(Upadhyay, et al. (2004)
LDPE film	RF discharge (13.56 MHz, 100W)	Ar plasma (15-90s, 25-100W, 15ml/min)	7 days	Non-linear decrease in contact angle	Ataeefard, et al. (2009)
HDPE film	RF discharge (13.56MHz)	Ar:O_2=1:9 /9:1 plasma (50-150W, 30sccm, 0.01 torr)	30 days	Decrease in aging effects by increasing crystallinity	Ataeefard, et al. (2002)
LDPE film	Corona discharge (1kW, 50Hz)	Air plasma (600W, 15m/min)	21 days	Partial hydrophobic recovery	Pascual, Balart, Sánchez, Fenollar, and Calvo (2008)
PET film	DBD plasma (3-20kV, 40-80kHz)	Air plasma (9.6, 14, 21.9W/cm^2)	3 months	Partial hydrophobic recovery	Cui, et al.(2007)
PET film (biaxially oriented)	Jet plasma (285V, 6A, 16kHz)	Air plasma (0.16-0.81m/s)	14 days	Partial hydrophobic recovery	Gotoh, et al. (2011)
PET film	Glow discharge (400V)	Air plasma (0.2mbar, 2-25min)	20 days	Increase in contact angle, No significant difference in 10 and 20 days stored samples	Pandiyaraj, et al. (2008)

2.5. Applications

2.5.1. Surface Sterilisation

Most regulatory guidelines specify microbiological requirements for food packaging materials and in many cases the packaging process is an important control point in an hazard analysis critical control point (HACCP) (Mittendorfer et al., 2002). Food packaging materials are intended to preserve food quality along the distribution and storage chain and also to protect it from deterioration, damage or outside contamination. If food packaging is not properly sterilized this may cause further contamination of the food from the packaging surface and consequently lead to health risk and economic losses (Misra et al., 2011). Conventional sterilisation methods such as dry heat, steam, UV light and chemicals like ethylene oxide and hydrogen peroxide have been traditionally used in sterilisation of medical instruments and implants as well as packaging materials for the food industry, but certain limitations have motivated the search of new approaches (Schneider et al., 2005, Lerouge et al., 2001). The main drawback related to these conventional sterilisation techniques is the generation of liquid effluents, for which the cost of treatment gets added to that of the process. In the case of cold plasma treatment there is no chemical utilisation, allowing fast and safe sterilisation of a wide range of packaging materials without leaving any residues. However, there are still some challenges with the technique to facilitate mass production in the food packaging sector, where time is the essential expense factor and sterilisation periods of several minutes are not affordable. Schneider, et al.(2005) investigated the scalability of a Muegge Array, a Duo-Plasmaline® based plasma source for industrial applications, and compared the approach to a laboratory scale Plasmodul® using PET foil substrates with a

treatment time of 5 s. Figure 4 shows the spore reduction kinetics for both systems, suggesting ease of scaling of the Duo-Plasmaline® plasma source.

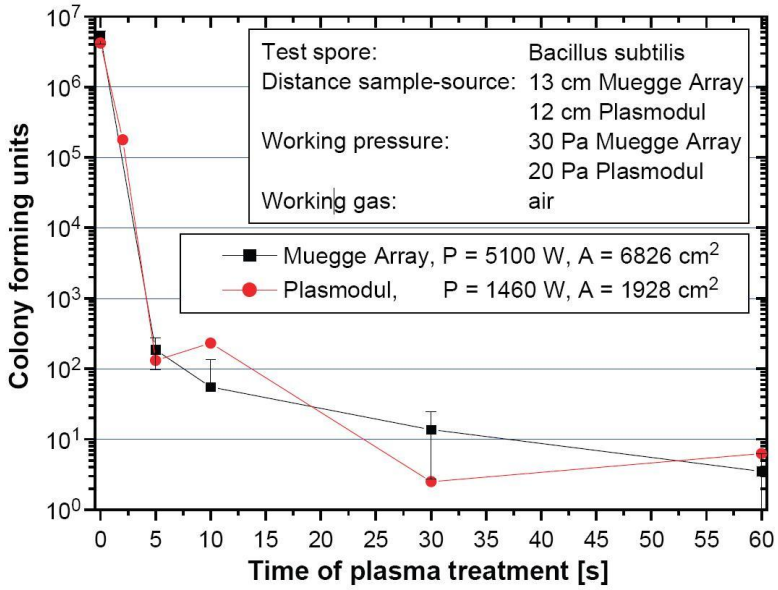

Figure 4. Comparison of two spore inactivation kinetics of *B. subtilis* test spores with an initial spore density of 2.0 10^4/cm^2, i.e. homogeneous spray contamination, obtained by the Muegge Array and the Plasmodul® (Schneider et al., 2005), with permission.

The group of Muranyi *et al*. has also widely reported the use of cold plasma treatments for sterilisation of PET foils as well as polystyrene and a multilayer packaging based on PET/PVDC/PE-LD (Muranyi et al., 2008, Muranyi et al., 2010). Increasing the relative gas humidity was firstly identified as key factor to achieve a minimum of $2\log_{10}$ inactivation of both *Aspergillus niger* and *Bacillus subtilis* at 1 s treatment. In the second study (Muranyi et al., 2010), damages in DNA of *Bacillus atrophaeus* endospores and vegetative cells were observed when treated with CDBD as a consequence of the synergistic combination of UV radiation and direct plasma. This combination allowed for very short treatment times, leading to minor changes in packaging materials which did not affect functionality. Other studies

(Yang et al., 2009a) report the effect of O_2 plasma excited by 13.56 MHz RF sterilisation of PET sheets depending on their position in the discharge area, afterglow area or remote area in the reaction equipment. A germicidal effect was found for the three approaches for *Pseudomonas aeruginosa* with lower time exposure than other traditional methods.

The immobilization of bioactive functional compounds like lysozyme, nisin, vanillin, sodium benzoate, glucose oxidase or antimicrobial peptides into the packaging material by plasma treatment has been studied in the emerging field of antimicrobial and active packaging (Buonocore et al., 2004, Misra et al., 2011, Lerouge et al., 2001, Ghanem and Ghaly, 2004, Fernandez-Gutierrez et al., 2010, Appendini and Hotchkiss, 2002a, Mastromatteo et al., 2011, Lee, 2010). Fernández-Gutierrez, Pedrow, Pitts, and Powers (2010) showed the feasibility of cold gas plasma for deposition of vanillin films over red delicious apples. The antimicrobial nature of vanillin against bacteria, yeasts and fungi has been shown in the literature (Fitzgerald et al., 2004, Cerrutti and Alzamora, 1996). Vanillin was selected for its capacity to form plasma-polymerized films although the formation of nodules due to condensation processes took place in the study, however no penetration of the apple's epidermis occurred. Other antimicrobial substances like chitosan, silver and triclosan have been immobilized on films by plasma treatment (Joerger et al., 2009, Nobile et al., 2004, Vartiainen et al., 2005, Zhang et al., 2006, Popelka et al., 2012). In the study of Joerger, *et al*. (2009), chitosan and chitosan/silver films were obtained by a relatively simple coating process by means of corona treatment showing good antimicrobial activity against *Escherichia coli* and *Listeria monocytogenes*. A recent study of Anton Popelka, *et al*. (2012) showed the immobilization of triclosan and chlorhexidine on LDPE via polyacrylic acid

(PAA) grafted on LDPE by low-temperature barrier discharge plasma (Figure 5), and shown its antibacterial efficacy for *E. coli and Staphylococcus aureus*.

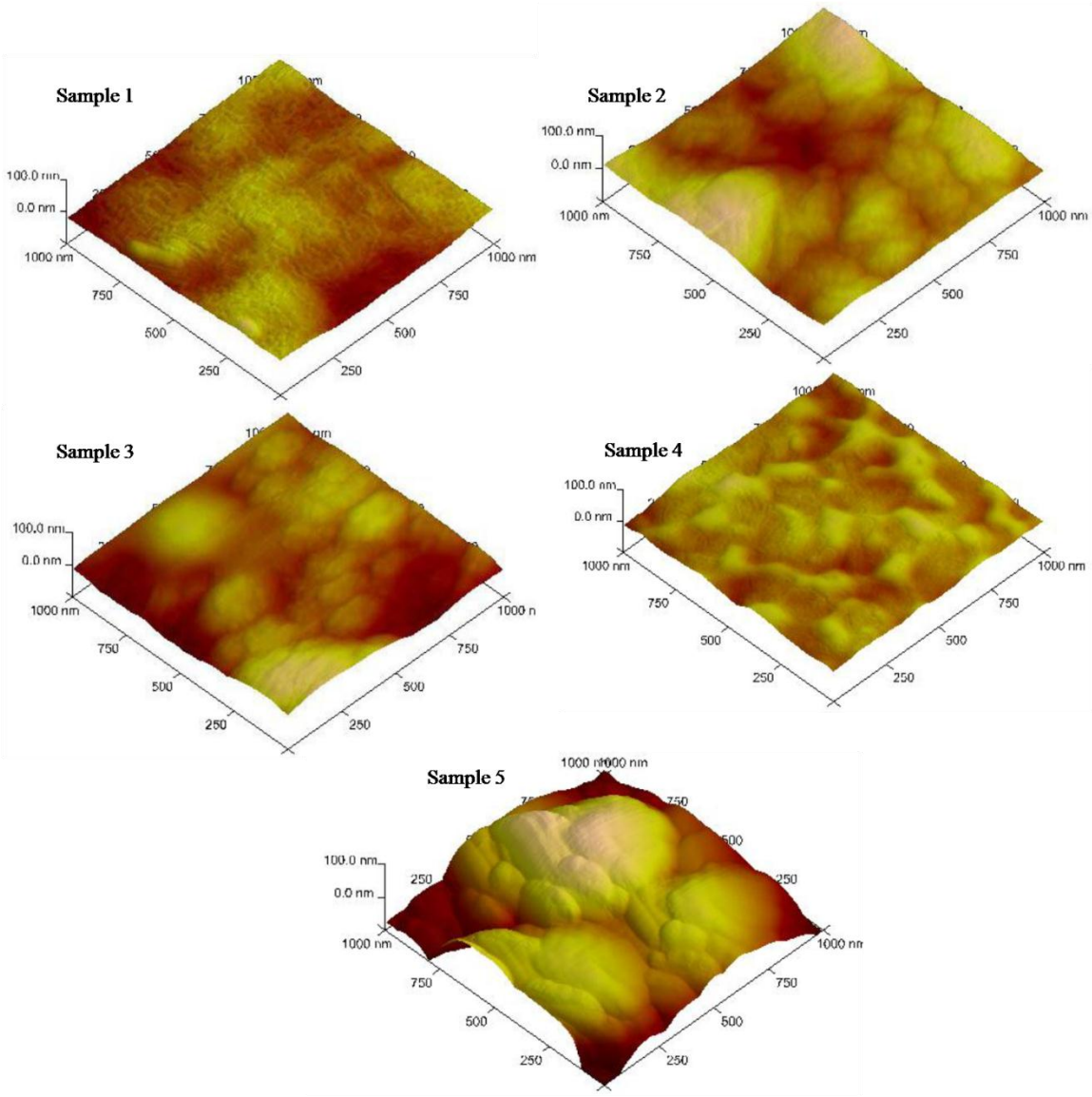

Figure 5. AFM surface changes for Sample 1–5: 1 - untreated LDPE; 2 - plasma-treated; 3 - AA grafted; 4 - triclosan coated; 5 - chlorhexidine coated. Adapted from (Popelka et al., 2012), with permission.

2.5.2. Surface activation and functionalisation

Surface activation and functionalisation by atmospheric-pressure plasma makes possible the processing of different materials and coatings that are, sometimes, very thin, for example in the production of composite packaging. Whether labelling jam jars, printing on glass containers, or sealing liquid packaging a key factor in the packaging industry is the ability to process materials reliably and at low cost (Banu, 2012, Ozdemir and Sadikoglu, 1998).

Imprints on packaging in the food and pharmaceutical industries are diverse (e.g. best-before dates or EAN codes) and it is essential that such imprints are secure against abrasion. Plasma treatment can fulfil the requirements for precise colour matching and high pixel accuracy when applying decoration to glass bottles or jars. Air bubbles are avoided and an optimum coating adhesion and high scratch resistance can be achieved safely and without any backside damage.

As it has been presented in section 3, a number of techniques are used to quantify the surface changes resulting from plasma treatment that will provide the printability property. Surface contact angle is often used to investigate wettability, which is closely related with ink adhesion (Strobel et al., 1991, Dixon and J. Meenan, 2012, Navaneetha Pandiyaraj et al., 2008). However, the wetting of a surface is not determined only by the magnitude of its surface energy, but also by the free energy of adhesion between the solid and liquid as well as the surface tension of the liquid (Bárdos and Baránková, 2010). Processing rates depend, additionally, on the plasma equipment used. Figure 6 shows a comparison of results on a PE surface (a) before and (b) after a 5 s exposure to a Ne FHC plasma treatment.

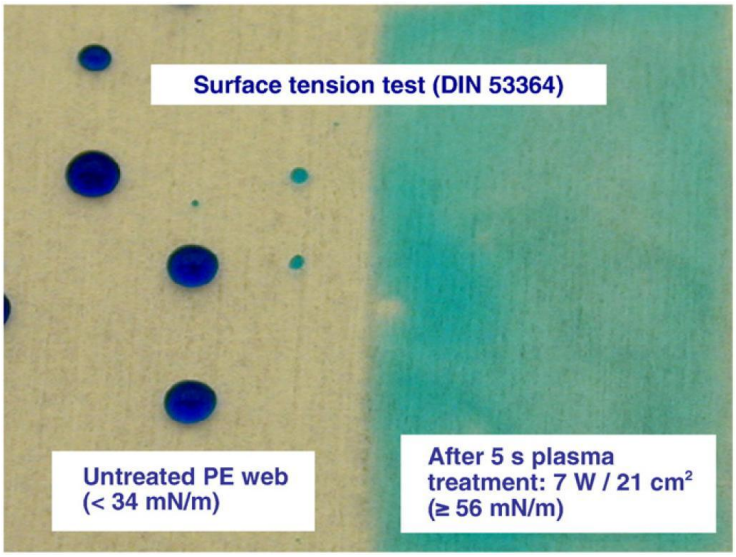

Figure 6. Effect of FHC plasma activation on PE web surface. Testing ink balls up and forms drops on an untreated surface (surface energy b34 mN/m), while on the plasma treated surface (surface energy ≥56 mN/m) the ink forms a continuous film (Bárdos and Baránková, 2010), with permission.

2.5.3. Mass transfer

Cold plasma treatments can be applied to food packaging materials as a sterilisation technique, aiming to pre-disinfect surfaces before contact to foods as it has been mentioned. However, treatment of food packaging materials with cold plasma can pursue other objectives such as the modification or enhancement of food packaging barrier properties. Whether it is used as a sterilisation method or for the surface modification of packages, cold plasma treatment can affect mechanical and mass transfer (barrier and migration) properties. The main types of mass transfer to be considered include: (i) Permeation of gases or vapors (oxygen, water vapour, aroma compounds, etc.) through the packaging materials from the external atmosphere into the food or the headspace and vice versa; and (ii) Migration of low-molecular weight substances from the packaging into the food (e.g. monomers, plasticizers,

solvents) that need to be evaluated for legislation and toxicological evaluation (Guillard et al., 2010).

Alteration of the barrier properties in materials for food contact applications has been one of the most studied applications in polymers treated by cold plasma (Lee, 2010, Ozdemir and Sadikoglu, 1998) since it is crucial factor to control the shelf life of fresh produce. Tenn, *et al*. (2012) carried out water vapour permeability measurements before and after plasma treatment in ethylene vinyl alcohol (EVOH) films with different percentages of ethylene content. They found that the hydrophobicity was significantly improved after plasma treatment for all films and consequently water permeability was decreased by up to 28% in some cases and the reported differences between samples were related to the polymer film composition, i.e., to the content of ethylene and hydroxyl groups, and the cross-linking reactions. Other studies focus on the improvement of barrier properties through deposition of thin layers of SiO_x on PET foils by plasma enhanced chemical vapour deposition (PECVD) (Plog et al., 2011, Deilmann et al., 2008a, Deilmann et al., 2008b). In these studies, a reduction by more than a factor of 2 in H_2O flux is reported for the coated PET foil. Films have the advantage of being colorless and they can be deposited on transparent packaging materials to allow customers a clear view of the packed food, which is highly desired for food packaging applications. Novel green bio-polymers like poly(lactic acid) (PLA), chitosan or arabinoxylans (AXs) are also being developed for food packaging applications, but the barrier properties in these materials are usually poorer than in traditional polymers, so cold plasma treatment may allow enhancement of gas permeability through cross-linking PLA with tetramethoxysilane (TMOS) (Uemura et al., 2006), deposition of hydrophobic silicon

coating onto chitosan polysaccharide film surfaces (Assis and Hotchkiss, 2007) or grafting omega-3 fatty acids onto AX polymeric chains (Péroval et al., 2003).

The second type of mass transfer, known as migration, can also be an important item in terms of consumer health. Few studies have been reported on the use of cold plasma for the decrease of migration in food packaging materials (Audic et al., 2001), but even less report the potential migration of low-molecular substances when plasma is applied with other objectives (surface sterilisation, increase in adhesion or printability, etc). In the case of poly(vinyl chloride) (PVC)-based commercial wrap films or gaskets in metal lids for glass jars, various processing aids like plasticizers and/or stabilizers may exude from the packaging material during storage or can be extracted by the foodstuff. This migration phenomenon causes pollution of the packaged food and a decrease of chemical and physical properties of the plastic material. Audic, *et al*. (2001) report the cold plasma modification of PVC flexible films with respect to the migrational properties of the resulting treated films. Different types of gases were used with both conventional (Bis(2-ethylhexyl)adipate -DEHA- ,and epoxidised soybean oil -ESO-) and non-conventional (permanent elastomeric EVACO) plasticizers for PVC. The overall migration decreased when DEHA and ESO were substituted by EVACO, but specific migration of DEHA and ESO increased in this sample. After plasma treatment with Argon (the most efficient gas), migration was significantly reduced for all plasticized PVC films.

Despite of the numerous efforts made from food safety institutions to control migration of polymer additives from food packaging materials to foodstuffs, the problem is still unresolved. In light of the few studies cited above for assessment of safety on packaging

materials regarding the use of plasma treatment to avoid migration effects or to study the degree of migration the technique should be studied as a function of the targeted polymers.

2.6. Biodegradable polymers

Biopolymer-based packaging is defined as packaging that contains raw materials originating from agricultural or marine sources (Cha and Chinnan, 2004). Plastics based on renewable resources do not necessary have to be biodegradable or compostable while the biodegradable polymers do not necessary have to be based on renewable materials because the biodegradability is directly correlated to the chemical structure of the materials rather than the origin (Siracusa et al., 2008). There are many ways in which biodegradable polymers are classified in the literature, one such classification based on the monomer source and polymer synthesis is presented in Figure 7 (Vieira et al., 2011).

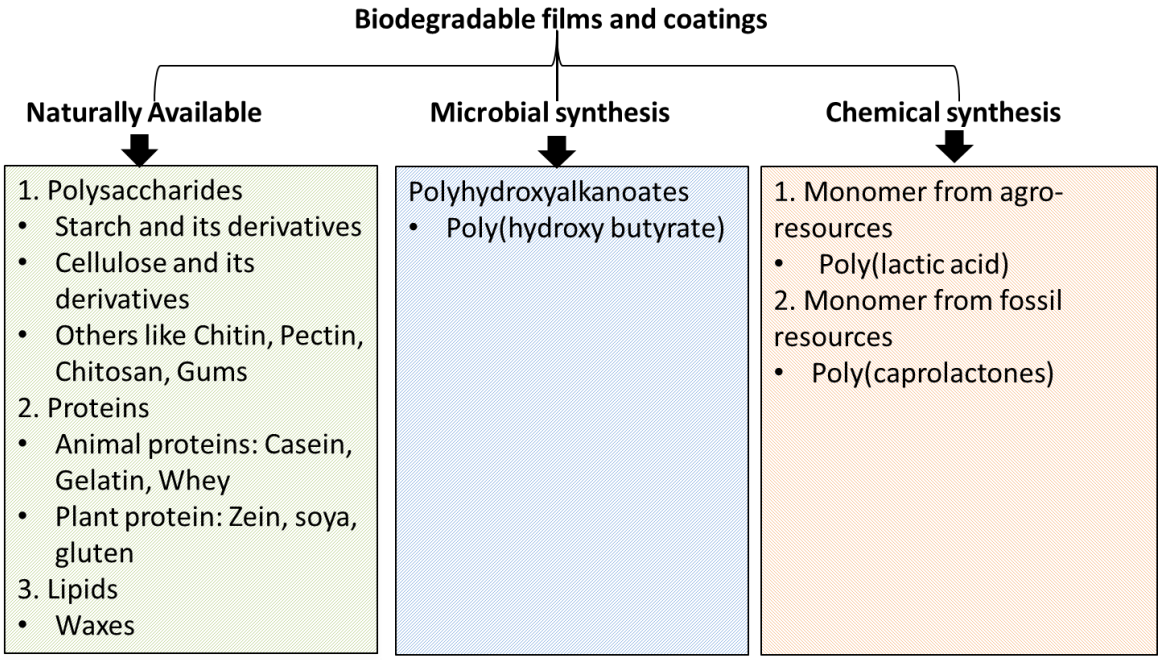

Figure 7. Classification of biodegradable films and coatings.

There are numerous types of biodegradable films which can be utilized as films and coatings in the food industries. For this work, it was essential to select a wide range of films to characterize the effects of cold plasma treatment. Due to this reason, PLA, zein, caseinate, starch, chitosan and gelatin were selected as the test samples to cover important classes of the natural and chemically synthesised films. Details of these films have been discussed later in the individual chapters.

2.7. Active packaging

Active packaging refers to the incorporation of certain additives/active ingredients into the packaging film or within the packaging containers to changes the condition of the packed food to extend shelf life or to improve safety or sensory properties, while maintaining the quality of the packaged food. Active packaging can be classified according to the desired application or intended use of the active ingredients and major types of active packaging systems are summarized in Table 5.

Table 5. Major types of active packaging systems (Adapted from Day (2003))

Active packaging systems	**Mechanisms/active compounds**	**Applications**
Oxygen scavengers	Ferro compounds, metal/acid, metal catalyst, ascorbate/metallic salts, enzyme based	bread, cakes, cooked rice, biscuits, pizza, pasta, cheese, cured meats and fish, coffee, snack foods, dried foods and beverages
Carbon dioxide	iron oxide/calcium hydroxide,	coffee, fresh meats and fish,

scavenger/ emitters	ferrous carbonate/metal halide, calcium oxide/activated charcoal, ascorbate/sodium bicarbonate	nuts and other snack food products and sponge cakes
Ethylene scavengers	potassium permanganate, activated carbon, activated clays/zeolites	fruit, vegetables and other horticultural products
Antimicrobials	Organic acids, enzymes, bacteriocin, fungicides, natural extracts, volatile oils, silver zeolite, antioxidants, volatile chlorine dioxide/ sulphur dioxide	cereals, meats, fish, bread, cheese, snack foods, fruit and vegetables
Moisture absorbers	PVA blanket, activated clays and minerals, silica gel	fish, meats, poultry, sandwiches, fruit and vegetables
Flavor/Odour absorbers	cellulose triacetate, acetylated paper, citric acid, ferrous salt/ascorbate, activated carbon/clays/zeolites	fruit juices, fried snack foods, fish, poultry, dairy products and fruit

Active packaging has been a focused area of research for many decades among food researchers due to its several potential applications for food preservation, consumer safety, and quality enhancement. Antimicrobial packaging is an important type of active packaging which has shown significant commercial applications. Based on this rationale, antimicrobial packaging was selected as the test samples for this work. Two different types of films were

used (one protein film-zein and one polysaccharide film-chitosan) with same active compound (thymol) for the cold plasma treatments.

2.8. Intelligent packaging

Intelligent packaging can be defined as a packaging system that is capable of carrying out intelligent functions (such as detecting, sensing, recording, tracing, communicating, and applying scientific logic) to facilitate decision making to extend shelf life, enhance safety, improve quality, provide information, and warn about possible problems (Yam et al., 2005). There are various types of intelligent packaging systems which are summarized in Table 6.

Table 6. Examples of indicators used in intelligent packaging. Adapted from Dobrucka (2013)

Indicators	**Principles**	**Applications**
Time-temperature indicators	Diffusion based, polymer based, enzymatic based	Foods stored under chilled and frozen conditions
Oxygen indicators	Redox dyes, pH dyes, enzymes	Foods stored in packages with modified oxygen concentration
Carbon dioxide indicator	Dyes based	Modified or controlled atmosphere food packaging
Microbial growth indicators/ Freshness indicators	Dyes sensitive to pH change, volatile nitrogen compounds, hydrogen sulphide and other metabolites	Perishable foods like meat, fish and poultry

Pathogen indicators	Various chemical and immunochemical methods reacting with toxins	Perishable foods such as meat, fish and poultry

Among all the different types of intelligent packaging systems, oxygen sensors are one of the most commercially exploited sensors in the food industry. Due to this reason, optical oxygen sensors were selected for this study to analyse the compatibility of presently available oxygen sensors with the novel in-package plasma processing.

2.9. Research objectives

Cold plasma has been used for decades for surface modification in polymer industry. However, the novel application of cold plasma in food industry for in-package decontamination raises concern of its effect on polymer properties important for food packaging applications. In recent decades food packaging has also evolved a lot and now can facilitate both passive and active roles in food preservation. This forms the impetus of this work to characterize the effects of cold plasma on different aspects of food packaging viz. primary packaging, active packaging and intelligent packaging. The idea was to access the compatibility of different packaging systems with process parameters found close to food decontamination processing.

For primary packaging materials, few studies have been reported on effects of cold plasma for traditional polymers but a wide gap was observed for biodegradable polymers. Along with the environmental concerns for using petrochemical based polymers, this formed the motivation to study the effects of cold plasma on biodegradable polymers. Based on these

rationales, a wide range of samples were selected for cold plasma treatments to cover most types of biodegradable polymers. The samples selected for this study were: PLA (commercial), protein from plant source (zein), protein from animal source (sodium caseinate), polysaccharide from plant source (corn starch), polysaccharide from animal source (chitosan) and polymer from waste utilization (bovine gelatin). The properties used for characterisation included surface properties including; topography and composition, bulk properties, crystal structure, chemical groups, thermal characteristics and film permeability to cover most of the important parameters pertaining to food packaging applications.

For the work on active packaging, the class of antimicrobial packaging was selected as it has been most widely used and shown good market potential. In this work, zein and chitosan films were selected with thymol as the active agent to cover both protein and polysaccharide active films. The properties analysed were surface, thermal and antimicrobial release kinetics of the active compound.

In case of intelligent packaging, oxygen sensors were selected as they are commercially available and can be quickly tuned for application with in-package cold plasma processing. Oxygen sensors were analysed for compatibility with plasma treatments under different gaseous environments for all the important parameters like calibration, reversibility, temperature dependence, humidity dependence and photo-degradation. Methodologies for film preparation, plasma treatment and different characterisation techniques are discussed in detail in chapter 3.

Chapter 3 Materials and Methods

3.1. Materials

Commercial PLA film (thickness = 42.8±1.3 µm) was purchased from Amcor Flexibles, UK. It is a tri-layer film with a PLA core covered with PLA skin layers on either side without any coating material or prior treatments.

Zein films were prepared as described by Mastromatteo et al. (2009) with slight modifications. 5 g of zein (Sigma-Aldrich, Ireland) were dissolved into 26 ml of ethanol at 50 °C. 3 g of glycerol (Sigma-Aldrich, Ireland) were added to the solution and stirred using a hotplate magnetic stirrer for 10 min. The film forming solutions were poured on Petri dishes (diameter 15 cm) and dried at ambient conditions under laminar flow until the solvent was completely evaporated and peeled off after 48 h. The cast zein films had a thickness of 385±10 µm.

Sodium caseinate films were prepared by the method reported by Arrieta et al. (2013). The film-forming aqueous dispersions of sodium caseinate (5 % w/w) was prepared using a hot-plate magnetic stirrer at 65 °C for 10 min. Glycerol as a plasticizer (protein:plasticizer ratio of 1:0.35) was added under the same conditions while stirring for another 15 min. Films were prepared by taking 30 ml of film-forming solution into Petri dishes (15 cm diameter) and dried at ambient conditions under laminar air flow until the solvent was completely evaporated and peeled off after 48 h. The thickness of films was 130±11 µm.

Corn starch film was prepared by the method described by Bertuzzi et al. (2007). High amylose unmodified corn starch (HYLON VII, Ingredion, UK) with an amylose content of

about 70 % was used for film preparation. Briefly, 1g of corn starch was dispersed in 10 ml of water and then 10 ml of 0.25 M sodium hydroxide was added. The resulting dispersion was stirred for 60 min on a magnetic stirrer and gelatinized at 78–80 °C for 15 min. Glycerol was added as plasticizer at 10 % level. The resulting film forming solution was cooled to 50 °C and poured on plastic Petri dishes (15 cm diameter) and dried at ambient conditions under a laminar flow hood until the solvent was completely evaporated and peeled off after 48 h. The cast corn starch films had a thickness of 70±18 µm.

Bovine hide gelatin film was prepared by the solvent casting method. 10g of bovine hide gelatin (Rousselot International, Belgium) was dissolved in 100 ml of distilled water for 30 min on a hot plate magnetic stirrer. It was then heated at 60 °C for 20 min and 4 ml of glycerol (Sigma Aldrich, Ireland) was added as a plasticizer and stirred for another 15 min. The film forming solution was cooled to 40 °C and poured on plastic 15 cm diameter Petri dishes (30 ml/plate) and dried at ambient conditions under laminar flow until the solvent was completely evaporated and peeled off after 48 h. The cast gelatin films had a thickness of 159±20 µm.

For chitosan films, medium molecular weight chitosan, analytical grade acetic acid and glycerol were purchased from Sigma-Aldrich, Ireland. Chitosan film was prepared by the method followed by Leceta et al. (2013) with minor modifications. Chitosan (1 % w/v) solution was prepared in 1 % acetic acid solution. Glycerol (10 %) was added after 15 min continuous stirring. Stirring was continued for 30 min until total homogenization of the mixture. Film forming solutions was filtered and 70 ml of the solution were poured into 15 cm petri dishes and dried at ambient conditions under laminar flow till the solvent was

completely evaporated and peeled off after 48 h. The cast chitosan films had a thickness of 64±16 µm.

Antimicrobial zein films were prepared as described by Mastromatteo et al. (2009) with slight modifications. 5 g of zein (Sigma-Aldrich, Ireland) were dissolved into 26 ml of ethanol at 50 °C. 3 g of glycerol (Sigma-Aldrich, Ireland) were added to the solution and stirred using a hotplate magnetic stirrer for 10 min. Then the solution was cooled to room temperature and 10 % and 20 % of thymol (weight of thymol/weight of dry polymer) (Sigma-Aldrich, Ireland) was added with final stirring for about 10 min. As a blank, zein solutions without active agent were also prepared. The film forming solutions were poured on Petri dishes (diameter 15 cm) and dried at ambient conditions under laminar flow, until the solvent was completely evaporated and peeled off after 48 h. The zein films had a thickness of 385 ± 8 µm.

For active chitosan film, medium molecular weight chitosan, analytical grade acetic acid and glycerol were purchased from Sigma-Aldrich, Ireland. Chitosan film was prepared by the method followed by Leceta et al. (2013) with minor modifications. Chitosan (1 % w/v) solution was prepared in 1 % acetic acid solution. Glycerol (10 %) was added after 15 min continuous stirring. Then 2 % and 5 % of thymol (weight of thymol/weight of dry polymer) (Sigma-Aldrich, Ireland) was added with final stirring for about 30 min until total homogenization of the mixture. As blank, chitosan solutions without active agent were also prepared. 70 ml of the film forming solutions was poured into 15 cm diameter petri dishes and dried at ambient conditions under laminar flow until the solvent was completely evaporated and peeled off after 48 h. The cast chitosan films had a thickness of 64±20 µm.

For preparation of oxygen sensors, the non-woven microporus polypropylene sheets (Type FS2192i, thickness=80 ± 20 mm, mean pore size=17 mm, and fibre size=8-12 µm) were purchased from Freudenberg, UK. Platinum (II)-benzoporphyrin dye (PtBP) was purchased from Luxcel Biosciences (Cork, Ireland). Tetrahydrofuran (HPLC grade) were purchased from Sigma-Aldrich, and N_2 and O_2 gases (99.999 % purity) from Irish Oxygen (Ireland). Commercial Optech™-O_2 platinum sensors (sensor A) were purchased from Mocon (Minneapolis, USA). These sensors were stored at room conditions and used without any further treatment. Soak sensors (Sensor B) were prepared by making a solution of PtBP dye 70:30 tetrahydrofuran/water (0.03 mg/mL) and placing 8 mL of the solution in each 15 ml disposable vial (Sarstedt) (Kelly et al., 2014). Strips of PP membrane (24 mm x 12 mm) were placed the solution ensuring strips were immersed fully in solution. The vials were then capped and incubated at 65 °C for 1 h. The samples were extracted, washed with water and air-dried for 4 h. Subsequently, the sensor strips were incubated in a dry oven at 70 °C for 16 hr.

3.2. Plasma treatment

An overall block diagram of the used plasma generation system has been shown in Figure 8. The DBD plasma source consists of two circular aluminium plate electrodes (outer diameter = 158 mm) over perspex dielectric layers (10 mm thickness). When the potential across the gap reaches the breakdown voltage the dielectric barrier acts as a stabilizing material forming of a large number of micro-discharges. The applied voltage to the electrode was obtained from a step-up transformer (Phenix Technologies, Inc., USA) using a variac. The input of 230 V, 50 Hz was given to the primary winding of high voltage step-up transformer from the mains supply.

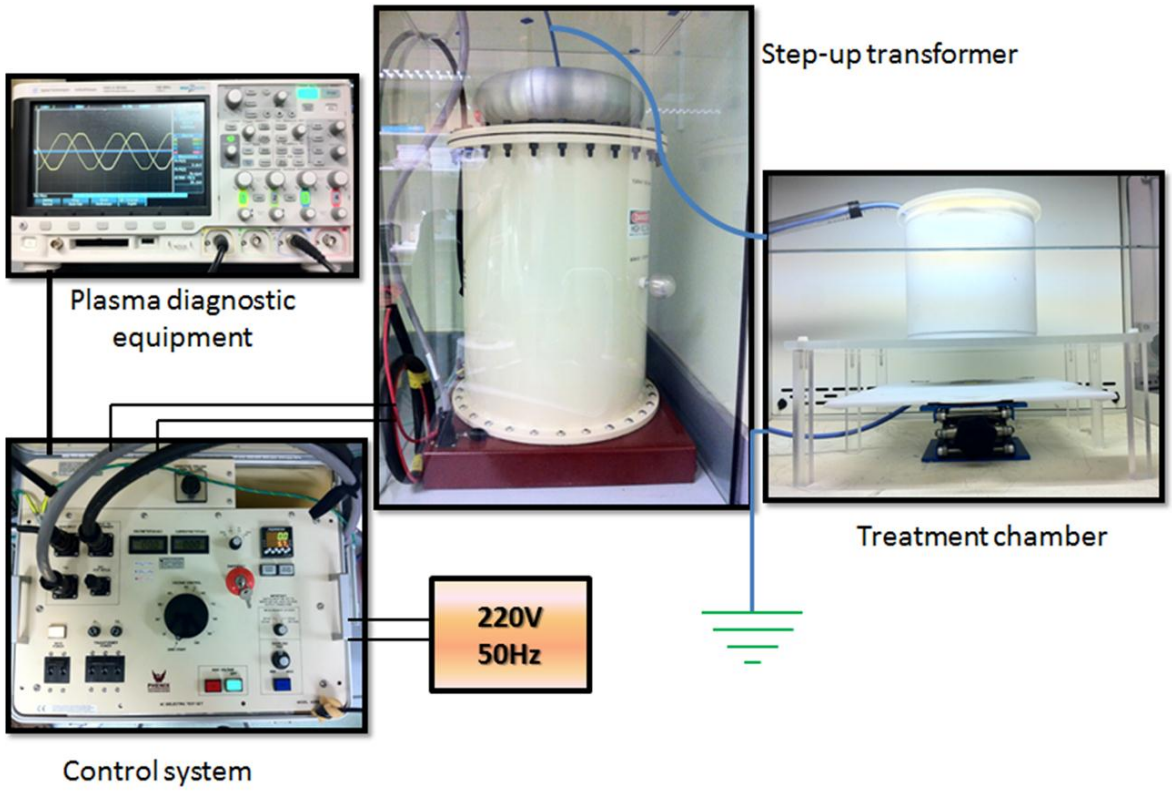

Figure 8. Block diagram of the cold plasma generation system

The excited and reactive species generated by the employed plasma source had been characterised previously (Pankaj et al, 2014c), using a computer controlled Stellarnet EPP 2000C-25 spectrometer for optical emission spectroscopy. The emission from the discharge was coupled to the spectrometer using an optical fibre having a numerical aperture of 0.22. Spectra were obtained at a resolution of 1.5 nm, over the range of 200 to 850 nm. Identification of spectral characteristics was carried out using NIST atomic spectra database which shows the most intense peaks near UV region by the excited species of nitrogen, namely nitrogen second positive system N_2 (C-B) and first negative system N_2^+ (B-X). The minor peak around 300 nm was resulting from OH excitation. Peaks associated with optical

transitions of the O atom were also observed at low intensities: 725.4 from O ($5s^3S \rightarrow 3p^3P$), 533.0 nm from O ($5d^5D \rightarrow 3p^5P$), and 777.4 from O ($2s^22p^33p^5P \rightarrow 2s^22p^33s^5S$). The dielectric barrier discharge setup was also found to generate significant amount of ozone. It may be noted that air plasma chemistry is highly complex with participation from over 75 species, in almost 500 reactions limiting the number of species that can be identified; especially the very short time scale species remain unidentified to this point. To conclude, the current dielectric barrier discharge setup was a potential source of reactive oxygen and reactive nitrogen species.

A schematic of the experimental setup has been presented in Figure 9. In the case of commercial PLA, the film was used as a pillow pouch packaging material for a polypropylene box of dimensions of 310 mm × 230 mm × 22 mm. The sample in contact with the high-voltage electrode is referred to as the top-positioned and the sample in contact with ground electrode is referred as bottom-positioned in chapter 4. The PLA samples were treated at 70 and 80 kV for 0.5, 1.5, 2.5 and 3.5 minutes and stored at normal room conditions before analysis. The atmospheric air condition at the time of treatment was 45 % relative humidity (RH) and 22 °C.

The zein, sodium caseinate, starch, gelatin and chitosan film samples were kept on a polypropylene sheet (2 mm) and treated at a distance of 10mm from the Perspex dielectric barrier (10 mm) at 60, 70 and 80 kV for 1, 2, 3, 4 and 5 min. The atmospheric air conditions at the time of treatment were about 48 % relative humidity (RH) and 20 °C in all the cases.

The antimicrobial zein and chitosan film samples were treated at 70 kV for 5 min. The atmospheric air condition at the time of treatment was about 50 % relative humidity (RH) and 22 °C in both cases.

For treatment of oxygen sensors, sensors were placed in commercial PET/PE trays (150 mm x 150 mm x 35 mm, Holfield plastic, Ireland) and sealed by tray sealer using anti-fog coated BOPA/PE/EVOH/PE films (thickness=0.043 mm, DAZA, Spain) as top film. Sensors were sealed using two different gas compositions: air and MAP (pre-blended 30% CO_2 + 70% N_2, BOC, Ireland). Sensors containing trays were treated at 80 kV for 5 minutes.

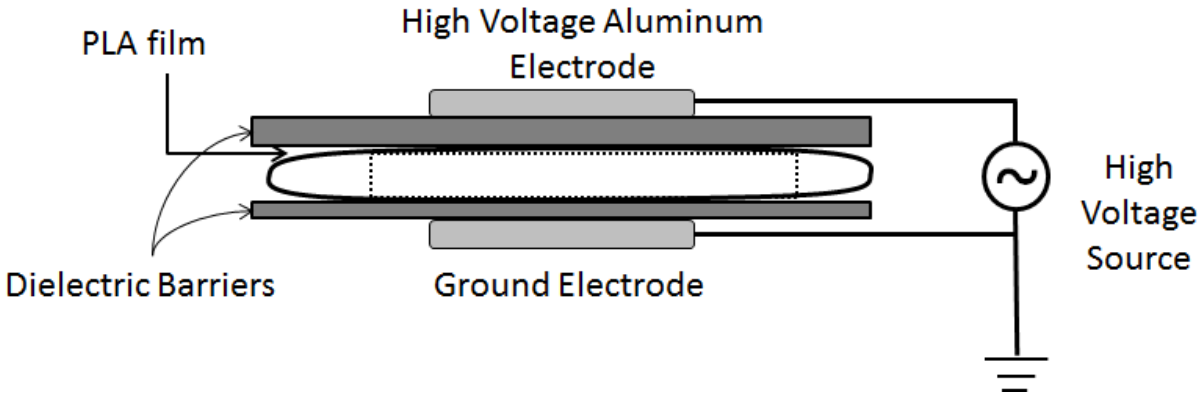

Figure 9. Schematic of the experimental setup for DBD plasma system.

3.3. Material characterisation

3.3.1. Atomic force microscopy (AFM)

AFM measurements were carried out to observe the surface topography of the samples before and after DBD plasma treatment. The AFM used was an MFP-3D BIO 1126 (Asylum

Research, Santa Barbara, CA, USA) operated in intermittent contact (tapping) mode. The images were collected at a fixed scan rate of 0.5 Hz. The sampling rate was 512 lines. The data was processed using MF3D software (version 111111+1219). The scanned area was 25 μm^2 and was repeated five times.

3.3.2. Thermogravimetric analysis (TGA)

TGA analysis were performed with a Mettler Toledo thermal analyser, model TGA/SDTA 851e (Schwarzenbach, Switzerland). Approximately 5g samples were heated at 10 °C min^{-1} from room temperature to 700 °C under nitrogen atmosphere (flow rate 50 ml min^{-1}). Initial degradation temperature (T_5) was determined as the temperature at which 5 % of mass was lost and maximum degradation temperature (T_{max}) was determined from the first derivative.

3.3.3. Differential scanning calorimetry (DSC)

DSC analysis was performed with a TA Instruments DSC Q2000 (New Castle, DE, USA) under a dry nitrogen gas flow rate of 50 ml min^{-1}. Approximately 3-5 mg samples were weighed in aluminium pans (40 µL) and subjected to two heating-cooling cycles from -30 °C to 200 °C at 10 °C min^{-1}. Glass transition temperatures (T_g) and melting endotherm were analysed during the first heating cycle.

3.3.4. X-ray diffraction (XRD)

Wide-angle X-ray scattering (WAXS) of PLA films was performed on a Bruker D8-Advance (USA) diffractometer, equipped with a Cu-Kα radiation source (λ = 1.546 Å), operating at 40 kV and 40 mA as the applied voltage and current, respectively. The incidence angle (2θ) was varied between 5°and 90° at a scanning rate of 2° min^{-1}.

3.3.5. Fourier transform infrared spectroscopy (FTIR)

FT-IR spectroscopy was carried out by using Nicolet Avatar 360 FT-IR E.S.P. (UK) and Perkin Elmer FT-IR/FT-NIR spectrometer (Spectrum 400) from 4000 to 400 cm^{-1} to measure any changes in the spectra intensities. A background spectrum was collected by keeping the resolution as 1 cm^{-1}. After the background scan, treated and untreated film samples were placed in the sample holder and analysed in triplicates.

3.3.6. X-ray photoelectron spectroscopy (XPS)

X-ray photoelectron spectroscopy (XPS, K-ALPHA, Thermo Scientific) was used to analyse sample surfaces. All spectra were collected using Al-Kα radiation (1486.6 eV), monochromatized by a twin crystal monochromator, yielding a focused X-ray spot with a diameter of 400 µm, at 3 mA × 12 kV. The alpha hemispherical analyser was operated in the constant energy mode with survey scan pass energies of 200 eV to measure the whole energy band and 50 eV in a narrow scan to selectively measure the particular elements. XPS was used to provide the chemical bonding state as well as the elemental composition of the samples. Charge compensation was achieved with the system flood gun that provides low energy electrons and low energy argon ions from a single source.

3.3.7. Oxygen transmission rate (OTR)

OTR analysis was conducted with an Oxygen Permeation Analyser 8500 from Systech Instruments (Metrotec S.A, Spain). Treated films were cut into circular samples (14 cm diameter) and clamped in the diffusion chamber at 25 °C. Pure oxygen (99.9 %) was introduced into the upper half of the chamber while nitrogen was injected into the lower half, where an oxygen sensor was placed. The oxygen volumetric flow rate per unit area of the

membrane and per time (OTR, $cm^3m^{-2}day^{-1}$) was continuously monitored until a steady state was reached. All samples were analysed in triplicates.

3.3.8. Water vapor transmission rate (WVTR)

WVTR was measured gravimetrically using the ASTM method E 96/E 96M-05 (ASTM, 2005). Briefly, 50 g of anhydrous calcium chloride, after drying at 100 °C for 24 h, was placed in each test jar to establish the dry conditions. Control and plasma treated film samples were placed over the jar, and its edge sealed using paraffin wax (T_m= 54–56 °C; Sigma-Aldrich, Ireland). After the films were mounted, the whole assembly was weighed and placed in a climatic chamber at a set temperature of 24 ± 1 °C and RH of 50 ± 1 %. The assembly was weighed with an accuracy of 0.001 g at 24 h intervals. WVTR was calculated in g $(m^2.day)^{-1}$ using equation 1.

$$WVTR = \frac{M_t - M_O}{\Delta t} . \frac{1}{A} \quad (1)$$

where M_0 is the initial mass of the test jar (g), M_t is the mass of the test jar at time t (g), Δt is the duration of the test period (day), and A is the effective surface area of the test film (m^2). The experimental values of WVTR represent average of measurements from the three replicate samples.

3.3.9. Water Sorption Kinetics

Water sorption kinetics was determined by the method of Pereda et al. (2009). Briefly, the films were dried at 40 °C for three days in a vacuum oven at 500 mm of Hg pressure at 25 °C. After drying, films were DBD plasma treated and placed in a versatile environmental test chamber (Model MLR-350H, Sanyo Electric Biomedical Co. ltd., Japan) at a controlled

humidity environment of 75 % at 23 °C. Samples were weighed gravimetrically at equal time intervals with a precision of ± 0.0001 g. This experiment was performed in triplicate to ensure the reproducibility of the results. The moisture content (M_t) of films as a function of time was obtained from the total mass balance of the sample as given in equation 2.

$$M_t(\%) = \frac{(W_t - W_0) \times 100}{W_0} \quad (2)$$

where M_t= moisture content of the sample at time t (%), W_t= weight of the sample at time t (g), W_0= initial dry weight of sample (g).

3.3.10. Overall Migration

The overall migration study was carried out according to EN 1186 standard (European Standard EN 1186-1:2002). Control and plasma treated samples (80 kV for 3.5 minutes) were cut into strips of 1 dm^2 area (10X10cm) and totally immersed in 100 ml of food simulant in a stoppered glass tube in triplicate. Four simulants viz. A (distilled water), B (3 % w/v acetic acid), C (10 %v/v ethanol) and D (95 %v/v ethanol) were used. The test condition used was 40 °C for 10 days corresponding to the food contact during long term storage at room temperature or below, including heating up to 70 °C for up to 2 h, or heating up to 100 °C for up to 15 minutes (European Standard EN 1186-1:2002). All simulants were subsequently evaporated to dryness and kept in air-dried oven until constant weight was achieved. The mass of the non-volatile residue was determined gravimetrically.

3.3.11. Contact angle and surface free energy

Static contact angle of all the films were analysed using Theta Lite Optical Tensiometer (Attension, TL100, Finland) by sessile drop technique. Three test liquids were used whose

properties are given in Table 7. A drop of each test liquid was uniformly placed on the film surface and the image was recorded at 15 frames per second for 10 seconds. Images were analysed using the OneAttension software (v 2.1). All the values reported are the mean of more than 130 data points done in triplicates.

Table 7. Surface free energy (γ^{tot}: total surface free energy, γ^{d}: dispersive component, γ^{+}: acid component, γ^{-}: base component) components of test liquids.

Test liquids	**γ^{tot}(mN/m)**	**γ^{d}(mN/m)**	**γ^{+}(mN/m)**	**γ^{-}(mN/m)**
Water	72.8	21.8	25.5	25.5
Ethylene glycol	48.0	29.0	3.0	30.1
Di-iodomethane	50.8	50.8	0.0	0.0

The surface free energy (SFE) for the plasma treated films was also calculated from the contact angle using the same software. The theory of contact angle is based on the Young equation (equation 3) (Young, 1805).

$$\gamma_L \cos\theta = \gamma_S - \gamma_{SL} \quad (3)$$

where γ_L is surface tension of liquid, θ is contact angle, γ_S is the surface free energy of the solid surface and γ_{SL} is the solid/liquid interfacial energy. It was the work of Fowkes to divide the total surface free energy into two components: dispersive (γ^{d}) and non-dispersive/polar (γ^{p}) (Fowkes, 1962). Owen and Wendt extended Fowkes' work and added the hydrogen bonding term; they also used the geometric mean to combine the components (equation 4) (Owens and Wendt, 1969).

$$\gamma_{SL} = \gamma_S + \gamma_L - 2\sqrt{\gamma_S^d . \gamma_L^d} - 2\sqrt{\gamma_S^p . \gamma_L^p} \quad (4)$$

Combining equation 3 and 4 gives equation 5, which is referred as Fowkes or Owen-Wendt approach or OWRK equation.

$$\frac{1}{2}.\gamma_L(1+\cos\theta) = \sqrt{\gamma_S^d . \gamma_L^d} + \sqrt{\gamma_S^p . \gamma_L^p} \quad (5)$$

One of the recent developments in surface free energy calculation is Acid-base approach or Van Oss-Chaudhury-Good method, which further divides the polar component into acid and base components (equation 6) (Van Oss et al., 1988).

$$\frac{1}{2}.\gamma_L(1+\cos\theta) = \sqrt{\gamma_S^d . \gamma_L^d} + \sqrt{\gamma_S^+ . \gamma_L^-} + \sqrt{\gamma_S^- . \gamma_L^+} \quad (6)$$

3.3.12. Thymol release kinetics

Thymol release was measured by the method described by Del Nobile et al. (2008) with slight modifications. The prepared active films were put into a glass beaker with 250 ml of distilled water (volume/surface ratio 4.5 ml cm^{-2}) and shaken at 25 °C and 150 rpm in an orbital shaker for 180 h. The thymol release kinetics was evaluated by monitoring thymol concentration in the surrounding solution using HPLC (Waters e2695 Separation module and Waters 2998 Photodiode array detector, Waters Corporation, Ireland), until equilibrium value was achieved. The chromatographic column used was a C18 Reverse phase column, 250 × 4 mm, particle size 5 µm. A linear gradient elution with acetonitrile-0.05 M orthophosphoric acid was used (Martel and Zeggane, 2002). Typical gradients used are given in Table 8. The flow rate was 1 ml min^{-1} with injection volume of 5 µl and the elution was detected at a

wavelength of 277 nm. The calibration curve was constructed for peak area against thymol concentration of standard solutions from 10 to 500 ppm.

Table 8. Gradient elution for determination of thymol

Time (min)	Acetonitrile	0.05 M orthophosphoric acid
0	40	60
7	46	54
8	60	40
11	60	40
20	40	60

3.3.13. Sensor characterisation

All the oxygen sensors were screened for the phosphorescence intensity and lifetime signals were recorded with a handheld instrument Optech™ (Mocon, Minneapolis, USA). The sensors were placed in a clear 20 ml polystyrene vial (Sarstedt, Ireland). Phosphorescence intensity and lifetime (µs) were measured in both air (21 kPa O_2) and N_2 (0 kPa O_2). Each sensor strip was measured three times in different locations and average values were reported. The experimental setup used for the analysis of sensors has been shown in Figure 10.

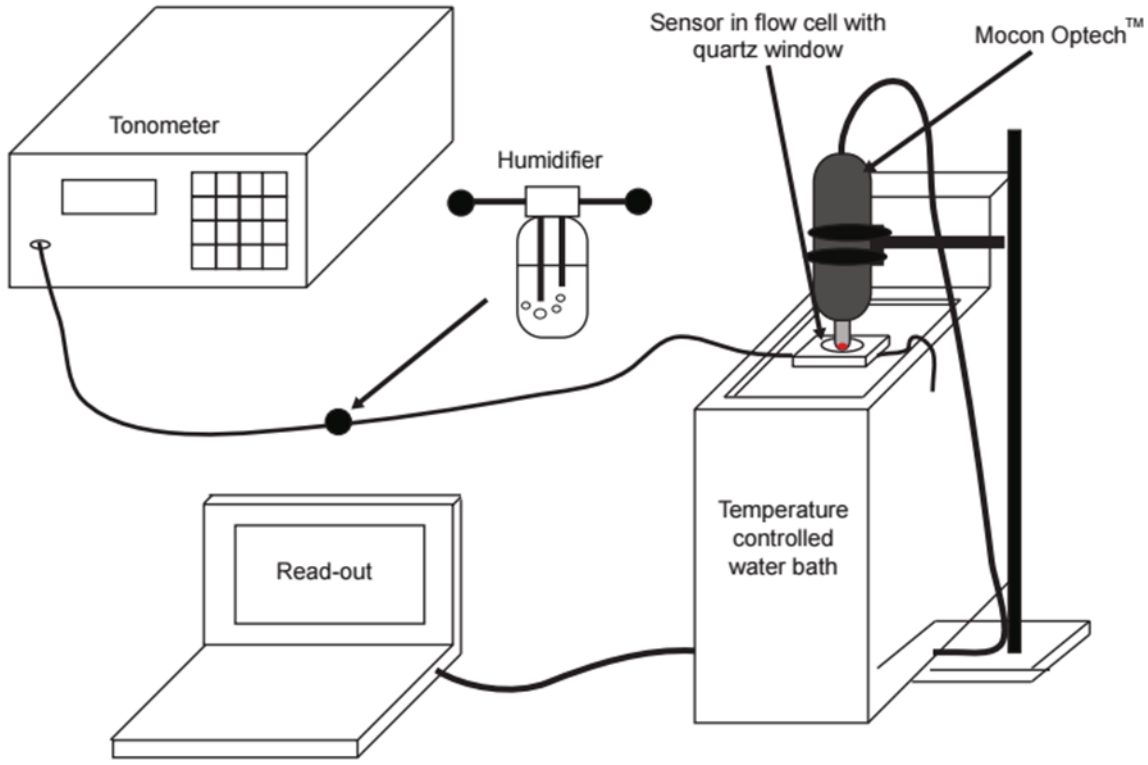

Figure 10. Schematic diagram of the experimental set up used for sensors analysis

For sensor calibration standard O_2-N_2 gas mixtures (0–100 kPa O_2), produced using a precision gas mixer (LN Industries SA, Switzerland), were pumped through a flow cell with a glass window through which an O_2 sensor was interrogated with the Optech™ instrument. The flow cell was submerged in a circulating water bath (Julabo) keeping the window and probe above the water level to equilibrate the gas to the correct temperature. Sensor A was calibrated at 21, 10, 5, 2, 1 and 0 kPa O_2 while sensor B was calibrated at 100, 21, 10, 5, 2 and 0 kPa O_2.

To analyse the effect of humidity on the sensors, both the sensors were also calibrated in the humid gas condition. In this case, the gases were purged through a glass jar filled with water and were then used to calibrate the sensors with the same setup as discussed before. Both sensors were also analysed at three different temperatures (10, 20 and 30 °C) to characterise the effects of temperature on the sensor phosphorescence intensity and lifetime signals.

In order to investigate the reversibility and response time, both oxygen sensors were exposed to alternating streams of pure N_2 (0 kPa O_2) and air (21 kPa O_2) and the phosphorescence intensity was measured. The response ($t_{90\downarrow}$) and recovery ($t_{90\uparrow}$) times were denoted as the time required for the phosphorescence intensity to decrease and recover by 90 % of the total change respectively upon alternating the gas mixture from pure N_2 to air and back again.

The photo-stability of the control and plasma treated oxygen sensors were also investigated under prolonged continuous illumination for 12 h using a Xenon lamp (150 W) and the sensors signals were recorded continuously at 30s intervals at 100 % intensity using a Firesting™ instrument (PyroSciences GmbH, Germany) which operates with a 1 mm plastic fibre probe under standard manufacturer's settings.

3.4. Statistical Analysis

Analysis of variance was done for all the treatments and significance of difference between treatments was assessed using Fisher and Tukey's multiple sample comparison tests. Significance levels were tested at $p \leq 0.05$. Analysis was carried out in SPSS statistical package (SPSS Inc., Chicago, USA) and Minitab software (Minitab Inc., USA). The mathematical model for thymol release kinetic was performed in Matlab 2012a (MathWorks, USA).

Chapter 4 Poly(lactic acid) film

4.1. Introduction

PLA is one of the most promising bio-based polymers which is biodegradable, recyclable and biocompatible requiring low manufacturing energy, with good processability, high transparency and water solubility resistance (Rasal et al., 2010, Gupta et al., 2007, Siracusa et al., 2008). Such properties coupled with a competitive market price have made it one of the first commercially available biopolymers widely used in the packaging of fresh produce. Although PLA offers a substitute for many non-biodegradable polymers, its application is limited due to its brittleness and barrier properties (Rasal et al., 2010, Chaiwong et al., 2010). The commercial success of PLA made it the first choice to access its compatibility with cold plasma under operating conditions closely associated with in-package food decontamination.

4.2. Results and Discussions

4.2.1. Surface topography

Figure 11 shows the surface topography of PLA films before and after DBD plasma treatments. The surface of the untreated sample was relatively smooth with structures randomly dispersed over the surface. The root mean square (RMS) roughness was 0.93 nm. Roughness parameters for all the samples are summarized in Table 9. It is clear from the results that roughness increased with increasing voltage and treatment time. The increase in roughness was more evident in the samples which were in contact with the high voltage electrode. It should also be emphasised at this point that the roughness of bottom-placed films at 70 kV were not significantly different ($p>0.05$) for all treatment times, although at 80 kV, significant differences ($p\leq0.05$) were observed after 2.5 and 3.5 minutes of treatment

time. The periodic cone-like structures appearing on the samples in contact with the high voltage electrode would be most likely due to the etching effect of the applied plasma. These structures presented a typical feature size and spacing of the order of few micrometers or smaller. These structures became wider and closer to each other as the voltage increased, so the area of the flat surface was reduced and the grooves appeared at higher heights, as shown by the data of the highest peak and lowest groove in Table 6. The height of the cone-like structures increased moderately from 70 to 80 kV. However, there is a large increase in the lowest groove, from 19.2 to 42.5 nm, when the voltage increases. The bombardment of energetic particles such as electrons, ions, radicals, neutrals and excited atoms/molecules and UV–vis radiations on the surface of polymer films results in etching of the surface (Yang et al., 2009b). Similar types of topographical features using air-plasma treatment were also observed by Teraoka et al. (2006).

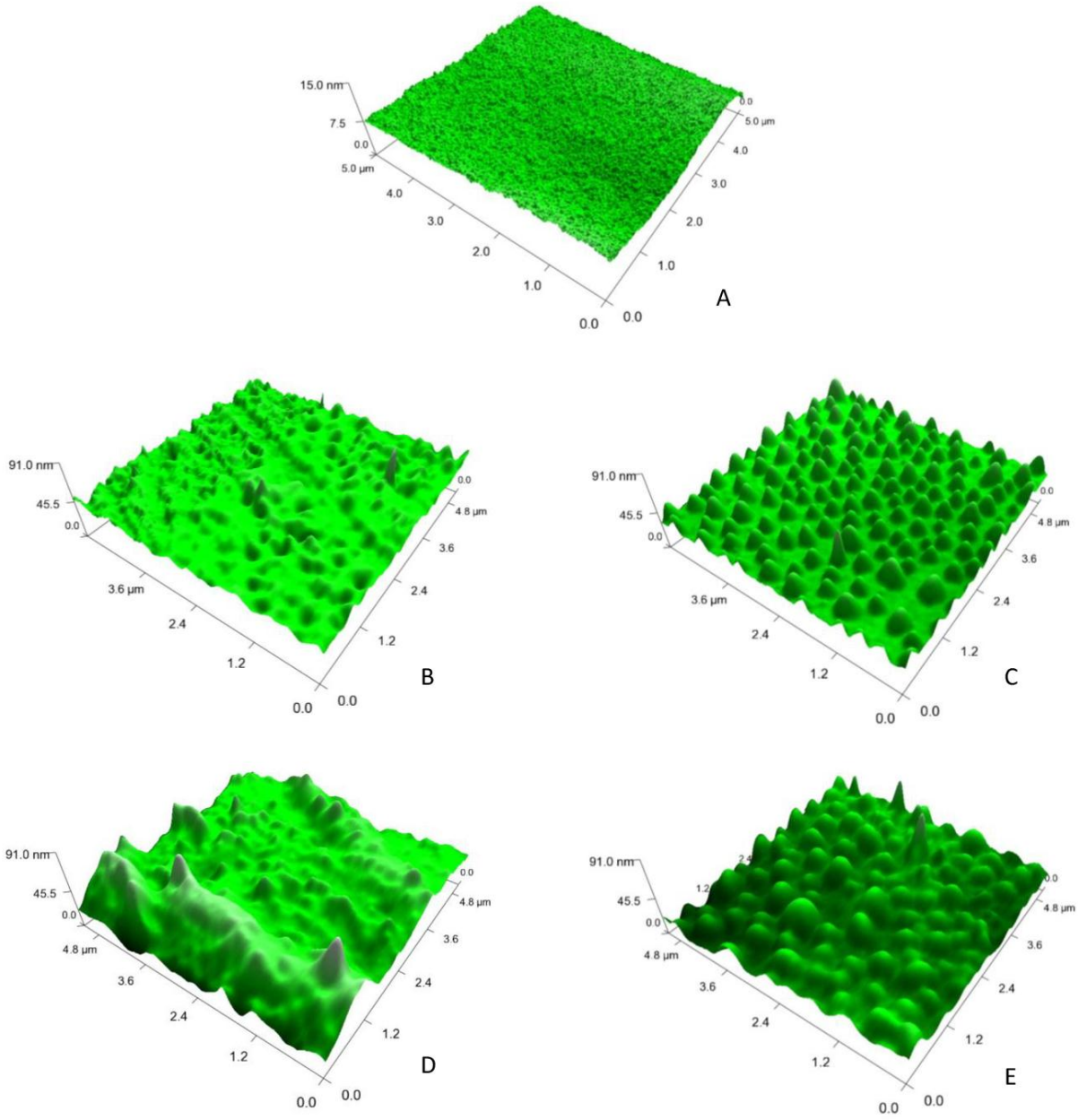

Figure 11. AFM images of the surface of untreated and plasma-treated PLA films (A. Untreated, B. 70 kV-3.5min-Bottom, C. 70 kV-3.5min-Top, D. 80 kV-3.5min-Bottom, E. 80 kV-3.5min-Top)

Table 9. Roughness parameters (mean value ±standard deviation) for control and DBD plasma treated samples (R_{rms}: root mean square roughness, R_{Peak}: Highest peak, R_{Groove}: lowest groove). Means that do not share a letter are significantly different ($p \leq 0.05$).

Voltage (kV)	**Time (min)**	**Position**	**R_{rms} (nm)**	**R_{Peak} (nm)**	**R_{Groove} (nm)**
	Control		0.9 ± 0.7^{c}	3.1	4.7
70	0.5	Bottom	$6.1 \pm 5.0^{b,c}$	30.9	6.2
		Top	$8.1 \pm 8.0^{a,b,c}$	33.4	16.7
	1.5	Bottom	$8.0 \pm 12.9^{a,b,c}$	45.7	21.6
		Top	$9.0 \pm 10.7^{a,b,c}$	48.2	38.2
	2.5	Bottom	$7.2 \pm 4.3^{b,c}$	37.9	29.8
		Top	$9.1 \pm 12.4^{a,b,c}$	52.0	39.7
	3.5	Bottom	$6.1 \pm 5.6^{b,c}$	21.4	31.2
		Top	$12.4 \pm 6.6^{a,b,c}$	42.5	19.2
80	0.5	Bottom	$4.9 \pm 3.0^{b,c}$	25.7	10.0
		Top	$8.8 \pm 4.7^{a,b,c}$	28.8	8.8
	1.5	Bottom	4.4 ± 3.8^{c}	18.4	17.4
		Top	$8.6 \pm 8.4^{a,b,c}$	39.9	15.7
	2.5	Bottom	$9.2 \pm 7.5^{a,b,c}$	32.2	36.2
		Top	$17.6 \pm 7.8^{a,b}$	52.6	38.8
	3.5	Bottom	$12.8 \pm 12.6^{a,b,c}$	55.4	26.1
		Top	20.9 ± 6.6^{a}	51.7	42.5

4.2.2. Thermal Properties

Thermal properties from TGA and DSC are presented in Table 10. The thermal stability of treated and untreated samples was studied by TGA. As expected for pure PLA, the thermal degradation of all the samples followed a one-stage weight loss. The initial degradation temperature (T_5) of the control PLA sample was 295 °C, with a maximum degradation

temperature of 316 °C. An increase in thermal stability was observed after DBD plasma treatment for all samples. The increase in T_5 was more evident at the top position at 70 kV treatments and for both positions at 80 kV treatments. A significant increase in T_{max} was also observed for all treatment voltages, times and positions (Figure 12). Although air plasma is likely to generate etching on the surface, the increase in thermal stability for all the samples after plasma treatment suggests that stable cross-linking at the surface level may be formed due to the oxygen enrichment of the PLA chain, which may retard thermal degradation.

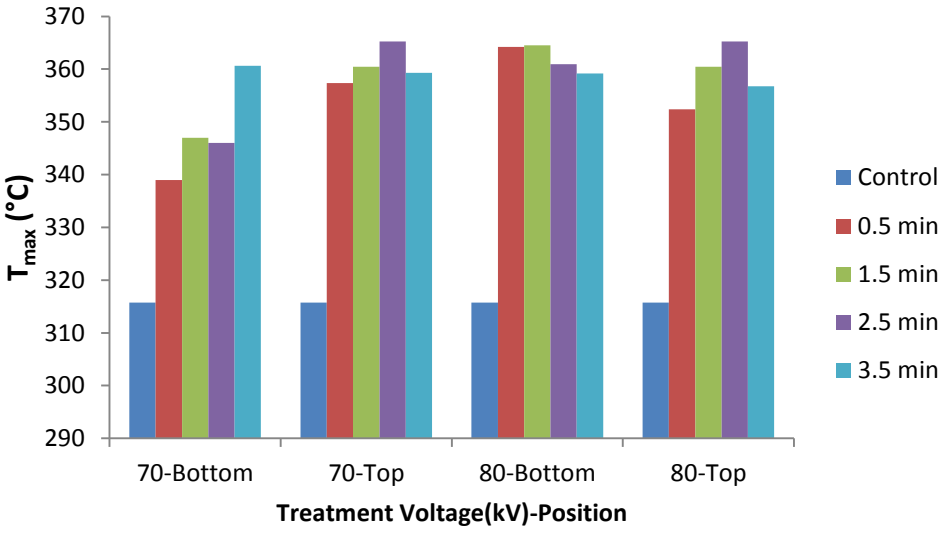

Figure 12. Effect of treatment voltage (kV), time (min) and position on maximum degradation temperature (T_{max}).

PLA thermogram (first heating cycle) consists of glass transition and melting endotherm events. The glass transition temperature (T_g) of the untreated samples was found to be 62.1 °C and for the treated samples no significant change in T_g was observed ($p<0.05$). The melting endotherm was observed at between 143 and 180 °C with a peak melting temperature between 164.4 and 165.9 °C for all the studied films. The melting enthalpy (ΔH_m) of all films

after DBD plasma treatment was found to be in the range of 29 and 32.5 $J.g^{-1}$ compared to the melting enthalpy of 29.7 $J.g^{-1}$ for the untreated film. In the second heating cycle a cold crystallization exotherm was also observed. Cold crystallization exotherm peaks were observed in all cases between 108 °C and 144 °C. Also it was found that $\Delta H_c + \Delta H_m \approx 0$ during the second heating step, which suggests the complete removal of thermal history from the PLA film by the first DSC heating-cooling cycle (Cao et al., 2003). From these DSC results, it can be concluded that DBD plasma did not have strong effects on the main structure of PLA, since glass transitions were maintained at approximately the same temperature relative to the control sample. It may be noted that T_g is an important parameter dictating the success in industrial processing of this polymer.

Table 10. TGA and DSC parameters for PLA samples

Voltage (kV)	**Time (min)**	**Position**	**T_5 (°C)**	**T_{max} (°C)**	**T_g (°C)**	**T_m (°C)**	**ΔH_m (J/g)**
	Control		295	316	62.1	165.4	29.7
70	0.5	Bottom	295	339	61.7	165.2	30.7
		Top	333	357	62.1	165.3	29.0
	1.5	Bottom	283	347	62.2	165.3	30.0
		Top	334	361	61.7	165.3	32.5
	2.5	Bottom	315	346	59.9	164.4	29.8
		Top	339	365	59.3	165.2	29.9
	3.5	Bottom	332	361	61.1	165.4	29.2
		Top	326	359	59.6	165.1	31.7
80	0.5	Bottom	337	364	61.2	165.9	31.5
		Top	323	352	61.5	164.9	29.8
	1.5	Bottom	337	365	61.8	165.3	31.1
		Top	302	361	61.1	165.3	30.6

2.5	Bottom	337	361	61.7	165.2	31.5
	Top	317	365	61.8	165.5	31.4
3.5	Bottom	330	359	61.3	165.1	30.6
	Top	314	357	61.8	165.9	31.2

4.2.3. Chemical characterisation

Wide-angle X-ray scattering tests were carried out for all samples. A clear peak was detected at 16.6° for all the studied films, which corresponds to the α-crystallographic form of the crystalline phase of PLA, described as a pseudo-orthorhombic unit cell (Kulinski and Piorkowska, 2005, Burgos et al., 2013). There was no significant change in this peak after plasma treatment under all treatment conditions, suggesting that DBD atmospheric plasma did not cause any change in the crystallization behaviour of PLA films.

Figure 13 shows the FTIR spectra of untreated and DBD plasma treated samples. An increase in the intensity of bands at 700 and 756 cm^{-1} was observed after DBD plasma treatment. These bands were assigned to -C-C- stretching. The intensity of the band at 2993 cm^{-1}, which was assigned to the –C-H stretching, also increased. The band intensity at 3501 cm^{-1} was found to increase for the top position samples when compared to the bottom position samples and was assigned to –O-H stretching (free) (Chaiwong et al., 2010). These results can be correlated with the surface oxygen enrichment after DBD plasma treatment which was also observed by Liu et al. (2004) and also to the increase in thermal stability found for all the treated samples by TGA.

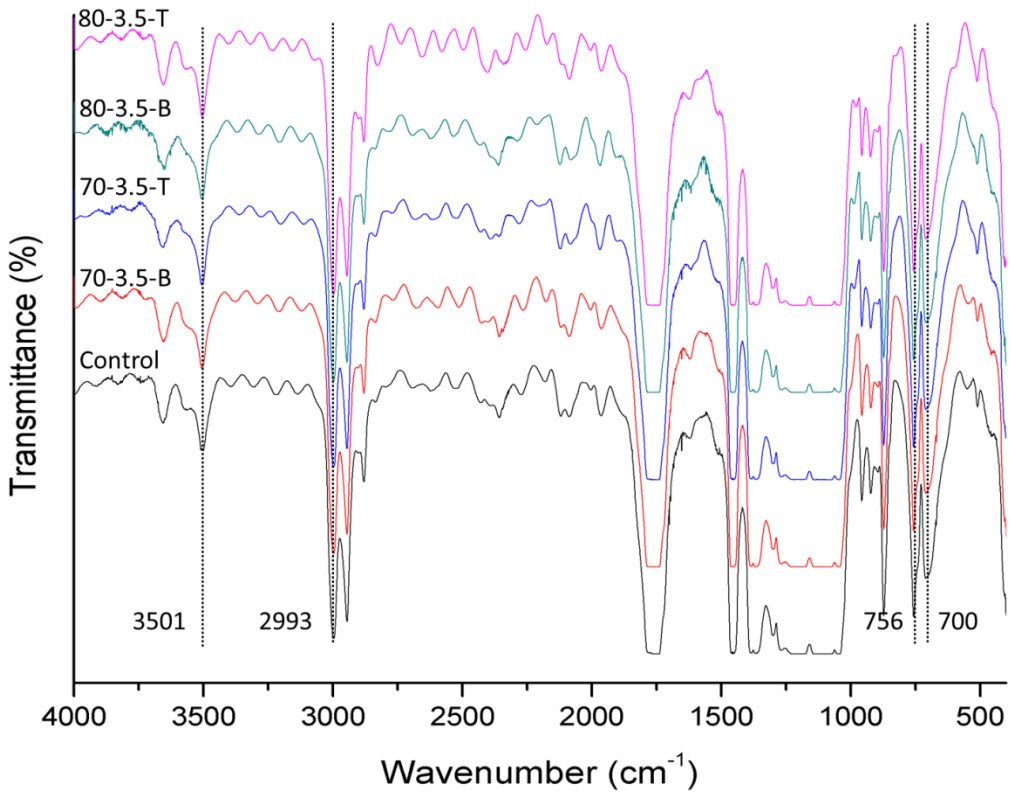

Figure 13. FTIR spectra of treated and untreated PLA films. [AA-BB-T/B=Treatment voltage (kV)-Treatment time (min)-T:top/B:bottom]

4.2.4. Contact angle and surface free energy

Film hydrophilicity was analysed by the contact angle method. The contact angle was analysed using three test liquids for both control and plasma treated PLA films (Table 11A). Control PLA film displayed a high contact angle for water of 75.1° which was significantly ($p<0.05$) reduced after DBD plasma treatment to 54.8°. This decrease in the water contact angle clearly demonstrates the increase in hydrophilicity of PLA films after plasma treatment (Figure 14). The surface free energy for the plasma treated films was also calculated from the contact angle using the Fowkes or Owen-Wendt approach or OWRK equation (Table 11B). Surface free energy analysis of control and plasma treated PLA films shows a significant

increase in the total SFE. The dispersive component was found to be in the same range but there was a significant increase in the polar component of the SFE. It may be due to the formation of polar groups on the polymer film surface upon reaction with plasma generated reactive species, increasing the polar component and finally the total SFE of the film.

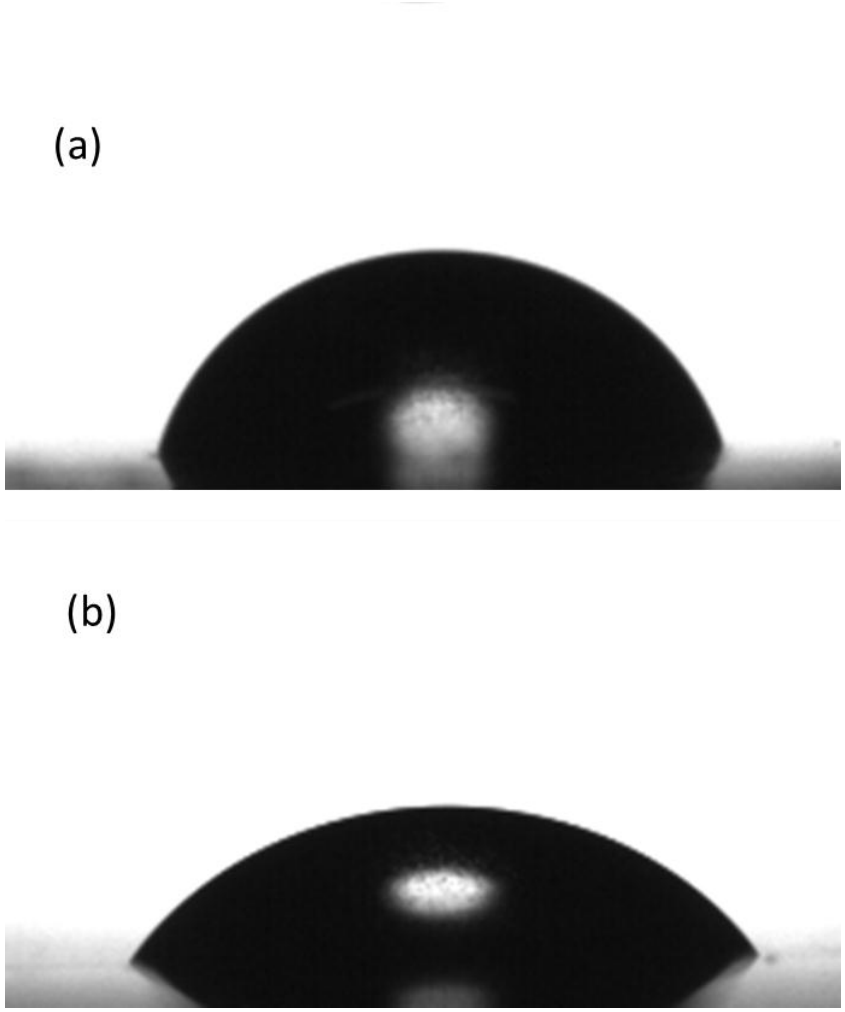

Figure 14. Water contact angle of PLA films (a) control and (b) plasma treated

Table 11. Contact angle (A) and surface free energy (B) analysis of plasma treated PLA films

A. Contact angle	**Parameters**	**Control**	**Plasma treated**
Water	θ_w	75.05±0.49	54.75±0.11
Ethylene glycol	θ_e	42.04±0.29	33.58±0.24
Di-iodomethane	θ_d	45.30±0.14	35.91±0.15
B. Surface free energy			
Fowkes	γ^{tot}	41.95	51.17
	γ^{d}	36.24	34.49
	γ^{p}	5.71	12.68

4.2.5. Barrier properties

Oxygen permeability is one of the most important properties of a packaging material governing its suitability for application in different food products. The most common food quality losses in packaged food are due to oxygen (Brown, 1992). Therefore, a high oxygen-barrier packaging material is critical for maintaining the initial high quality of the packaged product (Hong and Krochta, 2006). OTR**e* values (cm^3 mm m^{-2} day^{-1}) in the steady state were measured for untreated samples and after DBD plasma treatment for both the top and bottom-positioned films. The average OTR**e* value for the untreated sample was 23.37±0.66 cm^3 mm m^{-2} day^{-1} and no significant differences ($p>0.05$) were observed after the plasma treatment for all treatment voltages, times and positions. These results are particularly important for PLA to fit in as a competitive commercial food packaging material. For

commercial adoption it is necessary to ensure that the in-package food processing method does not adversely affect the oxygen permeability of the package.

Water vapor transmission rate for the control and treated films are shown in Figure 15. No significant differences were observed after plasma treatments at 70 kV for all the treatment times and both positions. At 80 kV, an increase in WVTR was observed for the film placed at the top position for all treatment times. It is worth recalling at this stage that permeation of water vapor is governed by vapor pressures and concentration gradients on the two surfaces of the polymer, while gas permeability of polymers, in general, is the combined effect of diffusion and solubility via voids of gaps present in between the segments of a polymer chain (Chaiwong et al., 2010). Results from this study indicated that although no significant change in the oxygen permeability was observed after plasma treatment, water vapor permeability slightly increased at higher voltage levels with treatment times, most significantly for the film in contact with the high voltage electrode.

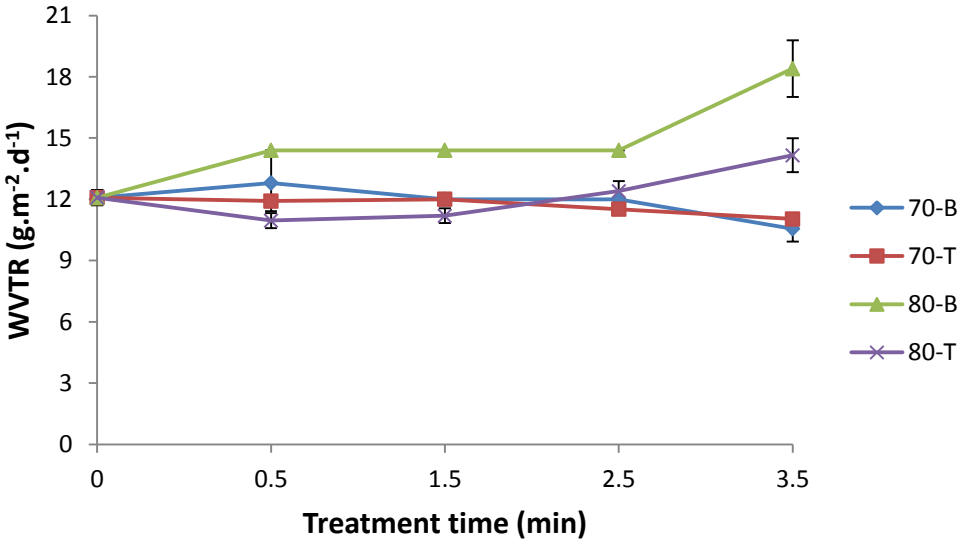

Figure 15. WVTR of treated and untreated PLA films. [AA-T/B=Treatment voltage (kV)-T:top/B:bottom]

4.2.6. Overall Migration

Overall migration tests were undertaken to determine the total amount of non-volatile substances that might migrate into foodstuffs from PLA films, following in-package plasma treatment. Overall migration results for the control and plasma treated samples (80 kV for 3.5 minute treatment) are shown in Figure 16. These samples were selected with consideration of their treatment at the maximum applied voltage and time. These results are based on mean values of triplicates. It is clear from the results that the DBD plasma treatment significantly increased the migration of non-volatile substances in acidic and high alcohol food simulants. Lactic acid being the lone monomer of PLA, migrated agents are mainly lactic acid monomers, dimers, and oligomers (Jamshidian et al., 2010). Therefore, it could be concluded that some PLA chains were broken after DBD plasma treatment resulting in the formation of low molar mass species prone to migrate through the polymer matrix under the test conditions. In addition, according to the studies conducted by Conn et al. (1995), very limited migration should be expected from PLA into foods and that small amount of migrant will be subsequently hydrolysed in the aqueous and acidic media commonly found in foods and in the stomach. It should be also highlighted that values obtained for the overall migration, even at the highest treatment conditions, are well below of the 10 mg dm^{-2} limit indicated in the current European Legislation (Commission Regulation N10/2011).

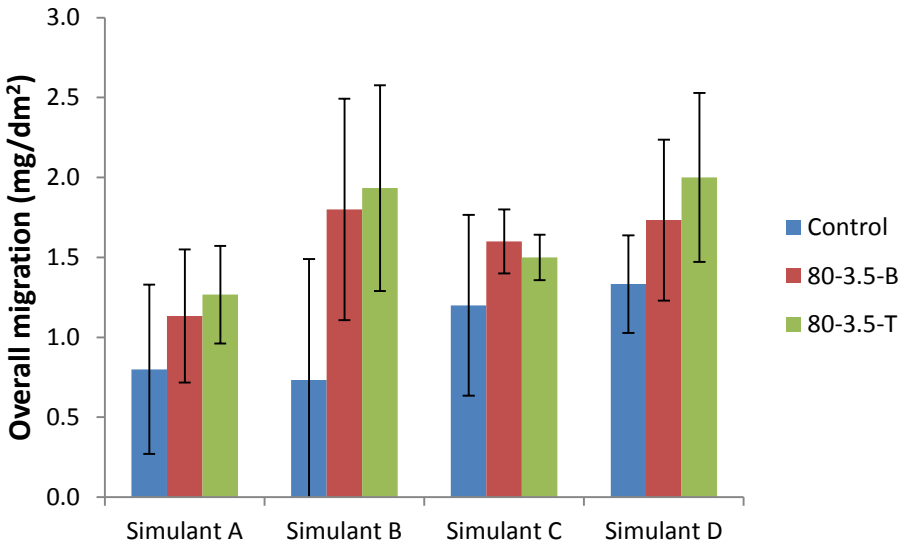

Figure 16. Overall migration (mg/dm^2) of control and treated PLA films. [AA-BB-T/B=Treatment voltage (kV)-Treatment time (min)-T:top/B:bottom]

4.3. Conclusion

Pure PLA commercial films were used in this study for testing its suitability as food packaging material for in-package NTP decontamination of foods. DBD plasma treatment increased the roughness of PLA film mainly at the site in contact with the high voltage electrode, but it did not adversely affect the glass transition temperature or oxygen and water vapor permeability. The increase in water vapor permeability at 80 kV level was also found to be within acceptable limits for food products. DBD plasma treatment resulted in significant improvement in the thermal stability of the treated polymer by increasing the initial and the maximum degradation temperatures. Lastly, the overall migration was found to be well below the regulatory limits. The combination of biodegradable food packaging materials and a novel energy efficient in-package plasma method for food decontamination offers a promising alternative to classical methods, whereby it permits an effective decontamination of the packaged food and avoids any post-process recontamination or hazards from the package itself.

Chapter 5 Corn zein film

5.1. Introduction

Zein was first described by John Gorham in 1821 after isolating the protein from corn and in 1909 the first patent was granted for preparing plastic from zein (Lawton, 2002, Goldsmith, 1909). Zein is a water-insoluble prolamin present in corn endosperm cells with a high content of hydrophobic amino acids (leucine, proline and alanine) (Shukla and Cheryan, 2001). Zein can be cast into films by dissolving it in a hydrated organic solvent, such as ethanol or acetone, and then drying (Yoshino et al., 2000). However, films made of 100% zein are brittle, therefore plasticizers are added to improve flexibility (Soliman and Furuta, 2009). Zein films are distinctive as they are tough, glossy, hydrophobic, greaseproof, and resistant to microbial attack ensuring its suitability as coatings, fibers and packaging films for the food and pharmaceutical industries (Shi et al., 2009, Shukla and Cheryan, 2001). The effectiveness of using zein films as edible coating for maintaining post-harvest quality has been demonstrated for produce including; apple, broccoli and tomato (Rakotonirainy et al., 2001, Bai et al., 2003, Zapata et al., 2008).

5.2. Results and discussions

5.2.1. Surface topography

DBD plasma is known for increasing the surface roughness of polymers due to the etching effect. Etching by DBD plasma can be due to chemical (breaking of bonds, chain scission, chemical degradation) or physical processes (physically removal of low molecular fragments) (Akishev et al., 2008, Mirabedini et al., 2007). The AFM topography of the zein surface is shown in Figure 17 and the roughness parameters are shown in Table 12. It is

evident that DBD plasma treatment increased the surface roughness of the zein film. There is a linear relationship between increases in surface roughness with applied voltage level.

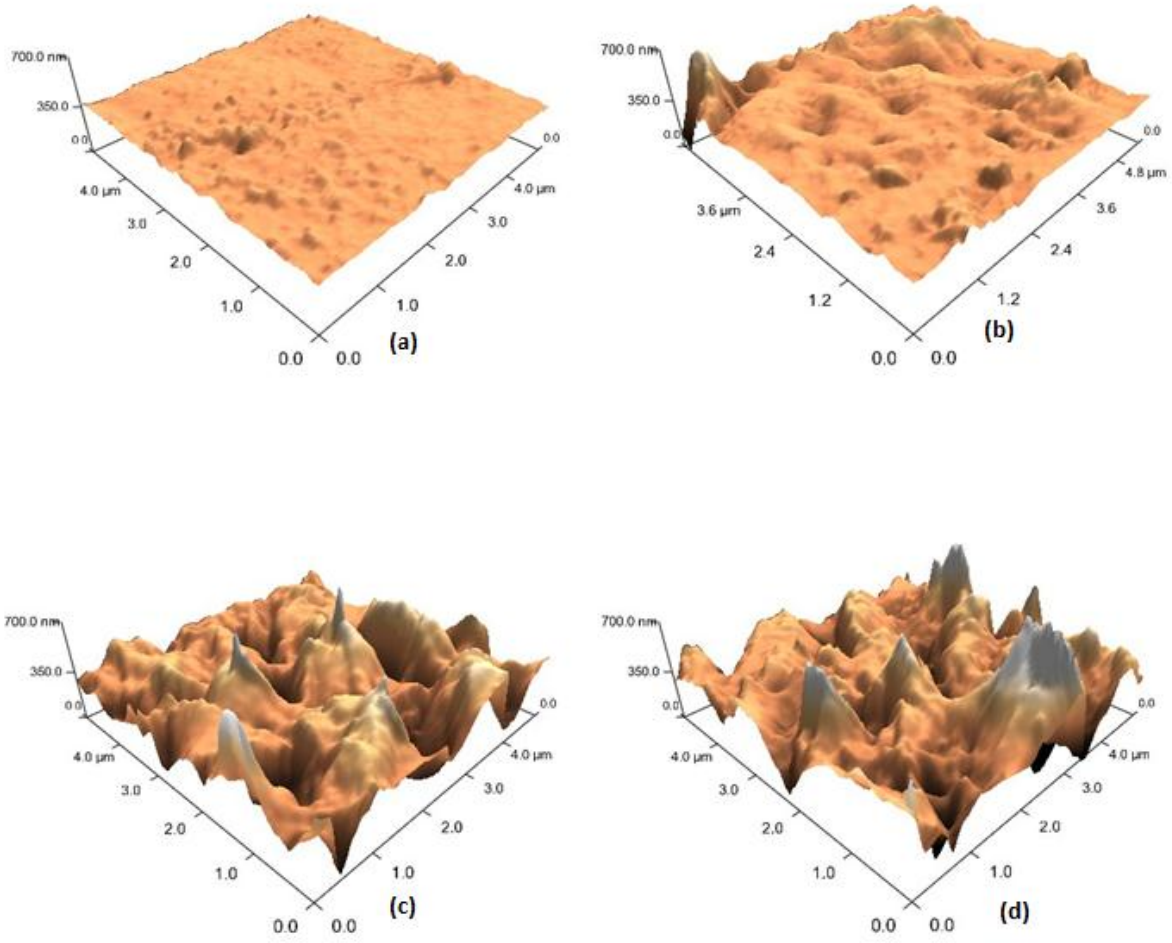

Figure 17. AFM images of the surface of untreated and plasma-treated cast zein films (a) Untreated, (b) 60 kV-5min, (c) 70 kV-5, (d) 80 kV-5.

Table 12. Roughness parameters for control and DBD plasma treated cast zein films (R_{rms}: root mean square roughness (mean value), R_{Peak}: Highest peak, R_{Groove}: lowest groove).

Voltage (kV)	Time (min)	R_{rms} (nm)	R_{Peak} (nm)	R_{Groove} (nm)
Control		16.41	125.99	67.00
60	5	52.04	295.15	337.62
70	5	126.16	496.31	506.47
80	5	132.87	641.02	651.89

5.2.2. Water Sorption Kinetics

Generally, protein films have poor moisture barrier properties due to their hydrophilic nature. Use of glycerol as a plasticizer further increases the moisture sorption capacity due to its hydrophilic nature as shown by Lawton (2004) and Wei and Baianu (1999). Water diffusion into hydrophilic polymers is associated with relaxation of the polymer chain and an increase in the volume. There are many empirical and fundamental models proposed in the literature for the absorption of water in hydrophilic films. In this study the Peleg equation was chosen for the empirical description of the sorption process. This equation relates the moisture content at a given time (M_t) with the initial moisture content (M_0) as given in equation 3.

$$M_t = M_0 + \frac{t}{K_1 + K_2.t} \quad (3)$$

where t is time (min) and K_1 and K_2 are fitting parameters. K_1 is Peleg's rate factor (min/%wt.) and is associated with the initial absorption rate, K_2 is Peleg's capacity parameter (% $wt.^{-1}$) and is related to the final absorption capacity.

As a fundamental model describing the water absorption on films, Fick's second law intended for a plane sheet with constant boundary conditions and uniform initial concentration was used as reported in equation 4.

$$M(t) = M_{eq}\left[1 - \frac{8}{\pi^2}\sum_{n=0}^{\infty}\frac{1}{(2n+1)^2}.\exp\left\{\frac{-D.(2n+1)^2.\pi^2.t}{h^2}\right\}\right] \quad (4)$$

where M(t) is the moisture content (%) at time t (s), M_{eq} is the moisture at equilibrium conditions (%), D is the diffusion coefficient ($cm^2\ s^{-1}$) through the swollen polymeric matrix and h is the film thickness (cm).

Experimental moisture sorption data were fitted with the Peleg equation and Fick's diffusion model and the fitting parameters are reported in Table 13. An increase in the equilibrium moisture content was observed after the DBD plasma treatment. This increase was found to be directly correlated with the treatment voltage. For the control film the equillibrium moisture content was 10.2 % while after plasma treatment at 80 kV for 5 minutes, it increased to 18.7 %. In the present study the Peleg equation was found to describe the process better than the Fickian model as evident from the root mean square error (RMSE) values (Figure 18). This can be explained by the fact that, Fick's model describes mass transport related to Brownian motions in which the penetrant flow is exclusively driven by a concentration gradient while water sorption in moderately hydrophilic polymers is a

complex phenomenon due to the presence of specific interactions between water molecules and the hydrophilic sites on the polymer backbone (Pereda et al., 2009).

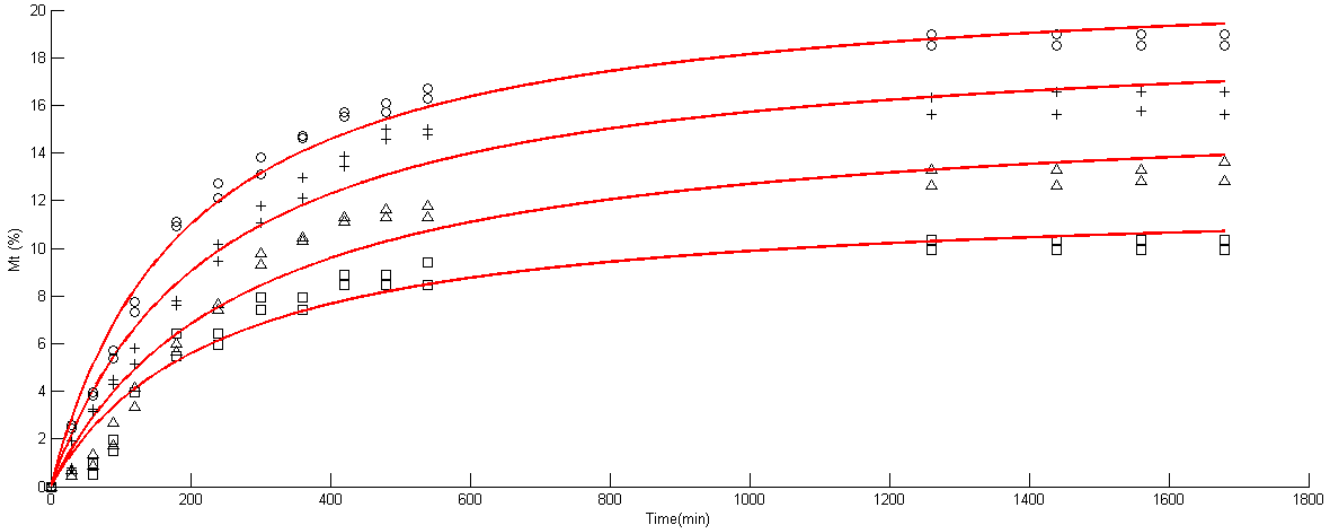

Figure 18. Moisture sorption of zein films after DBD plasma treatment at 23°C and 75% RH (solid lines represent the fitting from the Peleg equation, Control(□), 60kV-5min(Δ), 70kV-5min(+), 80kV-5min(○).

Table 13. Fitting Parameters of the Peleg Equation and Fickian model for DBD plasma treated zein films.

Treatments	**Peleg Equation**			**Fickian Model**		
	K_1(min/%wt.)	K_2(% wt.$^{-1}$)	RMSE	M_{eq} (%)	D (cm^2/s)	RMSE
Control	19.51	0.082	0.84	10.43	6.85 X 10^{-9}	1.246
60kV/5min	17.06	0.062	1.11	13.95	5.81 X 10^{-9}	1.709
70kV/5min	11.86	0.052	0.99	16.93	6.63 X 10^{-9}	1.602
80kV/5min	8.994	0.046	0.72	19.18	7.64 X 10^{-9}	1.472

5.2.3. Thermal Properties

The initial degradation temperature of zein film was not significantly ($p>0.05$) different after DBD plasma treatment. The T_5 for untreated control zein film was 148.1 °C while after plasma treatment it was in the range of 146.3 °C to 150.6 °C. The initial step of mass loss for the control film was found in the region of 78 °C while after plasma treatment it was in the region of 82 to 93 °C which also suggests an increase in water retention capacity of the zein film after plasma treatment.

In the DSC thermogram, no significant change was observed in T_g after plasma treatment and the values are in good agreement with other studies using glycerol as a plasticizer (Lawton, 2004, Lai et al., 1999). This implies that glycerol was effectively incorporated, by penetrating the protein network, forming hydrogen bonds with the protein molecules and thus increasing the separation between the protein chains. However, cold plasma treatment clearly changed the pattern of the thermograms of the plasticized zein films, since an endothermic event between 50 and 55 °C appears in all the treated samples, but it is not distinguishable in the control sample. This phenomenon was evident in the samples subjected to 5 min of treatment (Figure 19). It is also noted that as voltage increases, enthalpies associated with this event are higher and peak shapes also differ, with three small peaks for samples treated at 60 kV and one well-defined peak for samples treated at 80 kV observed. Given the fact that this event appears just before the glass transition in all the samples, it could be attributed to a breakdown of cross-linkages leading to a reorganisation of the protein conformational structure as the molecules obtain sufficient freedom of motion.

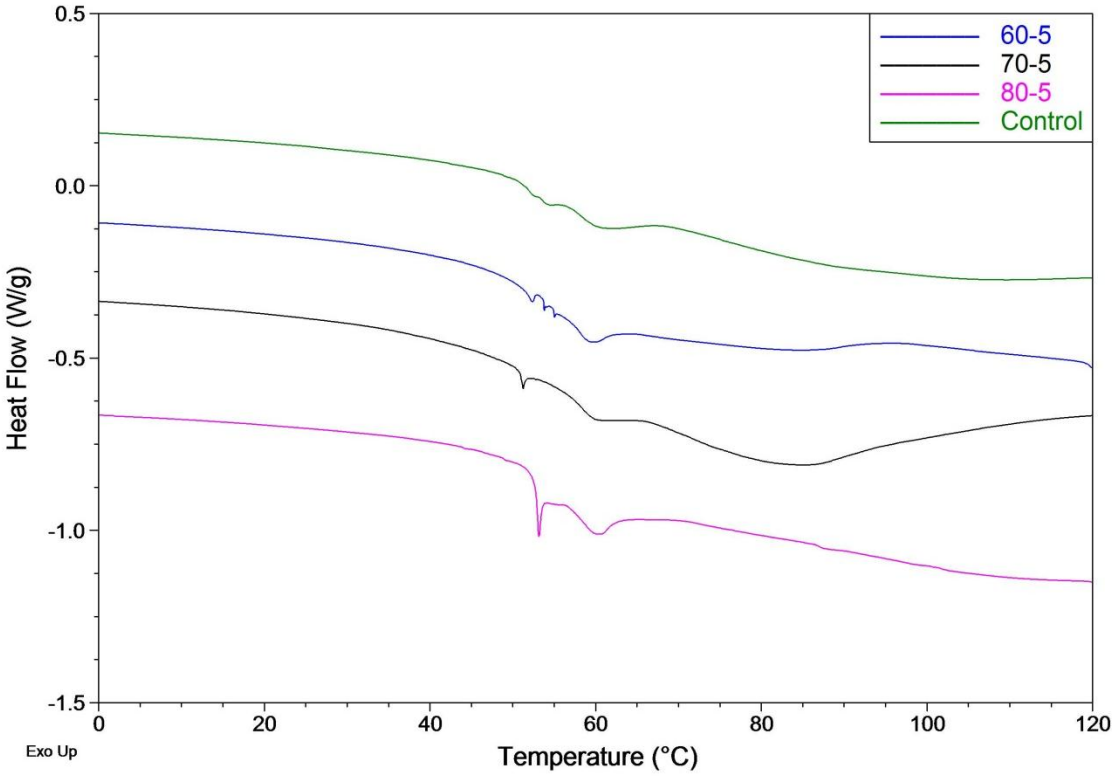

Figure 19. DSC thermogram of DBD plasma treated zein films. A-B: Voltage (kV)-Treatment time (min).

5.2.4. Chemical characterisation

The WAXS pattern of zein films is shown in Figure 20. Two broad peaks appear in all the diffractograms at 2θ = 8.7° and 2θ = 19.3°. By applying Bragg's law, distances of 10.1 Å and 4.6 Å respectively were calculated. The smaller distance (4.6 Å) corresponds to the average backbone distance within the α-helix. The larger distance (10.1 Å) is related to the lateral α-helix packing or the mean distance among neighboring helices (Lai et al., 1999, Wang et al., 2005, Wang et al., 2003). As evident from Figure 17a and 17b, after ACP treatment of zein films at 60 kV and 70 kV there is a decrease in the intensity of the first peak. Since the

10.1Å is related to the inter-helix packing, the decline of intensity implies the disruption of zein molecular aggregates, which was also observed by Wang et al. (2005) with the application of higher mechanical energy during film processing. At 80 kV, the reduction of the first peak's intensity was only observed after 1 minute of treatment. The second spacing corresponding to 4.6 Å (peak at 2θ = 19.3°) was clearly less affected in all the plasma treated samples, suggesting that the helical configuration of zein was not disturbed by plasma treatment.

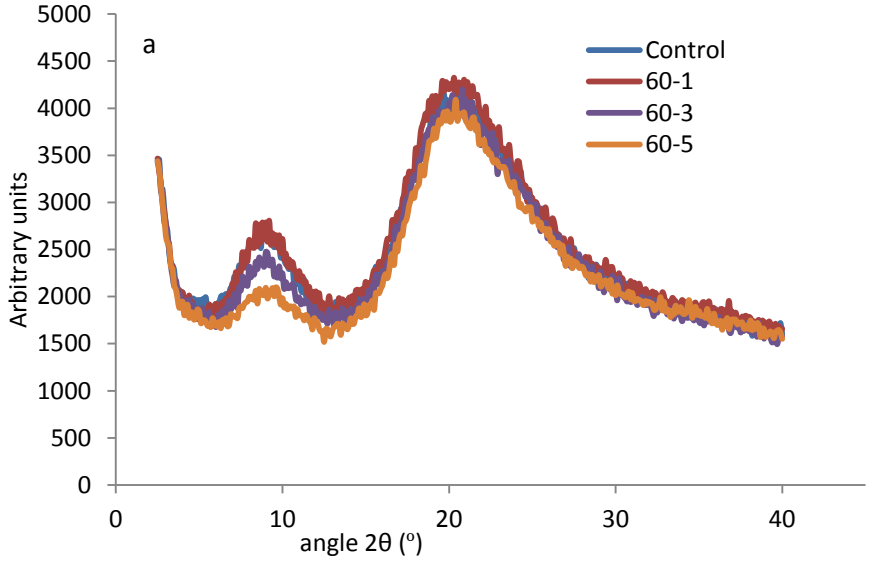

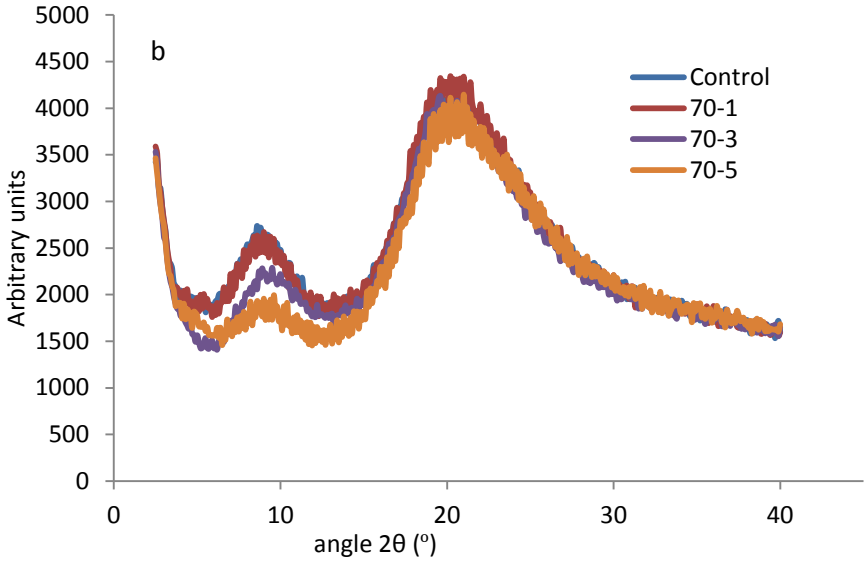

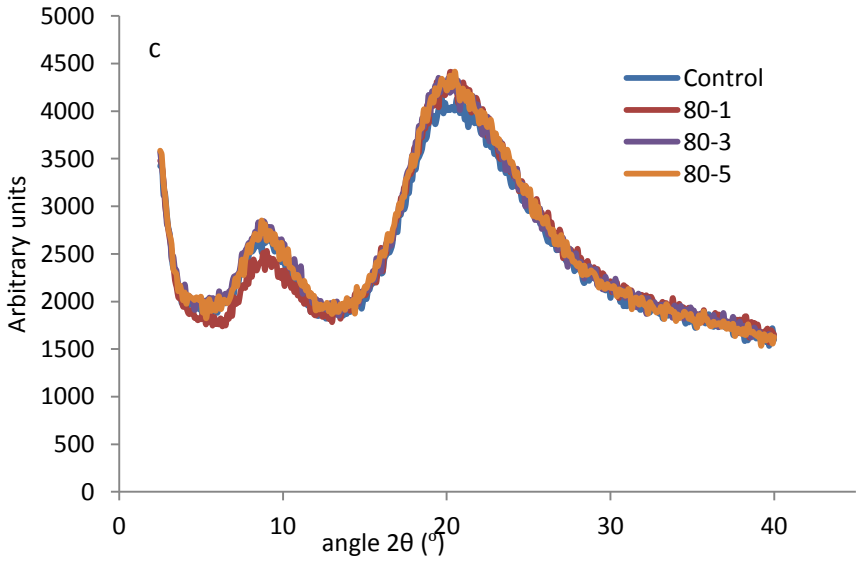

Figure 20. X-ray diffractogram of zein film after DBD plasma treatment at (a) 60kV (b) 70kV and (c) 80kV.

In the amide I region, the band around 1650 cm^{-1} can be assigned to α-helical and disordered conformation (stretching vibrations of the C=O bond of the amide) and the band at 1685 cm^{-1} is due to β-sheets (Singh et al., 2009). A broad peak was observed around 1650 cm^{-1}, which is consistent with α helical structure (Figure 21). The increase of intensity observed at this

band after DBD plasma treatment suggests that the ACP treatment increased the amount of α-helical and disordered conformations. The result is in agreement with the DSC thermograms and XRD diffractogram which also suggested a change in the protein conformation after plasma treatment. An increase in the intensity of the amide II band at 1540 cm^{-1} (bending vibrations of the N-H bond) after DBD plasma treatment was also observed. This change may be due to two main factors (i) more extensive hydrogen bonding between the protein, reducing the number of non-bonded peptide groups and (ii) a shift from a β-sheet structure, which absorbs around 1525 cm^{-1}, to a α-helical structure, which has its amide II maximum at 1545 cm^{-1} (Gao et al., 2006). Bands were also observed at the 2800-3000 cm^{-1} range, 1447 cm^{-1} and 720 cm^{-1} which are attributed to the vibrations of attached hydrocarbon chains (Shi et al., 2010).

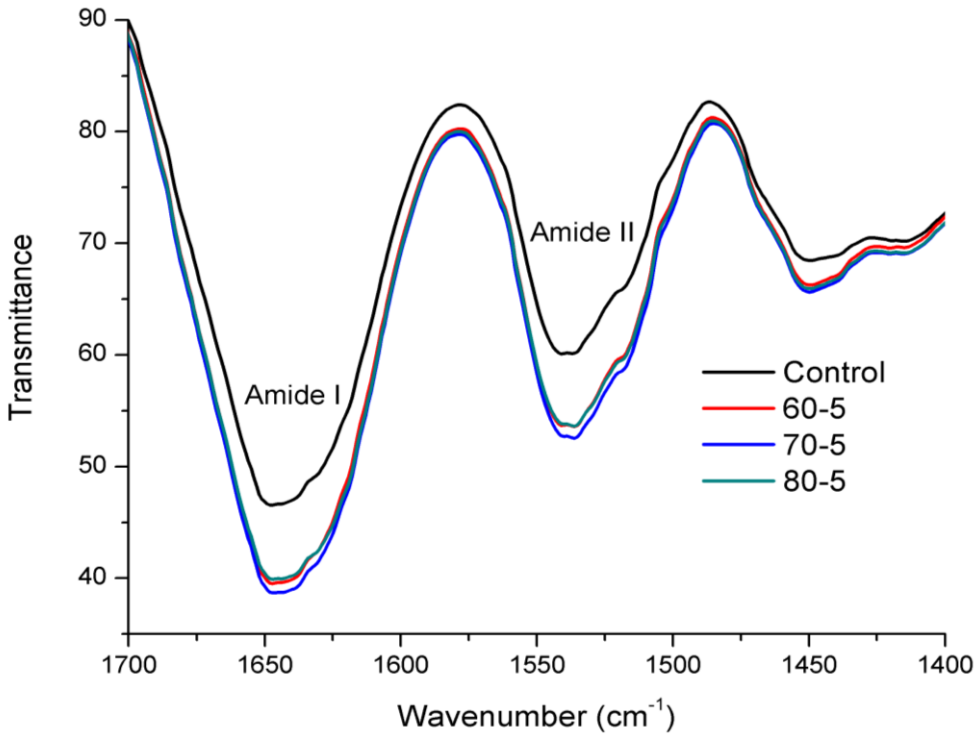

Figure 21. FTIR spectra of DBD plasma treated and control zein films in amide I and amide II region. A-B: Voltage (kV)-Treatment time (min).

5.2.5. Contact angle and surface free energy

Film hydrophilicity is an important property for any polymer and it was analysed by the contact angle method (Table 14). Control zein film displayed quite a high contact angle for water of 80.1° showing its hydrophobic nature which was significantly ($p<0.05$) reduced after DBD plasma treatment to 53.6°. This decrease in the water contact angle clearly demonstrates the increase in hydrophilicity of zein films after plasma treatment. The surface free energy for the plasma treated films was also calculated from the contact angle using Owen-Wendt approach. Surface free energy analysis of control and plasma treated zein films shows a significant increase in the total SFE. The dispersive component was not significantly different from the control films but a significant increase in the polar component of the SFE was observed for plasma treated film. It may be due to the formation of polar groups on the polymer film surfaces upon reaction with the plasma generated reactive species, increasing the polar component and finally the total SFE of the film.

Table 14. Contact angle (A) and surface free energy (B) analysis of plasma treated zein films

A. Contact angle	**Parameters**	**Control**	**80kV-5min**
Water	θ_w	80.19±1.23	53.62±1.54
Ethylene glycol	θ_e	41.57±0.97	39.44±0.85
Di-iodomethane	θ_d	46.96±1.34	41.15±0.45
B. Surface free energy			
Fowkes	γ^{tot}	40.54	49.40
	γ^{d}	36.25	35.49
	γ^{p}	4.29	13.91

5.3. Conclusion

DBD plasma treatment of zein film increases the surface roughness of the film. It also increases the equilibrium moisture content of the film. A significant increase in the thermal stability of zein was also observed for all the voltage levels and treatment times. ACP treatment led to a reorganisation of the protein conformational structure as evident from the DSC and XRD results. FTIR spectrum also confirms the changes in the amide I and amide II region after plasma treatment.

Chapter 6 Sodium Caseinate film

6.1. Introduction

Caseins are soluble in water despite their high content of non-polar amino acids (35 to 45% of total amino acid residues) (Chen, 2002). Commercially available caseinates are produced by precipitation of skim milk either by the addition of a dilute mineral acid or a microbial culture, after which the coagulated caseins are solubilized using an appropriate alkali (Chen, 1995, Fabra et al., 2010). Among caseinates, sodium and calcium caseinate are the most common, however magnesium and potassium caseinates are also commercially available (Fabra et al., 2010). Sodium caseinate is a mixture of casein monomers and small aggregates formed after removal of colloidal calcium phosphate from the casein micelles (Mendes de Souza et al., 2010). The primary mechanism for caseinate film formation is attributed to its random coil nature which allows it to form extensive inter-molecular hydrogen, electrostatic, and hydrophobic bonds, resulting in an increase of the inter-chain cohesion (Chen, 1995, Chen, 2002, Avena-Bustillos and Krochta, 1993). Caseinates have been extensively studied for various food products like fried cereal products (Albert and Mittal, 2002), cheese (Cao-Hoang et al., 2010), meat (Caprioli et al., 2009), Bing cherries (Certel et al., 2004) and other minimally processed fruits and vegetables (Baldwin et al., 1995).

6.2. Results and discussions

6.2.1. Surface topography

DBD plasma increases the roughness of the polymeric materials due to the etching effect caused by the bombardment of energetic particles such as electrons, ions, radicals, neutrals and excited atoms/molecules and UV–vis radiations on the surface of polymer films (Yang et

al., 2009b). The roughness parameters of control and plasma treated sodium caseinate films are given in Table 15. Surface roughness of plasma treated films at both 60 and 70 kV were found to be significantly ($p \leq 0.05$) higher than the control (Figure 22). Surface roughness (R_{rms}) was found to increase by up to 16.189 nm after treatment at 70 kV for 5 minutes.

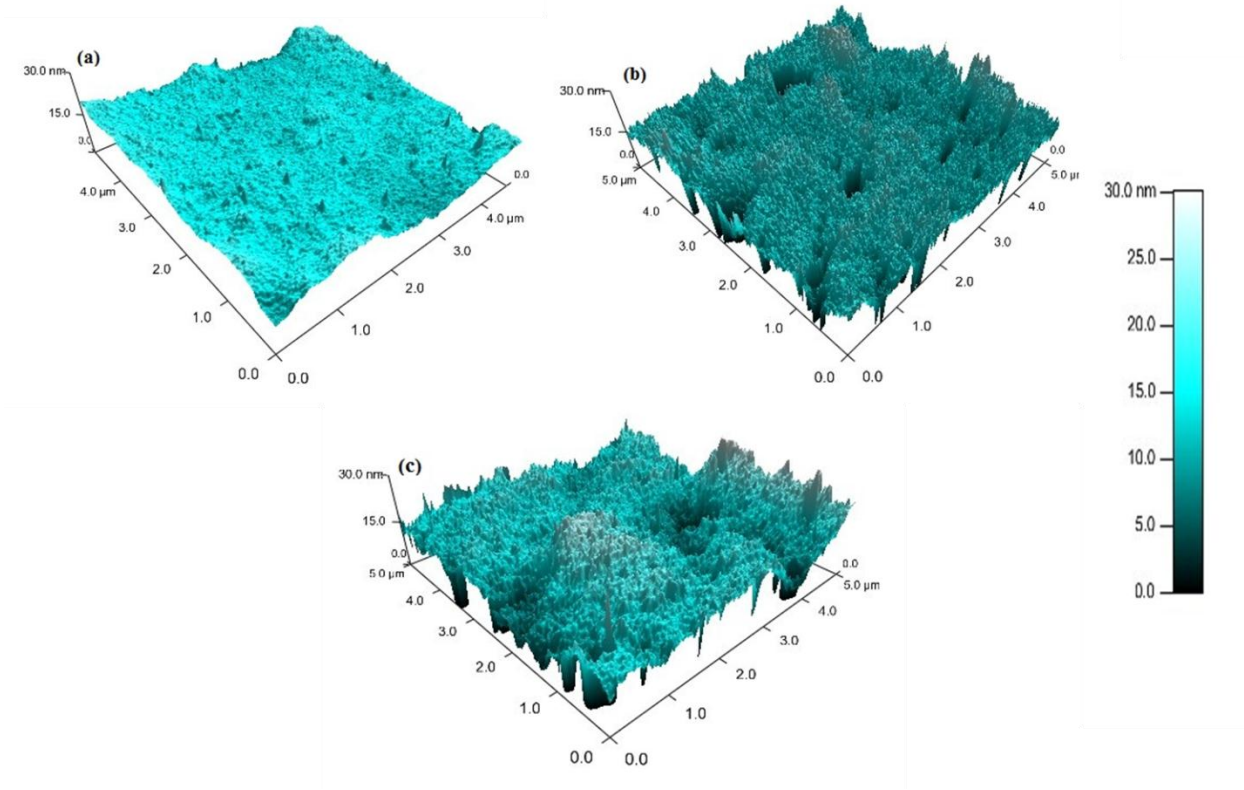

Figure 22. AFM images of the sodium caseinate film surface (a) Control (b) plasma-treated at 60kV for 5min (c) plasma-treated at 70kV for 5 min.

Table 15. Roughness parameters (mean value ±standard deviation) for control and DBD plasma treated samples (R_{rms}: root mean square roughness, R_{Peak}: Highest peak, R_{Groove}: lowest groove).

Voltage (kV)	**Time (min)**	**R_{rms} (nm)**	**R_{groove} (nm)**	**R_{peak} (nm)**
Control		1.70±1.2	7.29	10.44

60	**1**	2.24±1.3	12.98	11.39
60	**2**	6.92±2.9	10.38	18.64
60	**3**	13.84±4.4	24.22	25.63
60	**4**	12.64±4.7	29.54	16.48
60	**5**	9.24±7.6	14.68	20.06
70	**1**	12.69±8.2	19.87	18.38
70	**2**	8.97±3.3	11.99	16.16
70	**3**	12.69±4.8	10.88	22.24
70	**4**	12.13±8.5	23.34	24.45
70	**5**	16.19±4.4	15.08	15.39

6.2.2 Thermal Properties

The effect of DBD plasma treatment on the glass transition temperature of sodium caseinate film is shown in Figure 23. It is clear from the data that the T_g of all films after plasma treatment were found to be less than the control sodium caseinate film. The T_g of control sodium caseinate film was 61.1 °C which is in agreement with previously reported values (Kristo et al., 2008, Aliheidari et al., 2013). After plasma treatment the T_g varied between 46.8 to 50.9 °C. The decrease in the glass transition can be attributed to chemical etching by bond breakage, chain scission or chemical degradation of the plasma treated polymer which is also supported by the XRD results.

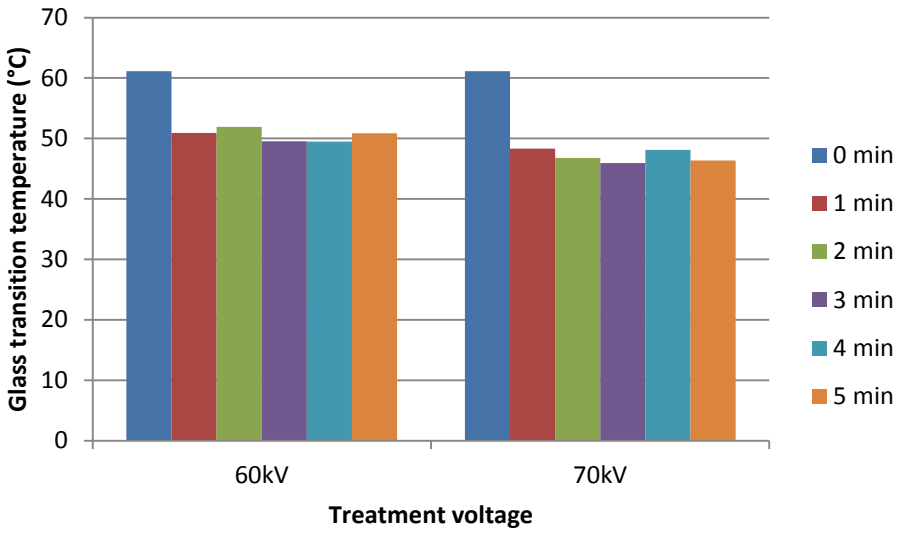

Figure 23. Glass transition temperature of control and plasma treated sodium caseinate films

6.2.3. Chemical characterisation

Surface chemical modifications induced by DBD plasma treatment were determined using XPS analysis. The elemental composition and ratio are summarized in Table 16, the control sodium caseinate film had an O/C ratio equal to 0.15, while after plasma treatment at 60 and 70kV for 5 minutes, the O/C ratio increased to 0.17 and 0.19 respectively. The increased O/C atomic ratio suggests the formation of new oxygen-containing groups on the film surface. This increase in the surface oxygen content may be the main reason for the increase in the hydrophilicity as discussed later. The wide scan spectra of the control and plasma treated sodium caseinate film is shown in Figure 24a which mainly contained C1s, O1s and N1s peaks. The C1s high resolution spectra of sodium caseinate films are shown in Figure 24b-d. The spectral peaks are at 284.9, 286.4, 288.1 and 289.0 eV, which may be assigned to C–C/C–H, C–O, C=O and O=C–O respectively (Wagner and Muilenberg, 1979). Data from the C1s peak deconvolution (Table 17) clearly show an increase in the C-O and O=C-O bonds

after DBD plasma treatment. Similar increases in the surface oxygen had also been reported for polypropylene (Leroux et al., 2008, Sorrentino et al., 2007) and polyethylene terephthalate films (Cui et al., 2007) after atmospheric air DBD plasma treatments.

Table 16. The elemental composition and ratio of the plasma modified sodium caseinate film surfaces

Sample	C1s(at%)	O1s(at%)	N1s(at%)	O/C
Control	82.91	12.53	4.54	0.15
60kV-5min	81.57	13.58	4.84	0.17
70kV-5min	81.3	15.14	3.55	0.19

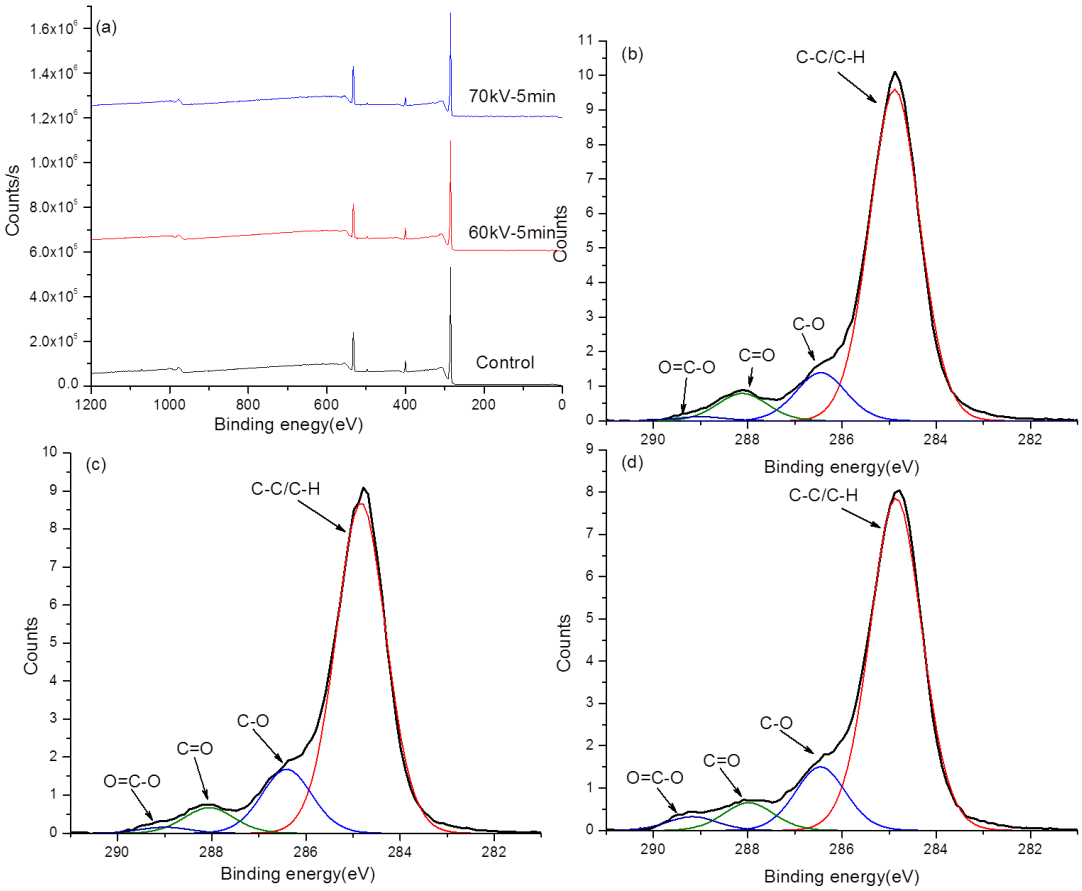

Figure 24. Wide scan XPS spectra and C1s peak of sodium caseinate films. (a) Wide scan XPS spectra (b) C1s spectra of control sodium caseinate film, (c) C1s spectra of plasma treated film at 60kV for 5 minutes, (d) C1s spectra of plasma treated film at 70kV for 5 minutes.

Table 17. High-resolution XPS of C1s peak deconvolution and possible groups.

Sample	**Contribution of C1s components (%)**			
	C-C/C-H	**C-O**	**C=O**	**O=C-O**
Control	80.65	11.71	6.65	0.99
60kV-5min	77.51	15.04	6.02	1.43
70kV-5min	76.61	14.20	6.14	3.06

Figure 25 shows the X-ray diffraction spectra of control and plasma treated sodium caseinate films. Two broad peaks were observed in all the diffractograms at $2\theta = 9.8°$ and $2\theta = 19.9°$. By applying Bragg's law, distances of 9.01 Å and 4.46 Å respectively were calculated. A decrease in the diffractogram peak at $2\theta = 9.8°$ (d=9.01 Å) after DBD plasma treatment was observed suggesting a disruption in the inter-helical structure (Lai et al., 1999, Lacroix et al., 2002). No significant change in the diffraction peak at $2\theta = 19.9°$ (d=4.46 Å) suggests that DBD plasma treatment did not induce any change in the helical configuration of the protein molecules. Peptide linkages were analysed using FTIR at all the main nine group frequencies in protein molecules: amide A (~3300 cm^{-1}), amide B (~3100 cm^{-1}), amide I (~1650 cm^{-1}), amide II (~1550 cm^{-1}), amide III (~1300 cm^{-1}), amide IV (~735 cm^{-1}), amide V (~635 cm^{-1}), amide VI (~600 cm^{-1}) and amide VII (~200 cm^{-1}) (Dong et al., 1995). No significant change in the peptide linkages were observed from the FTIR spectrum suggesting that DBD plasma treatment modified the film surface due to surface oxygenation without disrupting the prinicipal helical structure of the protein molecules.

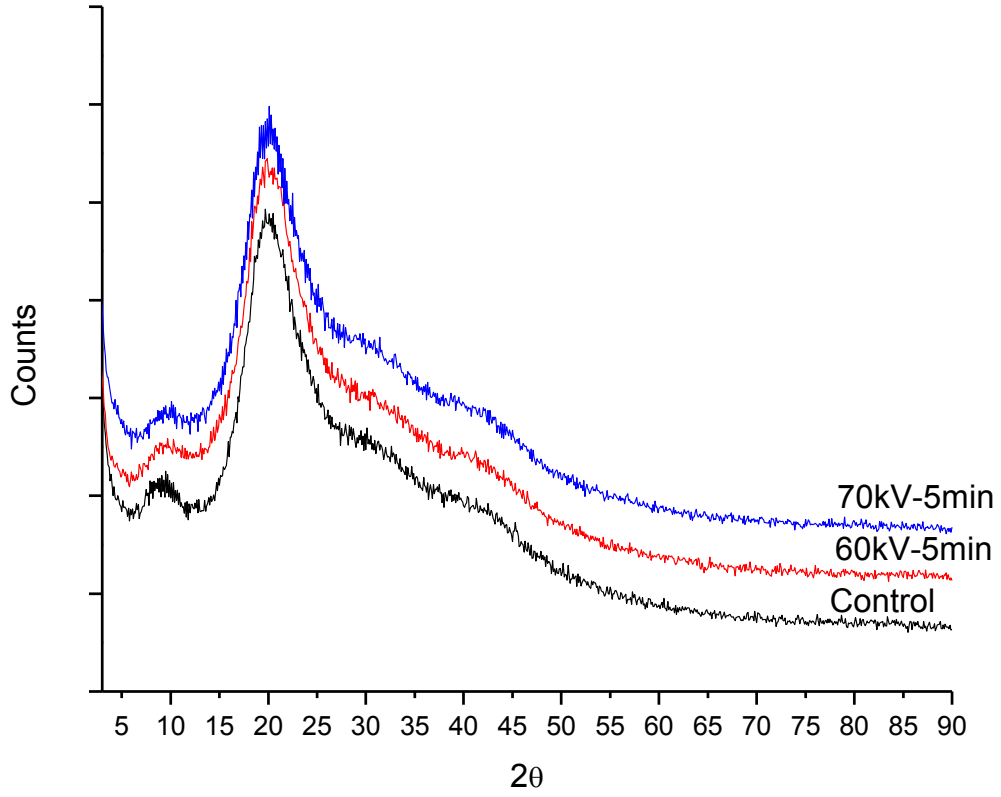

Figure 25. X-ray diffractogram of control and plasma treated sodium caseinate films

6.2.4. Water Sorption Kinetics

Water sorption kinetics for protein films have been described using many empirical and fundamental models. The two-parameter Peleg's equation and Fick's second law were chosen for the empirical and fundamental description of the sorption process respectively. Details of the equations and parameters have been discussed previously in chapter 5.

Water sorption kinetics for control and plasma treated sodium caseinate films are shown in Figure 26. Peleg's equation and the Fick's diffusion fitting parameters are shown in Table 18 along with their root mean square errors (RMSE). The first constant (K_1) in the Peleg's equation is inversely related to the initial rate of water absorption by the film. No significant

($p>0.05$) increase in the initial rate of water absorption after the DBD plasma treatment was observed at 60 kV, but for 70 kV treatment it was found to be significantly ($p\leq0.05$) higher than the control sample. The same conclusion can be obtained from the analysis of the diffusivity parameter suggesting an increase in the hydrophilicity of the sodium caseinate film after DBD plasma treatment at the higher voltage level. The low K_2 value of the plasma treated sample also indicates its higher final absorption capacity than the control and can be correlated with equilibrium moisture content values. The increase in the hydrophilicity after plasma treatment can be explained by higher surface oxygen as discussed earlier. Among the two models employed, the Peleg's equation was found to be better in explaining the experimental data as evident from the RMSE values.

Table 18. Fitting Parameters of the Peleg's Equation and Fickian model for DBD plasma treated samples. Means values not followed by a common superscript letter, are significantly different ($p \leq 0.05$) for each parameter.

Sample	**Peleg's Equation**			**Fickian Model**		
	K_1(min/%wt.)	**K_2(% wt.$^{-1}$)**	**RMSE**	**M_{eq} (%)**	**D (cm^2/min)**	**RMSE**
Control	12.59^{a}	0.051^{d}	1.31	16.35^{h}	4.97x10^{-8f}	1.98
60kV-5min	9.74^{a,b}	0.039^{e}	1.55	21.48^{i}	4.86x10^{-8f}	2.42
70kV-5min	10.45^{b}	0.040^{e}	1.08	20.83^{i}	4.51x10^{-8g}	1.95

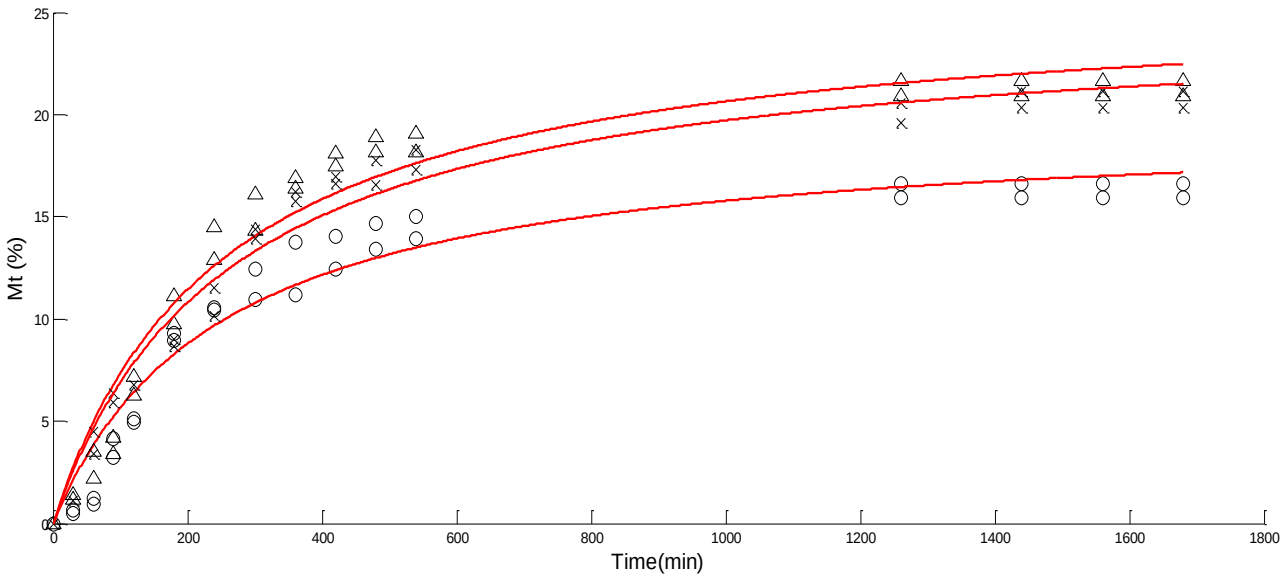

Figure 26. Moisture sorption of sodium caseinate films after DBD plasma treatment at 23°C and 75% RH (solid lines represent the fitting from the Peleg equation, Control(○), 60kV-5min(x), 70kV-5min(Δ)).

6.2.5. Contact angle and surface free energy

Static contact angle and the surface free energy of the control and plasma treated sodium caseinate films are shown in Table 19. Significant decrease ($p<0.05$) in the contact angle was observed after cold plasma treatment for all the test liquids. The water contact angle for control sodium caseinate film was 73.4° which was reduced to 52.4° after DBD plasma treatment at 70 kV for 5 min. Similarly, the total surface energy of the films was also found to be significantly higher after cold plasma treatment. Based on the Owen and Wendt model, polar and dispersive components of total surface were calculated. As shown in the Table 19, the increase in the total surface free energy was mainly due to the significant increase in the polar component of surface energy. The increase in the polar component suggests an increase in the polar groups on the film surface after cold plasma treatment. This result also supports

the findings of XPS analysis, which shows the formation of new oxidized polar groups on the film surface after DBD plasma treatment.

Table 19. Contact angle (A) and surface free energy (B) analysis of plasma treated sodium caseinate films.

A. Contact angle	**Parameters**	**Control**	**70 kV-5min**
Water	θ_w	73.37±1.03	52.37±0.18
Ethylene glycol	θ_e	38.86±1.90	30.86±0.42
Di-iodomethane	θ_d	49.86±0.24	38.86±0.37
B. Surface free energy			
Fowkes	γ^{tot}	40.24	51.69
	γ^{d}	34.80	37.18
	γ^{p}	5.44	14.51

6.2.6. Barrier properties

The water vapor and oxygen transmission rate of the sodium caseinate film are reported in Table 20. The WVTR of control sodium caseinate film was 26.06 ± 2.04 $g.m^{-2}.day^{-1}$. No significant differences ($p>0.05$) were observed in the WVTR after DBD plasma treatment at any treatment level. Oxygen transmission rate (OTR*e) of the control sodium caseinate film was 0.54 ± 0.03 $cm^3.mm.m^{-2}.day^{-1}$ and was also not significantly ($p>0.05$) different after DBD plasma treatment.

It is important to emphasise at this point that sorption and permeability properties of any polymer are governed by different mechanisms. In the case of water absorption, the state of

absorption equilibrium is controlled by dissolution properties of the solvent and solute whereas permeation of water vapor is governed by the vapor pressure and concentration gradient on the two surfaces of the polymer dependent on the diffusion and solubility mechanism. Gas permeability is also a combined effect of diffusion and solubility in which permeant is transported via voids of gaps present between the segments of a polymer chain (Chaiwong et al., 2010). Based on the mechanisms of action, it can be interpreted that water sorption is affected by the surface composition while WVTR and OTR are more dependent on the bulk properties of the polymer.

Table 20. Water vapor and oxygen transmission rate of sodium caseinate film after DBD plasma treatment (Mean±standard deviation). Means values not followed by a common superscript letter, are significantly different ($p \leq 0.05$).

Sample	WVTR ($g.m^{-2}.day^{-1}$)	OTR*e ($cm^3.mm.m^{-2}.day^{-1}$)
Control	26.06 ± 2.04^{a}	0.54 ± 0.03^{b}
60kV-5min	23.64 ± 1.87^{a}	0.42 ± 0.08^{b}
70kV-5min	23.28 ± 0.00^{a}	0.47 ± 0.01^{b}

6.3. Conclusion

DBD plasma treatment increased the surface roughness of sodium caseinate films. It also decreased the glass transition temperature of the film. Plasma treatment increased the surface oxygen content and hydrophilicity of the film. No significant ($p \leq 0.05$) change in the WVTR and OTR was observed after plasma treatment. The results indicate that the DBD plasma treatment have mainly modified the surface properties of the sodium caseinate film with minimal effects to the bulk properties of the film.

Chapter 7 Corn starch film

7.1. Introduction

Starch, being a low cost, inherently biodegradable, renewable and produced by various plant sources, is an obvious choice as green polymer. Starch serves as the energy reserve material in higher plants and found in leaf chloroplasts and amyloplast of storage organs like seeds and tubers (Wang et al., 1998). Chemically, starch is composed of carbon, hydrogen, and oxygen in a ratio of 6:10:5 [$C_6H_{10}O_5$] belonging to carbohydrate class of organic compounds. It is made up of two fractions namely amylose and amylopectin. Amylose is a linear molecule (molecular weight-5×10^5 to 10^6) composed of anhydroglucose units connected through α(1,4) linkages whereas amylopectin (molecular weight of several millions) is a branched polymer with anhydroglucose chain linked with α(1,4) with α(1,6) linked branches. The majority of starch used is derived from maize, potato, wheat and tapioca with smaller amounts from rice, sorghum, sweet potato, arrowroot, sago, and mung beans (Wang et al., 1998). The high molecular weight and branched structure of amylopectin reduces the mobility of the polymer chains preventing close orientation for significant levels of hydrogen bonding, consequentially causing the loss of some desired properties as a packaging material (Liu et al., 2009a). Potential application of starch as a food packaging material and edible coating has been previously studied on various products like carrots (García et al., 1999), strawberries (García et al., 1998), tomatoes (Das et al., 2013) and Brussels sprouts (Viña et al., 2007).

7.2. Results and Discussions

7.2.1. Surface topography

The root mean square roughness of control corn starch film was 17.05±10.49 nm. The roughness parameters for plasma treated samples are shown in Table 21. An increase in surface roughness was observed after DBD plasma treatment at all voltage levels and treatment times. Surface roughness was found to be significantly higher ($p<0.05$) after 5 minutes of plasma treatment at all the voltage levels (Figure 27).

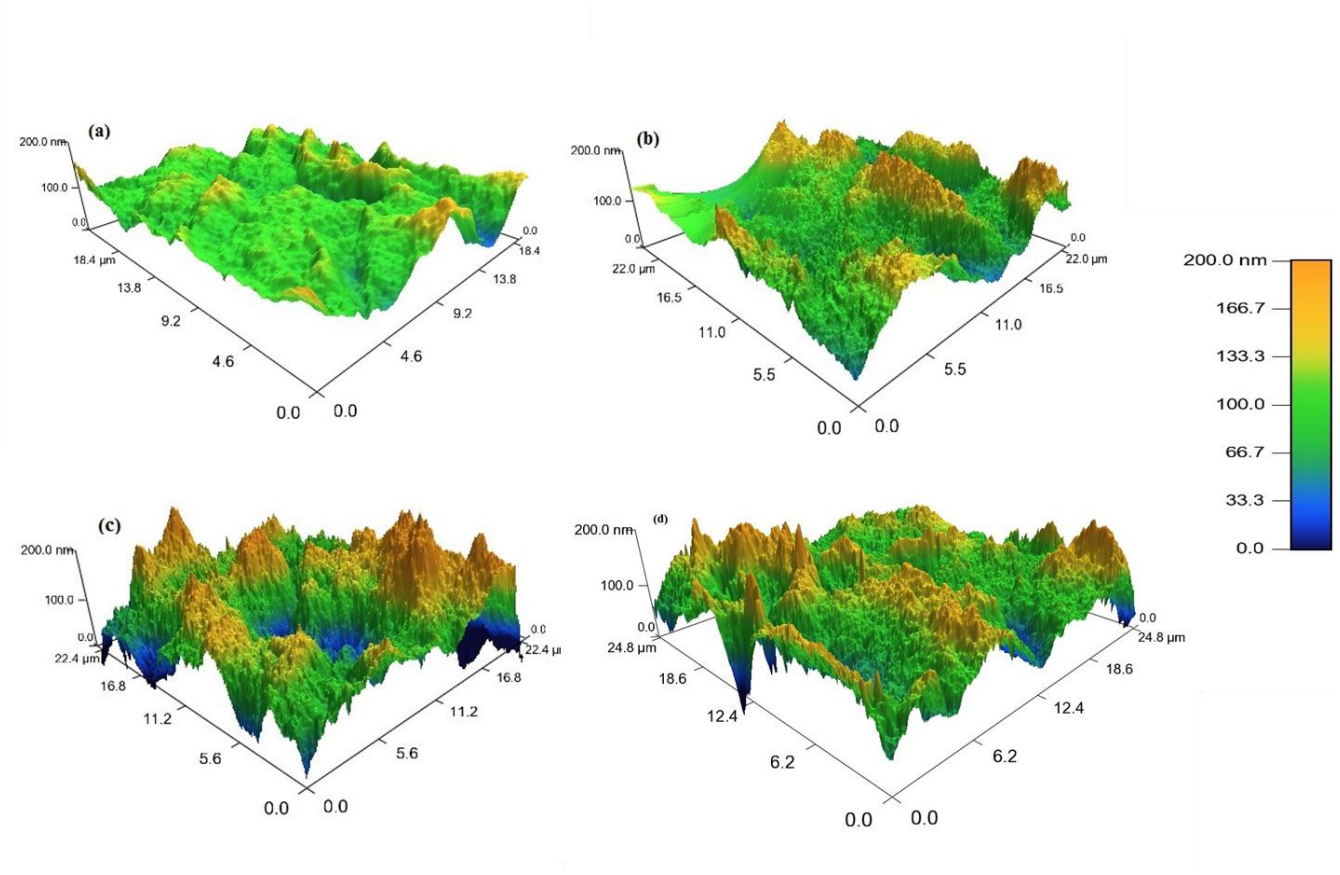

Figure 27. Surface topography of DBD plasma treated starch film (a) control (b) 60 kV-5min (c) 70 kV-5min (d) 80 kV-5min.

Table 21. Roughness parameter for DBD plasma treated corn starch films

Time↓/Voltage→	60 kV	70 kV	80 kV
1	29.97±28.97	39.85±25.09	49.54±30.47
2	31.39±26.38	40.93±32.71	38.35±35.72
3	43.85±31.75	52.61±46.26	49.95±39.44
4	65.68±32.05	57.43±41.35	55.57±42.43
5	58.21±20.91	53.22±22.08	62.56±26.73

7.2.2. Thermal Properties

The DSC thermogram was analysed to find the onset temperature, peak temperature and end temperature of the endothermic transition after plasma treatment. The onset temperature, peak temperature and end temperature for control corn starch film were 105°, 149° and 190 °C respectively (Figure 28). No significant difference ($p>0.05$) was observed after DBD plasma treatment. The endothermic transition was attributed to the remained granular structures after the thermal treatment during the casting process and any recrystallized structure (Li et al., 2011). The glass transition temperature was not clearly observed in the thermogram due to weak signal of heat flow, which is common for starch-based polymers (Liu et al., 2009b).

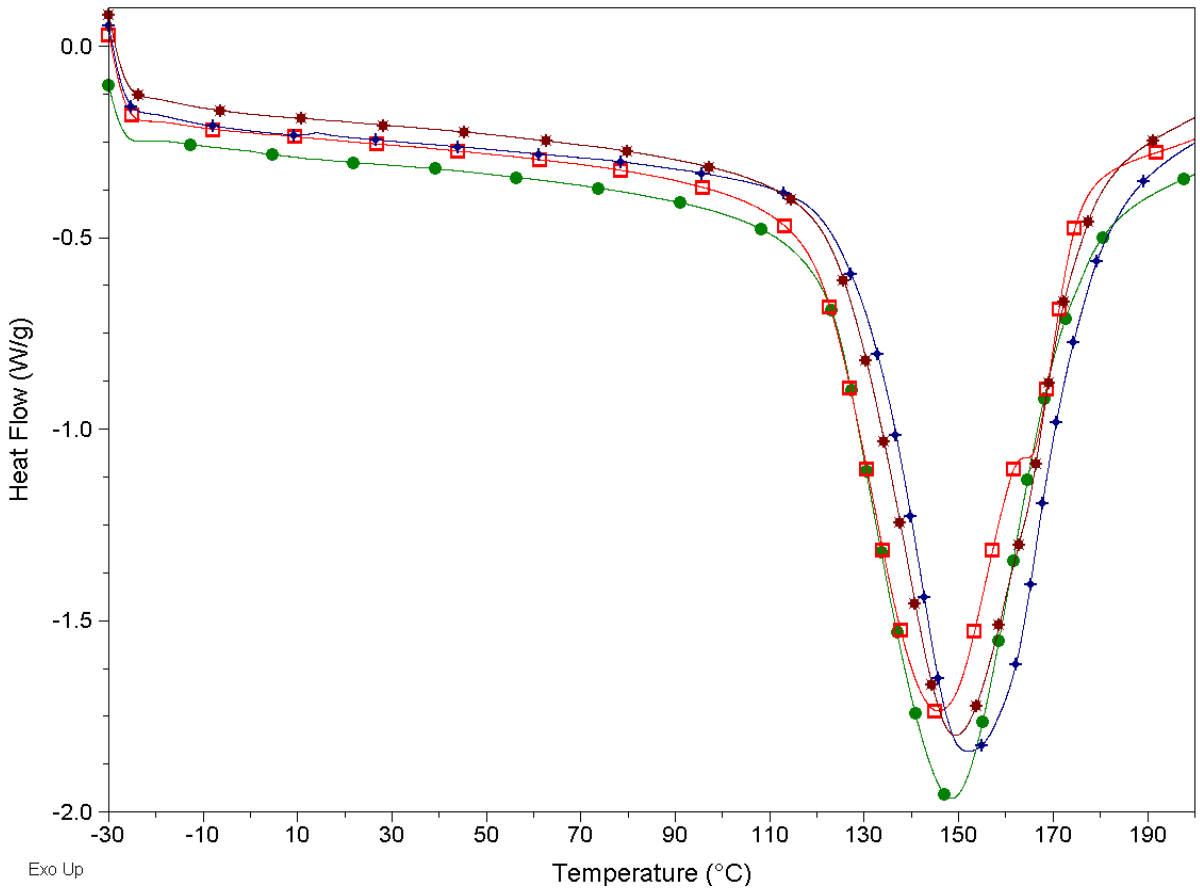

Figure 28. DSC thermogram of control and plasma treated corn starch films: Control (●), 60kV-5min (□), 70kV-5min (+) and 80kV-5min (✸).

TGA of control and plasma treated corn starch films displayed a similar thermal behavior of weight loss in three different phases. The first phase of weight loss was observed in the region of 70 to 130 °C, which was related to the loss of free and absorbed water from the film. The thermal degradation of corn starch started at 170 °C and the maximum degradation temperature for control film was 242.5 °C. After plasma treatment a decrease in maximum degradation temperature was observed in the range of 235.5 to 241 °C as shown in Figure 29. The third phase of weight loss was observed in the range of 420.8 to 425.8 °C. A similar three phase weight loss of corn starch film has also been reported earlier (Soares et al., 2005).

The decrease in the maximum degradation temperature can be attributed to the etching and random chain scission of the starch polymer after DBD plasma treatment.

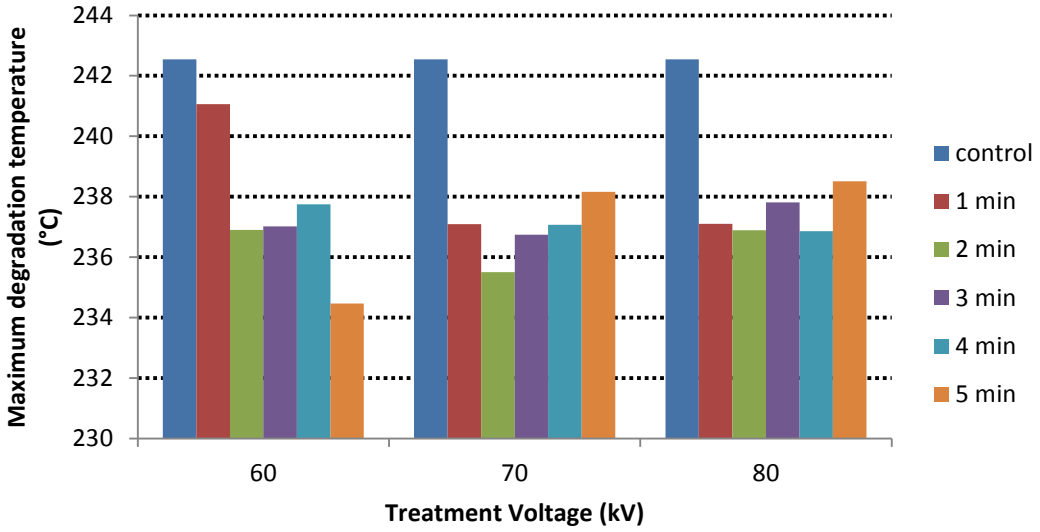

Figure 29. Maximum degradation temperature of control and plasma treated high amylose corn starch film.

7.2.3. Chemical characterisation

The surface elemental composition and ratio of control and DBD plasma treated corn starch films were determined using XPS analysis and summarized in Table 22. No significant increase in the surface oxygenation was observed after DBD plasma treatment at 60 kV, but the O/C ratio increased significantly after plasma treatment at 70 and 80 kV for 5 minutes. The increased O/C atomic ratio suggests formation of new oxygen-containing groups on the film surface after plasma treatment.

Table 22. The elemental composition and ratio of the plasma treated corn starch film surfaces

Sample	C1s(at%)	O1s(at%)	O/C
Control	81.51	18.50	0.23
60kV-5min	79.76	20.24	0.25
70kV-5min	71.51	28.49	0.40
80kV-5min	68.58	31.41	0.46

The C1s peaks of the control and plasma treated corn starch films were further deconvoluted to identify the chemical groups and are shown in Figure 30. Three spectral peaks were observed in the control and 60kV-5min plasma treated samples at 284.6, 286.5 and 288.2 eV which were assigned to C–C or C–H, C–O–H or C–O–C and C=O respectively. In the DBD plasma treated samples at 70 and 80 kV for 5 min, an extra peak was observed at 289.3 eV which can be assigned to O=C–O group (Xiong et al., 2008, Wagner and Muilenberg, 1979). The appearance of this peak suggests that DBD plasma treatment at higher voltage levels increased the contribution of higher binding energy carbon species and resulted in formation of new oxidized species on the film surface.

The concentrations of all chemical groups on the corn starch film surface before and after DBD plasma treatment were calculated from deconvulated high-resolution C1s peaks (Table 23). The control starch film contains 79.2 % C–C/C–H which decreased to 42.7 % after plasma treatment. The DBD plasma treatment significantly increased the C–O–H/C–O–C and C=O groups from 11.5 and 9.4 to 40.4 and 15.4 % respectively. The concentration of the newly introduced group O=C–O reached 1.6 % after treatment. This suggest that DBD

plasma leads to breakage of C–H/C–C bonds creating free radicals, which can react with the activated oxygen species in the discharge leading to the formation of oxygen-containing groups like C–O–H/C–O–C, C=O and O=C–O (Morent et al., 2008).

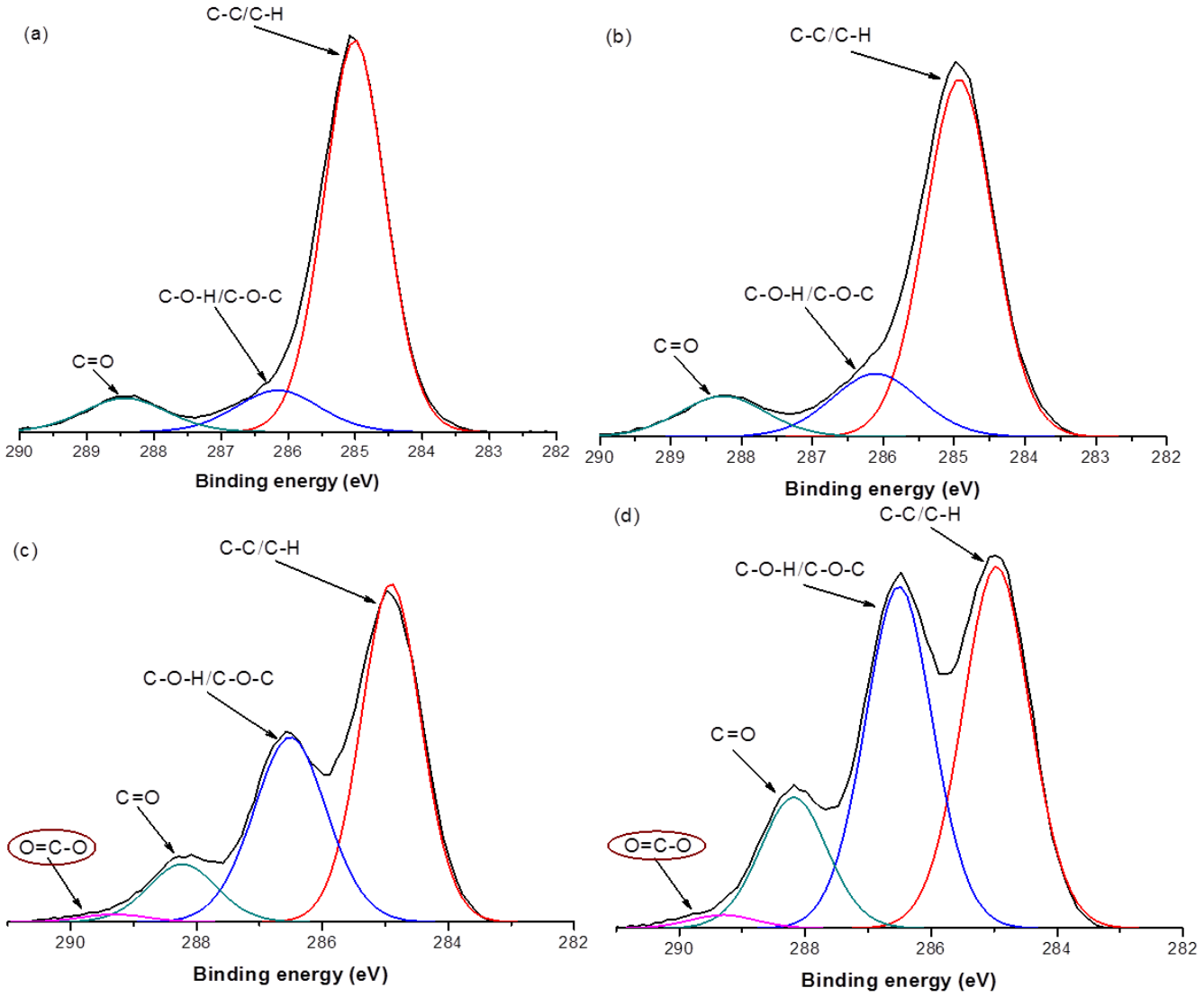

Figure 30. Deconvoluted C1s peaks of control and plasma treated corn starch films. (a) Control (b) 60kV for 5min, (c) 70kV for 5 minutes, (d) 80kV for 5 minutes.

Table 23. High-resolution XPS of C1s peak deconvolution and possible groups.

Sample	Contribution of C1s components (%)			
	C-C/C-H	**C-O-H/C-O-C**	**C=O**	**O=C-O**
Control	79.20	11.45	9.35	0
60kV-5min	72.90	16.59	10.52	0
70kV-5min	52.82	35.37	10.43	1.38
80kV-5min	42.65	40.36	15.42	1.58

X-ray diffraction was used to evaluate the changes in the crystalline structure of the corn starch films after DBD plasma treatment. Starch films displayed typical A-type crystal structure with peaks at 17.3º (5.12ºA), 19.9º (4.46ºA) and 22.3º (3.98ºA) (Cheetham and Tao, 1998). No change in the peak position was observed after plasma treatment, which indicates that DBD plasma treatment did not cause any change in the crystal structure of the starch films (Figure 31). Although an increase in the peak height was observed after plasma treatment suggesting an increase in the crystallinity of the films which may be due to changes in the orientation of the double helices within the crystallines (Xia et al., 2013, Jayakody et al., 2005).

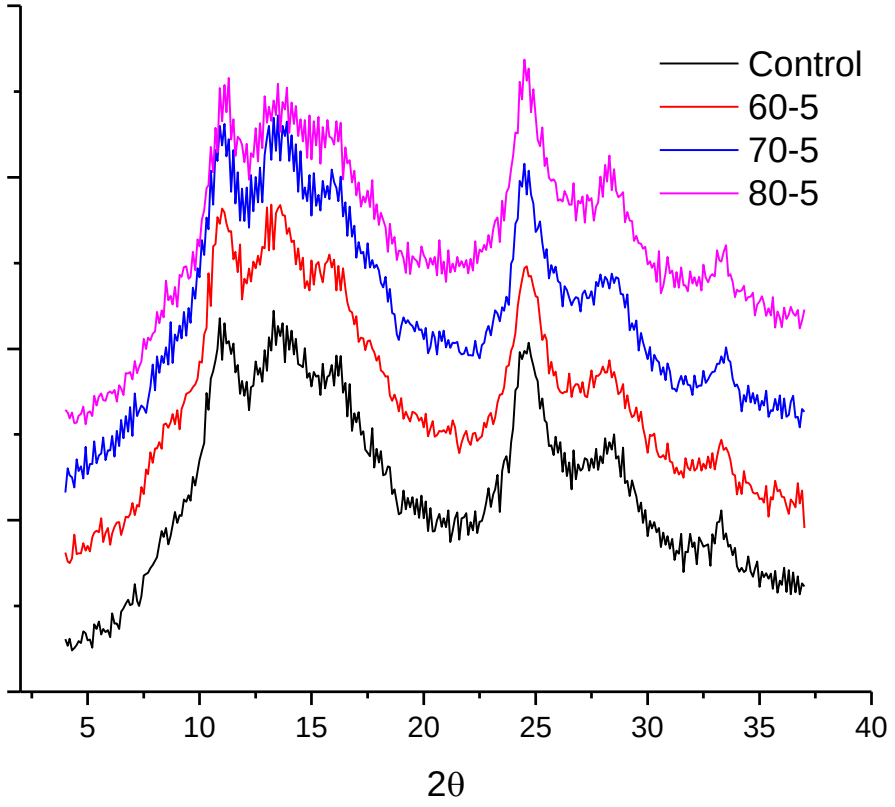

Figure 31. X-ray diffraction peaks of control and plasma treated corn starch films.

FTIR spectra of control and plasma treated corn starch films are shown in Figure 32. Characteristics absorption peaks were observed from the FTIR spectra of starch films at 929 and 857 cm^{-1} due to anhydroglucose ring stretching vibrations (Han et al., 2013). A shift in the absorption bonds at 1648 and 1580 cm^{-1} were observed for films treated at 70 and 80 kV, corresponding to δ(O–H) bending due to the tightly bound water (H_2O) in the starch (Xu et al., 2005). The shift may be the result of an increase in the hydrogen bonding due to surface oxygenation after DBD plasma treatment as evident from the XPS results (Xiong et al., 2008). An increase in the absorption peaks after plasma treatment were also observed at 1154 and 1081 cm^{-1} which corresponds to stretching vibration of C–O in C–O–H groups and the

band at 1016 cm^{-1} which is attributed to stretching vibration of C–O in C–O–C groups. These observations further validate the XPS results indicating an increase in C–O–H and C–O–C groups after plasma treatment.

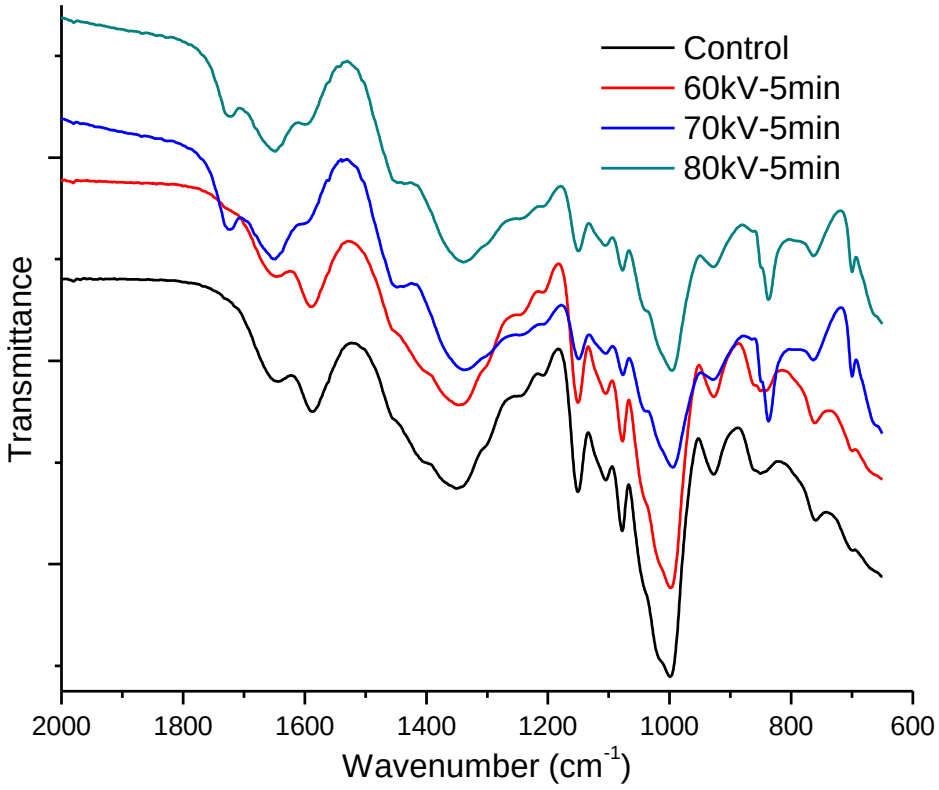

Figure 32. FTIR spectra of control and plasma treated corn starch films.

7.2.4. Contact angle and surface free energy

Static contact angle and the surface free energy of the control and plasma treated starch films are shown in Table 24. A significant decrease ($p<0.05$) in the contact angle (water) was observed after cold plasma treatment at all treatment levels. However, insignificant change in the contact angle was observed with increased treatment voltages. Similarly, the total surface energy of the films was found to be significantly higher after cold plasma treatment. Based

on the Owen and Wendt model, polar and dispersive components of total surface were calculated. As shown in the Table 24, the increase in the total surface free energy was due to the increase in the polar component of surface energy. The increase in the polar component suggests an increase in the polar groups on the film surface after cold plasma treatment. This result can be explained in collaboration with the XPS analysis, which also shows the formation of new oxidized functional groups on the film surface after DBD plasma treatment.

Table 24. Contact angle (A) and surface free energy (B) analysis of plasma treated corn starch films.

A. Contact angle (°)	**Control**	**60 kV-5 min**	**70 kV-5 min**	**80 kV-5 min**
Water	54.33±1.31	25.54±0.63	22.62±0.61	21.14±3.45
Ethylene glycol	28.64±2.75	8.75±2.20	3.00±0.97	4.05±0.82
B. Surface free energy(mN/m)				
Total (γ^{tot})	49.10	62.31	64.24	64.16
Dispersive (γ^{d})	32.81	34.70	37.92	36.51
Polar (γ^{p})	16.29	27.61	26.32	27.65

7.2.5. Barrier properties

Corn starch films generally are hydrophilic in nature and have high water transfer rates due to clustering of water molecules in their diffusion through micro-cavities, which is one of the major limitations for its use in commercial applications (Arvanitoyannis et al., 1996). It is desirable that the food processing technologies employed should not further adversely affect its water vapor permeability, to maintain its packaging utility. The WVTR for the control

corn starch film was found to be 7.7±0.2 $g.m^{-2}.day^{-1}$. No significant difference ($p>0.05$) in the water vapor permeability was observed even after DBD plasma treatment at maximum level of 80 kV for 5 minutes. The water vapor permeability of all the starch films was found in the range of 8.1 to 11.0 $g.m^{-2}.day^{-1}$. The results are in close agreement with the previously published results (Arvanitoyannis et al., 1996, Bertuzzi et al., 2007).

7.3. Conclusion

DBD plasma treatment of high amylose corn starch film significantly increased the surface roughness of the films. Control and plasma treated corn starch films were similar in thermal degradation profiles, although a decrease in the maximum degradation temperature was observed. XPS and FTIR spectra confirmed the increase in surface oxygen content and appearance of new oxygenated chemical groups on the film surface after treatment. DBD plasma did not induce any change in the crystal structure of the starch film. Also, no change in the water vapor permeability was observed after plasma treatment. These results demonstrate the potential of corn starch to be used as biodegradable packaging material with cold plasma technology.

Chapter 8 Bovine gelatin film

8.1. Introduction

Among protein films, gelatin-based films have shown a lot of potential for commercial application. Gelatin can be obtained from waste utilization from the meat industries, so it does not compete with the protein required for human or animal consumption. Also, the unique properties of gelatin such as its thermo-reversibility and melting point are close to human body temperature, making it suitable for edible and pharmaceutical applications (Achet and He, 1995). Gelatin is a water soluble protein biopolymer derived from partial hydrolysis of native collagen-high molecular weight, water insoluble and the most abundant structural protein found in skin, tendon, cartilage and bone of animals (Prasertsung et al., 2010). Collagen is made from three parallel alpha-chains forming a triple stranded super-helical structure. Gelatin is formed when collagen is partially denatured by mild heat treatment under acidic or alkaline conditions, and consists of a partially reformed triple helix structure and some unstructured domains rich in proline, hydroxyproline, lysine and hydroxylysine (Dangaran et al., 2009).

8.2. Results and discussions

8.2.1. Surface topography

Surface topography of the control and plasma treated bovine gelatin films are presented in Figure 33. The control film was relatively smooth with a root mean square roughness value of 2.73 nm. DBD plasma treatment increased the roughness of all treated films with R_{rms} ranging between 4.5 and 12.8 nm. The effects of plasma control parameters of voltage and treatment time on the surface roughness are shown in Figure 34. The increase in the surface

roughness was found to be largely dependent on the treatment time rather than treatment voltage. No significant difference ($p>0.05$) was observed between the surface roughness of films treated at different voltages. However, the roughness was significantly ($p<0.05$) higher for films treated for 4 and 5 minutes irrespective of the treatment voltage.

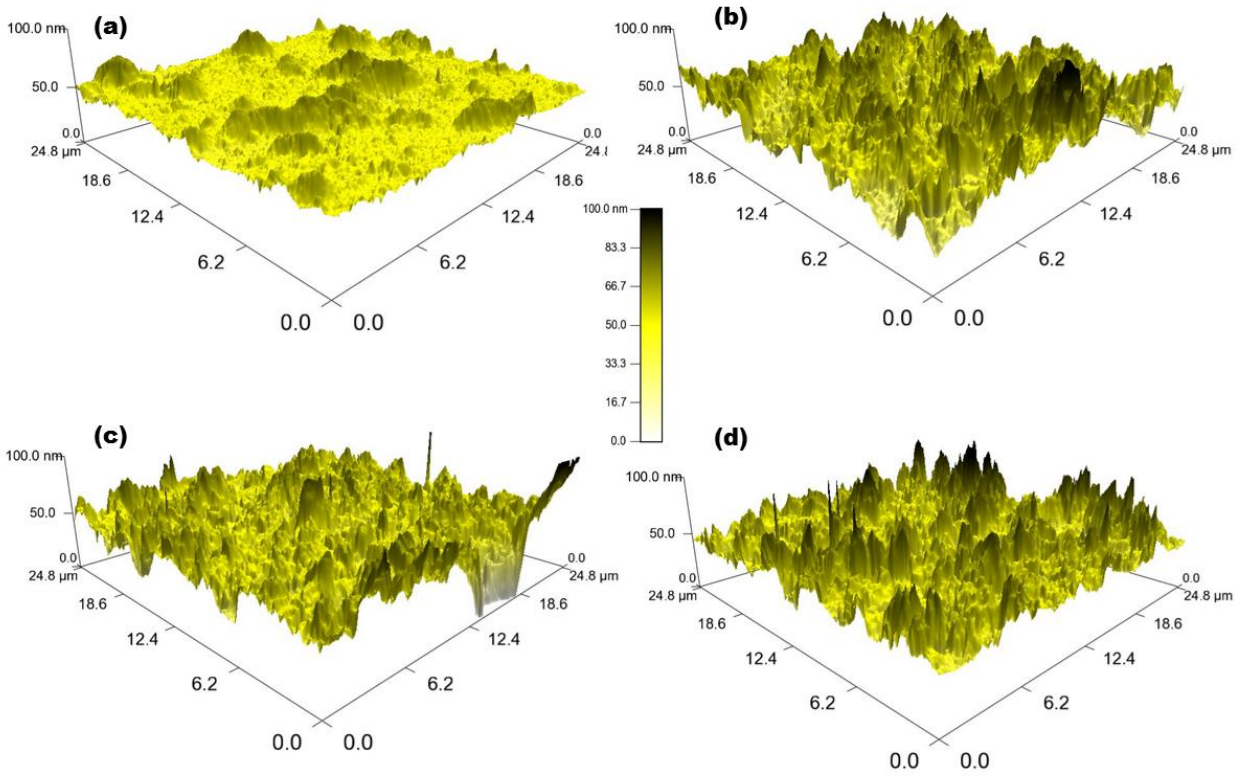

Figure 33. Surface topography of DBD plasma treated bovine gelatin films (a) control, (b) 60kV-5min, (c) 70kV-5min, (d) 80kV-5min.

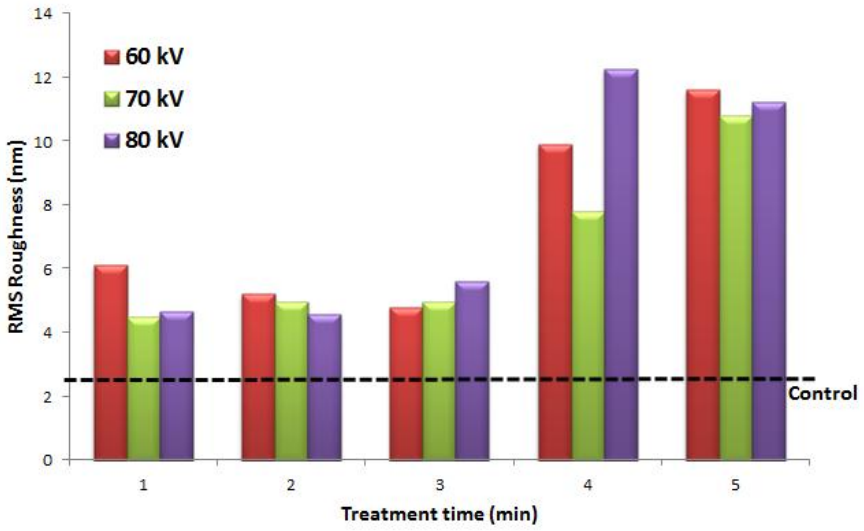

Figure 34. Surface roughness (R_{rms}) of DBD plasma treated bovine gelatin films at different voltages and treatment times

8.2.2. Chemical characterisation

XPS was carried out to analyse the effects of plasma treatment on the chemical composition of the film surface. The survey spectra identified carbon (C1s) and oxygen (O1s) on the film surface. The elemental compositions of the film surface are shown in Table 25. The control gelatin film has an O/C ratio of 0.26 which was significantly increased after plasma treatment. The increase in the surface oxygenation was also found to be more dependent on the treatment time than voltage with the same O/C ratios observed at 70 and 80 kV for 5 min.

Table 25. The elemental composition and ratio of the DBD plasma treated bovine gelatin film surfaces

Sample	C1s(at%)	O1s(at%)	O/C
Control	79.56	20.45	0.26
60kV-5min	77.69	22.33	0.29
70kV-5min	76.43	23.57	0.31
80kV-5min	76.60	23.40	0.31

Further analysis of the surface chemistry of the control and plasma treated films was obtained by the deconvolution of the high resolution C1s peaks. The deconvoluted peaks are presented in Figure 35. Four C1s peaks were identified at 284.88, 286.3, 287.95 and 288.72 eV which can be assigned to C-C/C-H, C-O-H/C-O-C, C=O and O=C-O groups (Wagner and Muilenberg, 1979). The percentages of each deconvoluted peak area are presented in Table 26. It is evident from the data that there has been a decrease in the C-C/C-H bonds after the plasma treatment. A significant increase was observed for both the peaks for C-O-H/C-O-C and C=O groups. However, a decrease in the peak area for O=C-O group was also noted. The increase in the O/C ratio after plasma treatment lead to an increase in the C-O-H/C-O-C and C=O groups on the film surface.

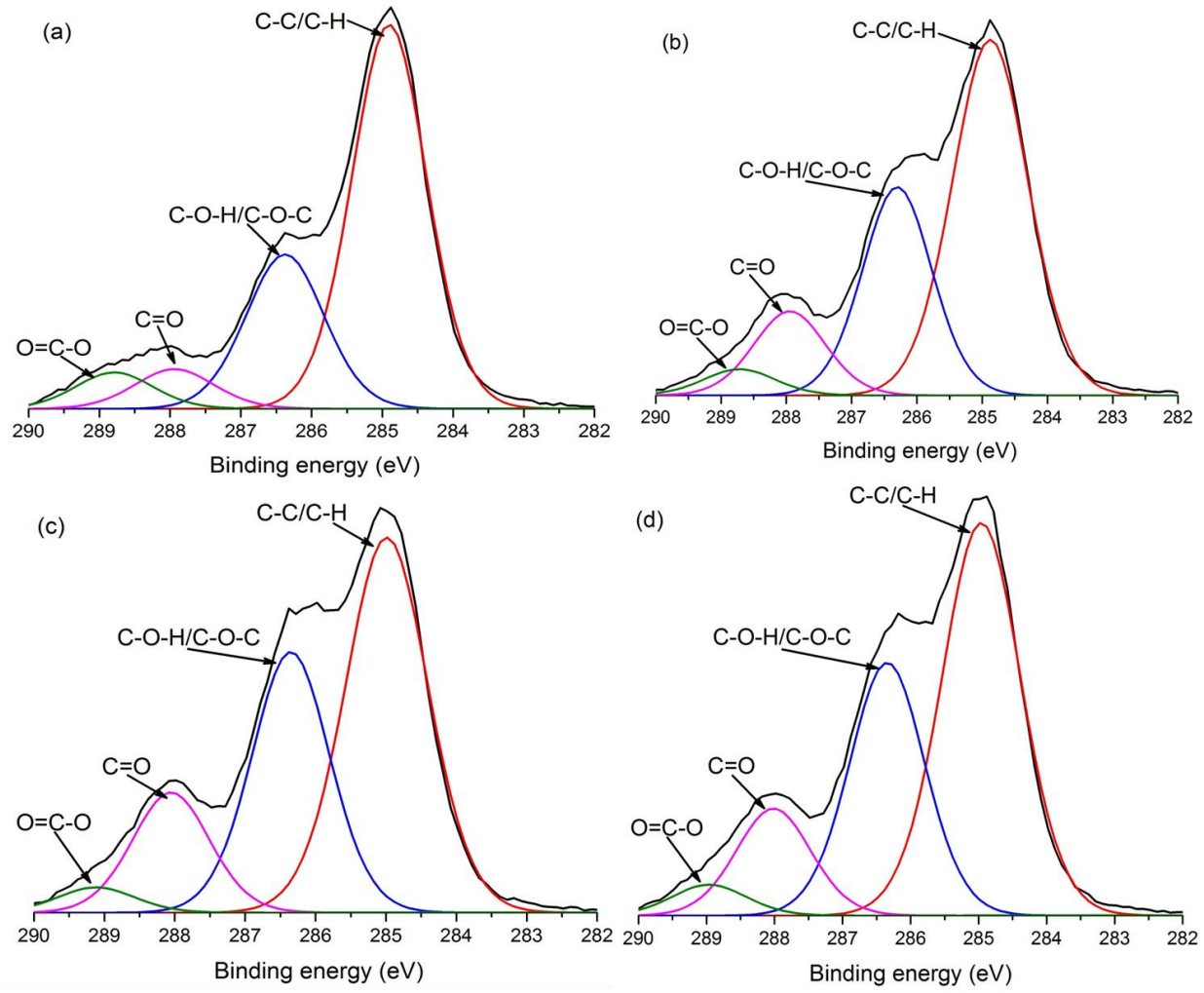

Figure 35. Deconvoluted C1s peaks of control and DBD plasma treated bovine gelatin films. (a) Control (b) 60kV-5min, (c) 70kV- 5 minutes, (d) 80kV- 5 minutes.

Table 26. High-resolution XPS of C1s peak deconvolution and possible groups.

Sample	Contribution of C1s components (%)			
	C-C/C-H	**C-O-H/C-O-C**	**C=O**	**O=C-O**
Control	61.43	25.76	6.75	6.06
60kV-5min	54.55	29.31	12.31	3.83
70kV-5min	49.67	32.32	14.86	3.14
80kV-5min	51.41	31.43	13.30	3.86

X-ray diffractograms of control and plasma treated bovine gelatin film are shown in Figure 36. Bovine gelatins were of type B and presented an X-ray diffraction pattern characteristic of a partially crystalline material. The diffractogram showed one sharp peak at 2θ=7.7° (d=11.47°A) and another broad peak at 2θ=20.3° (d=4.37°A). The peak at 7.7° is related to the diameter of the triple helix and its intensity relates with the triple helix content of the film whereas the peak at 20.3° is related to the distance between amino acidic residues along the helix (Bigi et al., 2004). No significant change was observed between the control and 60 kV-5 min plasma treated gelatin films but an increase in the peak intensity was observed for 70 kV-5 min and 80 kV-5 min plasma treated films, suggesting an increase in the triple helix content after DBD plasma treatment. Significant increases in the second peak intensity were also observed for 70 kV-5 min and 80 kV-5 min treatments. This change in the triple helix content and distance between amino acid residue along the helix, after plasma treatment can be attributed to the change in the polar groups make up, which lead to reconstitution of some

collagen-like triple helical structure in the films (Kozlov and Burdygina, 1983, Rivero et al., 2010, Tanioka et al., 1976).

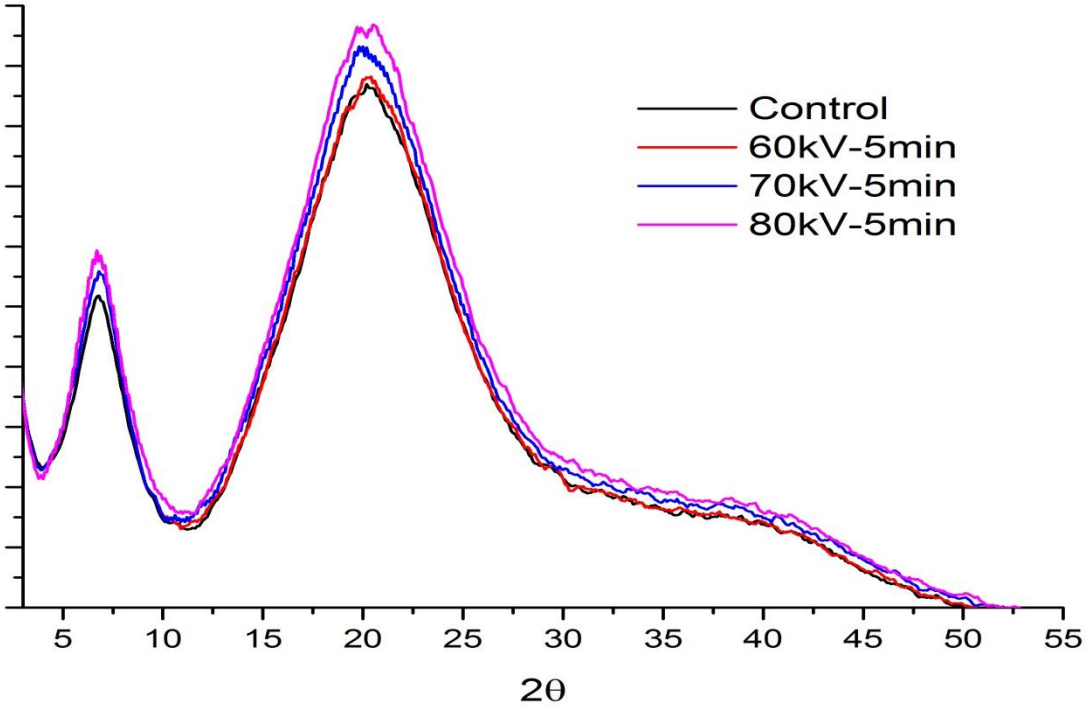

Figure 36. X-ray diffractograms of DBD plasma treated bovine gelatin films.

Bovine hide gelatin film displayed a typical protein film FTIR spectrum. A broad peak was observed at 3300 cm^{-1} due to the extension of the N–H group of amide A (Andreuccetti et al., 2009). A strong amide I band at 1635 cm^{-1} was observed which was attributed to the C=O stretching vibrational frequency of the amorphous, random coil peptides (Yannas, 1972). The amide II band was observed most strongly at 1545 cm^{-1} which was assigned to the extension of C-N and angular deformation of N-H ligations. The amide III bands seen at 1450 and 1235 cm^{-1}, represent extension of C-N and N-H on the flexion surface of amide bonds and vibrations due to CH_2 and CH_3 groups (Andreuccetti et al., 2009). However, no significant

difference in the peaks were observed after plasma treatment suggesting that the changes due to DBD plasma treatment were mostly limited to the chemical changes on the film surface without affecting the bulk chemical nature of the film.

8.2.3. Contact angle and surface free energy

Film hydrophilicity is an important characteristic for deciding the packaging application of any polymeric film. The contact angle was analysed for all three test liquids on the control and films treated at the maximum voltage and treatment time (80 kV-5 min) and are shown in Table 27. Control gelatin film displayed a high contact angle for water of 126.3° showing its hydrophobic nature. Gelatin is composed of single and double unfolded chains of hydrophilic moieties, which in highly hydrated states form a three-dimensional network called a hydrogel. The hydrophobic moieties of this hydrogel can have preferred orientations at the hydrogel-air interface resulting in a high contact angle (Białopiotrowicz and Jańczuk, 2001). Similar orientations in this case can also explain the hydrophobic nature of the control gelatin film.

After plasma treatment, a significant ($p<0.05$) decrease in the contact angle for all the test liquids was observed. This decrease in the water contact angle clearly demonstrates the increase in the hydrophilicity of gelatin films after plasma treatment. It may be due to the formation of hydrophilic groups on the plasma treated polymer film surfaces which may be explained as: plasma creates radical species on the polymer surface which can combine with oxygen in the air, increasing the amount of polar groups such as –OH, C=O, COOH on the plasma treated polymer surfaces.

Table 27. Contact angle (A) and surface free energy (B) analysis of plasma treated bovine gelatin film

A. Contact angle	**Parameters**	**Control**	**80 kV-5 min**
Water	θ_w	126.27±0.39	58.10±0.34
Ethylene glycol	θ_e	53.31±0.17	15.56±0.59
Di-iodomethane	θ_d	39.15±0.44	32.58±0.09
B. Surface free energy			
Fowkes	γ^{tot}	48.32	53.00
	γ^{d}	45.80	41.61
	γ^{p}	2.52	11.39
Acid-base approach	γ^{tot}	13.37	50.08
	γ^{d}	40.04	43.12
	γ^{p}	-26.67	6.96
	sqrt[γ^{+}]	2.48	0.85
	sqrt[γ^{-}]	-5.38	4.11

Surface free energy analysis of control and plasma treated bovine gelatin films shows a significant increase in the total SFE. The dispersive component was not significantly different but there has been a significant increase in the polar component of the SFE. And from the acid-base approach, we can deduce that there has been increase in the base component of the SFE. These observations show that DBD plasma treatment increased the amount of polar groups on the film surface, increasing the polar component and finally the

total SFE of the film. These results also support the results of XPS which has shown the increase in surface oxygen content and possible increase in polar groups like C-O-H and C=O.

8.2.4. Barrier properties

Water vapor and oxygen permeability are important parameters governing the suitability of polymeric films for packaging applications. WVTR of the control gelatin film was found to be 10.56 g $(m^2.day)^{-1}$. After plasma treatment at the maximum voltage level and treatment time of 80 kV for 5 min, no significant ($p>0.05$) difference was observed. The WVTR of 80 kV-5 min film was found to be 14.16±3.39 g $(m^2.day)^{-1}$. Also in the case of OTR, the OTR*e of the control film was 0.35±0.06 $cm^3.mm.m^{-2}.day^{-1}$, while after plasma treatment OTR*e was found to be between 0.23 to 0.34 $cm^3.mm.m^{-2}.day^{-1}$. No significant ($p>0.05$) difference was observed for OTR*e also, after plasma treatment. These results further supports the fact that DBD plasma treatment largely affected the surface features of the film, but bulk properties were mostly unchanged. These results also show the potential of bovine gelatin films to be successfully used with DBD plasma treatments and merit further studies with suitable food systems.

8.3. Conclusion

DBD plasma treatment of bovine gelatin film increased the surface roughness and surface oxygen content. An increase in the polar groups C-O-H and C=O was observed after plasma treatment. The increase in the O/C ratio was found to be largely dependent on the treatment time rather than treatment voltage. This increase in the surface polarity has also increased the hydrophilicity of the gelatin film and increased the polar component of the surface free energy. No change in the water vapor and oxygen permeability was observed after the

plasma treatment. Results demonstrate that although, cold plasma treatment have a slight impact on the film surface, but even at maximum treatment parameters, it did not significantly alter the bulk properties of the films, indicating the compatibility of bovine gelatin film with DBD plasma treatments.

Chapter 9 Chitosan film

9.1. Introduction

Chitosan is a linear polysaccharide consisting of (1,4)-linked 2-amino-deoxy-β-d-glucan, is a deacetylated derivative of chitin, which is the second most abundant polysaccharide found in nature after cellulose (Aider, 2010). Chitosan can be either used as edible coatings (<30 μm) for direct application on food or as films (>30 μm) to improve the food safety and shelf-life (van den Broek et al., 2015). Chitosan has been reported to be used as for various food products like peach, pear, kiwifruit (Du, 1997), strawberry (El Ghaouth et al., 1991a), tomato (El Ghaouth et al., 1992), cucumber, bell pepper (El Ghaouth et al., 1991b), longan fruit (Jiang and Li, 2001) and shrimps (Simpson et al., 1997) for extension of their quality attributes and shelf-life.

9.2. Results and discussion

9.2.1. Surface topography

The surface topography of control and plasma treated chitosan film was characterised using AFM. The surface of control chitosan film was observed to be smooth and homogenous without any sharp features with a root mean square roughness of 1.01 ± 0.96 nm. After DBD plasma treatment, the surface roughness was observed to be increasing with appearance of sharp protuberances (Figure 37). The increase in surface roughness after DBD plasma treatment was found to be more dependent on the treatment time rather than the treatment voltage. After DBD plasma treatment for 5 min at 60, 70 and 80 kV, root mean square surface roughness of chitosan films were 2.02, 2.82 and 3.39 nm respectively. The increase in the surface roughness of chitosan films were observed to be significantly less prominent

compared to other bio-based polymers like corn starch, zein and caseinate films. The DBD plasma treated chitosan films had less pronounced etching effects which may be attributed to the densely packed two-fold helical structure of chitosan films (Ogawa et al., 2004).

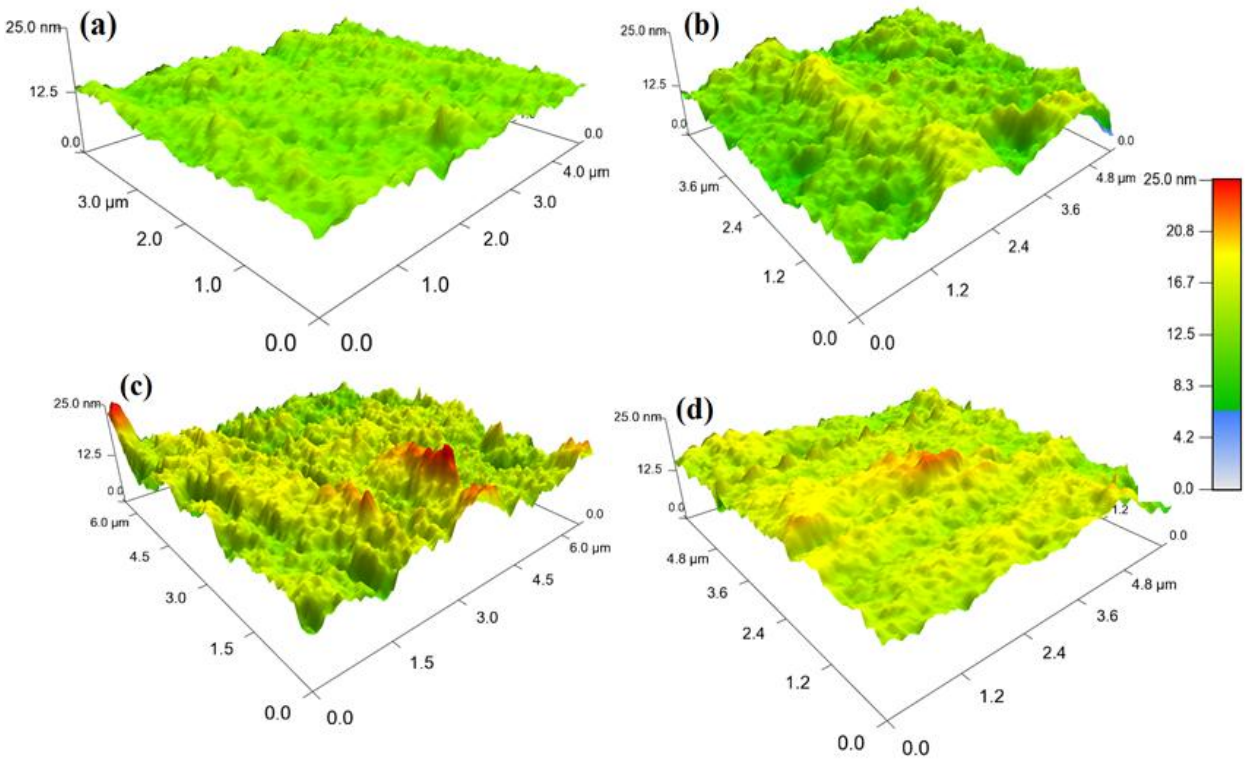

Figure 37. Surface topography of DBD plasma treated chitosan films (a) control (b) 60 kV-5min (c) 70 kV-5min (d) 80 kV-5min.

9.2.2. Chemical characterisation

XPS analysis was carried out to characterise the effects of DBD plasma treatment on the surface chemical composition of the chitosan films. Elemental composition of carbon (C1s) and oxygen (O1s) were recorded on the control and plasma treated film surfaces (Table 28).

The control chitosan film has an O/C ratio of 0.36. After plasma treatment a gradual increase in the surface oxygen content was observed with an increase in the treatment voltage levels.

Table 28. The elemental composition and ratio of the DBD plasma treated chitosan film surface

Sample	C1s (%)	O1s (%)	O/C
Control	73.75	26.26	0.36
60kV-5min	72.81	27.19	0.37
70kV-5min	71.45	28.56	0.40
80kV-5min	66.94	33.06	0.49

Further analysis of the surface chemistry of control and plasma treated chitosan films were done by deconvoluting the high resolution C1s peaks. The deconvoluted peaks are presented in Figure 38. Four C1s peaks were identified at 285, 286.6, 288.4 and 289.3 eV which were assigned to C-C/C-H, C-O/C-O-H, O-C-O and O=C-O bonds respectively (Amaral et al., 2005, Wagner and Muilenberg, 1979). Significant increases in the O-C-O bonds were observed after DBD plasma treatment which can be linearly correlated with the increase in treatment voltage levels. The O-C-O bond contribution increased from 7.17% in control film to 12.45 % after DBD plasma treatment at 80 kV for 5 min. This clearly indicates that DBD plasma treatment of chitosan leads to the formation of more oxygen-containing groups containing O-C-O bonds on the film surface hence increasing the overall surface oxygen content.

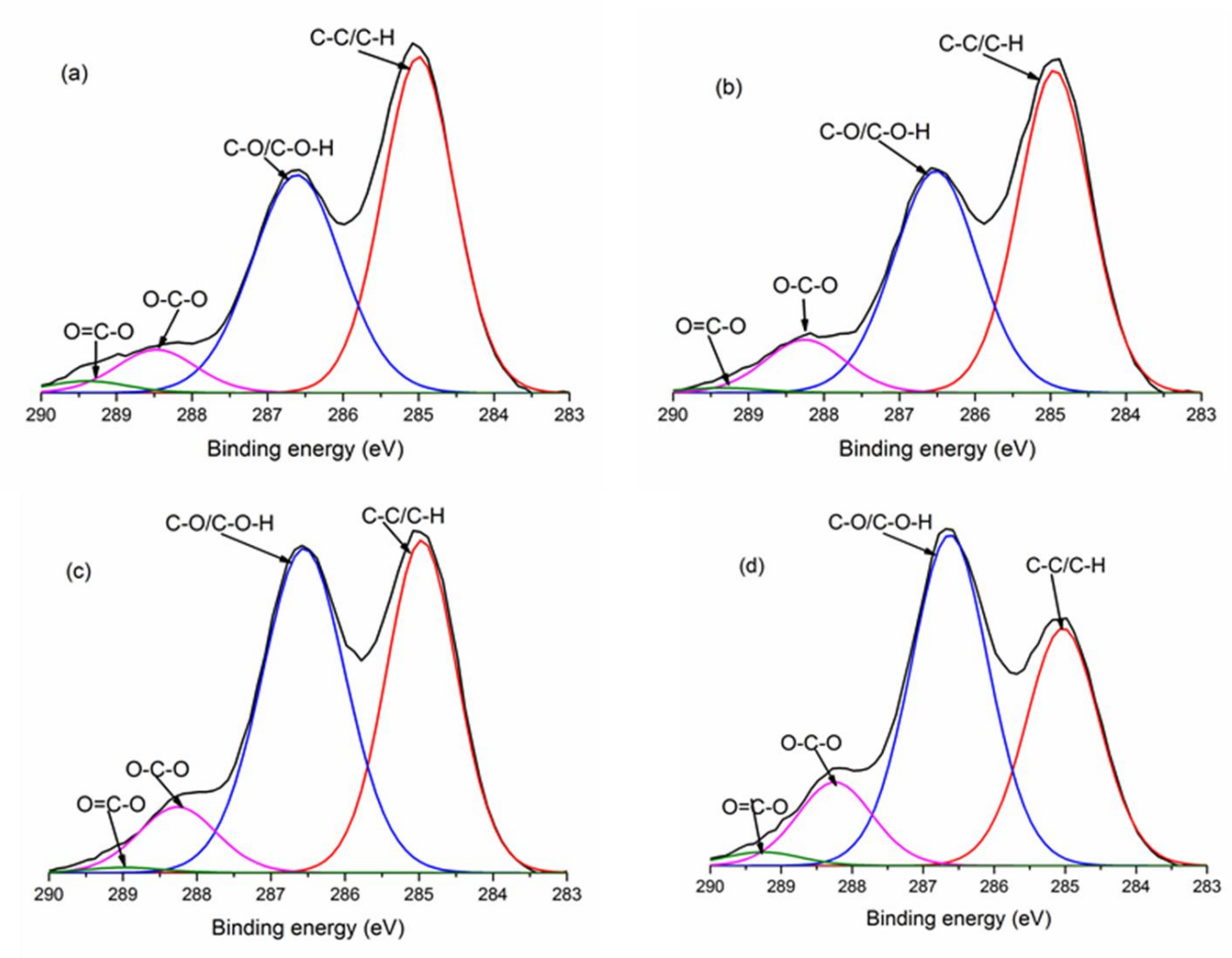

Figure 38. Deconvoluted C1s peaks of control and DBD plasma treated chitosan films. (a) Control (b) 60 kV-5 min, (c) 70 kV- 5 min, (d) 80kV- 5 min.

XRD was used to study the changes in the chitosan film structure after plasma treatment. Both control and plasma treated films have shown only one dominant peak at 2θ=20.3° (d=4.37 °A) (Figure 39). This peak correspond to the 'Form II' crystals having a constrained chain conformation (Fan et al., 2009). Form II crystals are orthorhombic having a unit cell of a=4.40 °A, b=10.0 °A and c=10.30 °A (fiber axis). Although, no shift in the peak was

observed after plasma treatment, the peak intensity was observed to be significantly higher after DBD plasma treatment. This increase in the peak intensity suggests the increase in regularity of the low *d*-spacing structure and development of more compact crystalline form leading to structural compactness of chitosan films after DBD plasma treatment (Qun et al., 2007).

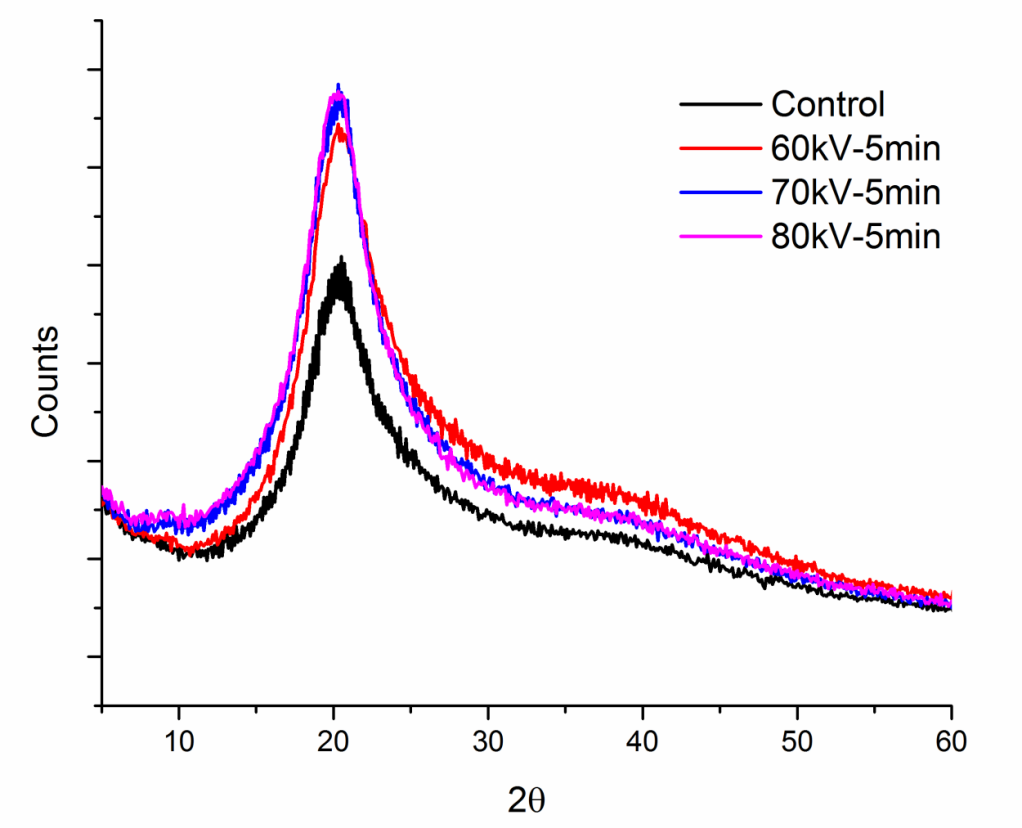

Figure 39. X-ray diffraction patterns of control and DBD plasma treated chitosan films.

The spectrum of control and DBD plasma treated chitosan films showed no change in the characteristic peaks of amide I at 1650 cm^{-1} (C=O stretching), amide II at 1554 cm^{-1} (N-H in plane deformation coupled with C-N stretching), amide III (C -N stretching coupled with NH in plane deformation) and CH_2 wagging coupled with OH in plane deformation at 1317 cm^{-1}

(Amaral et al., 2005). In the fingerprint region (Figure 40), peaks were observed at 1150 cm^{-1} (asymmetric bridge oxygen stretching), 1060 and 1030 cm^{-1} (C-O stretching in ether group), 990 and 950 cm^{-1} (CH_3 rocking), 900 cm^{-1} (C-O ring stretching), 925 and 850 cm^{-1} (C-C bond). The increases in the oxygen containing peaks are in good agreement with the results obtained from XPS analysis. It can be concluded from these results that DBD plasma treatment increase the oxygen content of the chitosan film without any significant change in the amide bonds.

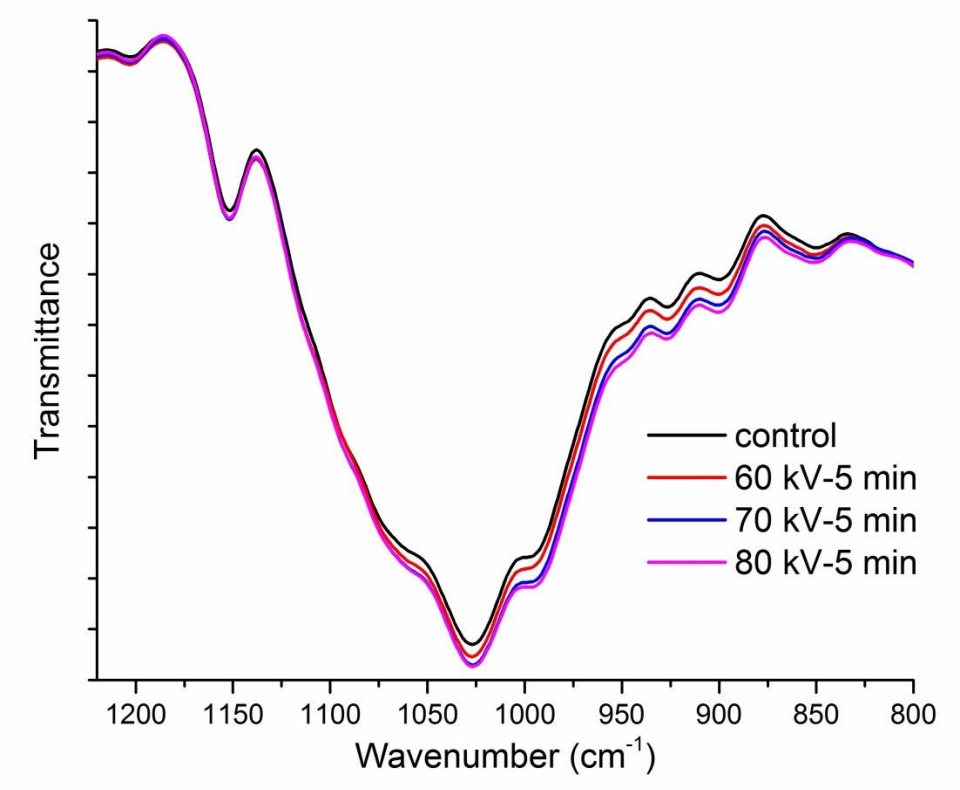

Figure 40. FTIR-ATR spectra of control and DBD plasma treated chitosan films

9.2.3. Contact angle and surface free energy

Film hydrophilicity is an important characteristic for deciding the packaging application of any polymer. The contact angle was analysed for the control and plasma treated films and results are shown in Table 29. Control chitosan film has a contact angle of 76° which was significantly reduced after plasma treatment showing an increase in the hydrophilicity of the film.

Table 29. Contact angle (A) and surface free energy (B) analysis of control and plasma treated chitosan films

A. Contact angle	**Parameters**	**Control**	**60kV-5min**	**70kV-5min**	**80kV-5min**
Water	θ_w	76.09±0.71	57.69±0.23	46.43±1.80	27.56±0.07
Ethylene glycol	θ_e	57.68±1.14	51.54±1.73	40.21±1.23	22.42±0.20
B. Surface free energy					
Fowkes	γ^{tot}	28.83	46.86	57.94	75.33
	γ^{d}	13.38	3.64	3.58	2.84
	γ^{p}	15.45	43.22	54.36	72.49

The surface free energy for the plasma treated films was also calculated from the contact angle (Table 4B). Surface free energy analysis of control and plasma treated chitosan films shows a significant and linear increase in the total SFE. A significant decrease in the dispersive component and simultaneously, significant increase in the polar component of the SFE was observed. These observations show that DBD plasma treatment of chitosan films increased the amount of polar groups on the film surface, increasing the polar component and

total SFE of the films. These results also support the XPS observation which shows an increase in surface oxygen content and possible increases in polar groups like O-C-O.

9.2.4. Barrier properties

Water vapor and oxygen permeability are important barrier properties for any polymer and it is desired that any new processing technology should not adversely change the barrier properties of the packaging films. WVTR of control chitosan film was found to be 37.32 ± 1.53 $g.m^{-2}.day^{-1}$. No significant difference ($p>0.05$) were observed in the WVTR of DBD plasma treated films all voltage levels and treatment times. OTR*e of control chitosan film was observed to be 0.17 ± 0.11 $cm^3.mm.m^{-2}.day^{-1}$ and no significant difference ($p>0.05$) were observed after the plasma treatment for all treatment voltages and times. These results are particularly important for potential application of chitosan films and to fit in as a competitive commercial food packaging material for DBD plasma processing.

9.3. Conclusion

DBD plasma treatment of chitosan films increased its surface roughness. However, the surface etching by plasma was found to be significantly less compared to other biopolymers. XRD results also demonstrated an increase in the structural compactness of plasma treated chitosan films. XPS and FTIR spectra confirm the increase in the oxygen containing groups in the chitosan film after plasma treatment. No significant change was observed in barrier properties of the chitosan film after DBD plasma treatment. These results indicate that chitosan films are robust for use along with DBD plasma treatment and serve as good potential to be used for plasma processed products.

Chapter 10 Antimicrobial zein film

10.1. Introduction

Zein, the major storage corn protein having a high content of hydrophobic amino acids, which has been extensively used to produce biodegradable films (Shukla and Cheryan, 2001). Zein films are glossy, hydrophobic, greaseproof and resistant to microbial attack ensuring its suitability as coatings and packaging films for food products (Shi et al., 2009, Shukla and Cheryan, 2001). An important factor that could promote zein as industrial polymeric material for food packaging applications is the incorporation of antimicrobial compounds into its matrix (Del Nobile et al., 2008). Antimicrobial food packaging is a form of active packaging, which acts to reduce, inhibit or retard the growth of microorganisms that may be present in the packed food or packaging material itself (Appendini and Hotchkiss, 2002b). The use of antimicrobial packaging material offers promise for enhancing the efficacy of existing antimicrobial agents and minimising environmental problems by reducing their residual toxicity, increasing efficiency and selectivity, and prolonging their lifetime (Kenawy et al., 2007).

The uses of natural plant extracts, like essential oils, as antimicrobial additives are perceived safe and are claimed to alleviate safety concerns (Suppakul et al., 2003). Essential oils are aromatic oily liquids obtained from plant material like flowers, buds, seeds, leaves, twigs, bark, herbs, wood, fruits and roots (Burt, 2004). Essential oils are complex natural mixtures containing hydrocarbons (mainly terpenoids) and oxygenated compounds (alcohols, esters, ethers, aldehydes, ketones, lactones, phenols and phenol ethers) (Stefanakis et al., 2013). Essential oils, such as eugenol, thymol, and plants extracts and spices, like rosemary or

cinnamon are the most commonly used natural active compounds for development of effective packaging systems (Mastromatteo et al., 2009). Thymol is most abundantly found in thyme (*Thymus vulgaris*) (10-64%) and oregano (*Origanum vulgare*) (traces-64%), formed via p-cymene from γ-terpinene (Marino et al., 1999, Burt, 2004, Kokkini et al., 1997). The study conducted by Dorman and Deans (2000) on the effect of six plant volatile oils against twenty-five bacterial strains concluded that thymol has a very wide spectrum of antibacterial activity.

10.2. Results and discussion

10.2.1. Surface Characteristics

The surface topographies of control and plasma treated antimicrobial zein films by atomic force microscopy are shown in Figure 41. The roughness parameters for the control and plasma treated zein film surface is presented in Table 30. It is clear from these results that the DBD plasma treatment leads to increase the surface roughness of zein films. The surface topography of untreated antimicrobial zein films is very smooth with root mean square roughness of only 26 nm while after DBD plasma treatment at 70 kV for 5 minutes, the R_{rms} of treated films is in the order of 100 nm. The increase in surface roughness after DBD plasma treatment was attributed to the etching effect of DBD plasma. The etching effect of plasma is already being employed for surface functionalisation and cleaning purposes (Pankaj et al., 2014a), but this study also suggests that the etching effect of plasma also plays an important role in controlling the release kinetics of active compounds from an active packaging material.

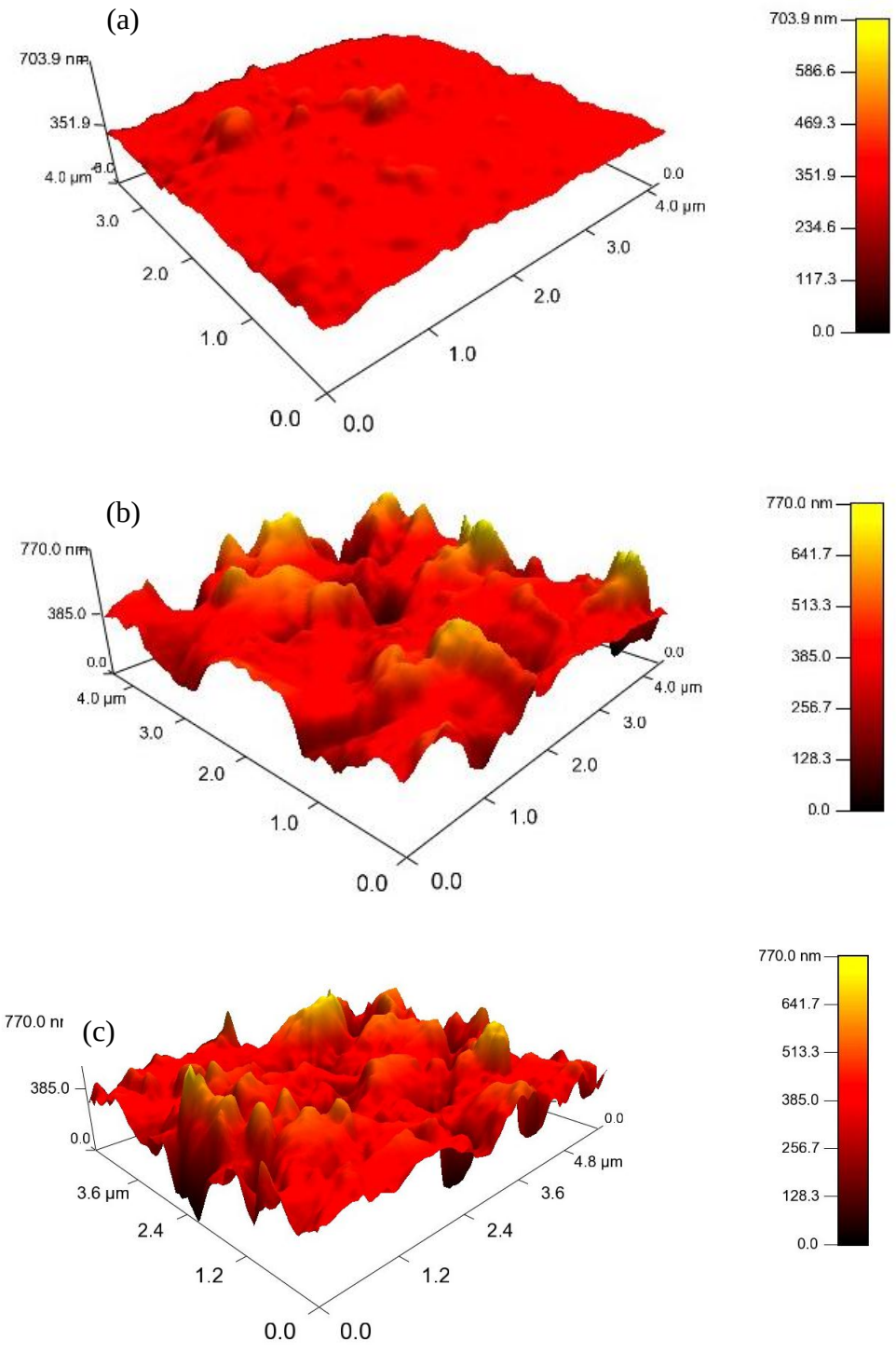

Figure 41. AFM images of the surface of (a) untreated and (b) plasma-treated antimicrobial zein (10 %) film (c) plasma-treated antimicrobial zein (20 %).

Table 30. Roughness parameters for untreated and plasma treated antimicrobial zein films (R_{rms}: root mean square roughness, R_{Peak}: Highest peak, R_{Groove}: lowest groove)

Characteristics	Untreated	Plasma-treated antimicrobial zein (10 %)	Plasma-treated antimicrobial zein (20 %)
R_{rms} (nm)	26.0 ± 18.9	118.1 ± 88.9	99.9 ± 74.7
R_{Peak} (nm)	143.4 nm	519.9 nm	337.9
R_{GROOVE} (nm)	-100.1	-466.9	-398.0
Skew	0.88	-0.109	-0.527
Kurtosis	2.86	1.23	1.3

10.2.2. Thermal Properties

The main indicators of thermal and structural changes are presented in Table 31. In general terms, TGA curves for films showed more than one degradation step. Large changes in the initial degradation temperature were observed after plasma treatment for the blank film. A strong thermal stabilization of the zein film without the antimicrobial agent was achieved after plasma treatment, which is consistent with the observations recorded for neat poly (lactic acid) films (Pankaj et al., 2014b). However, for the samples containing thymol, slight changes were observed after plasma treatment, suggesting that the thermal stabilization in these films could be predominantly due to thymol.

On the other hand, plasticized films with thymol showed three degradation steps. The first event was observed at temperatures around 80 °C and it was related to the loss of ethanol remaining from the casting process. The second stage at temperatures between 200 and 300 °C could be related to the loss of glycerol and thymol from the material. Finally, the third

degradation process, at temperatures above 300 °C, was associated with the protein thermal degradation.

The glass transition temperature of untreated films decreased as thymol concentration increased in the blends, as it was expected, since the organic nature of thymol makes it highly compatible with the zein protein and also acts as natural plasticizer in the blends, promoting chain mobility. Blank zein films showed a slight increase in the T_g after plasma treatment, which can be also correlated to the increase in T_5, suggesting some degree of crosslinking at the surface level, limiting the chain motion in the rubbery state. A similar increase in Tg was also observed for the treated antimicrobial films although it remained below the control zein film for all plasma-treated antimicrobial films. DSC thermograms also suggested that the plasticizer and protein remained a homogeneous material throughout the cooling and heating cycle due to the absence of any phase separation (separated glass transition temperature or melting and crystallization peaks) between the plasticiser and film.

Table 31. Initial degradation temperature (T_5, mass loss = 5 %) and glass transition temperature (T_g) for treated and untreated zein films.

Sample	T_5 (°C)	T_g (°C)
Control-0%	88.1	57.3
Control-10%	146.5	53.3
Control-20%	146.1	47.9
Plasma treated-0%	157.9	59.4
Plasma treated-10%	147.1	53.5
Plasma treated-20%	142.1	50.9

10.2.3. Release kinetics of thymol

Methodologies for determining the diffusion of additives from the packaging films have been widely discussed in literature (Han and Floros, 1998, Gnanasekharan et al., 1997, Arvanitoyannis et al., 1994, Buonocore et al., 2003). In the present study, the antimicrobial compound (thymol) was entrapped into the polymer matrix of zein film. When the film comes in contact with aqueous solution, firstly the water molecules penetrate into the matrix leading to its swelling and making the meshes of the polymeric network wider, allowing the active compound to diffuse through the matrix into the outer solution until a thermodynamic equilibrium between outer solution and polymer is reached. Therefore, the release of thymol from zein films depends upon the following phenomena: (1) water diffusion; (2) macromolecular matrix relaxation kinetics; (3) diffusion of the active compound trough the swollen polymeric network (Buonocore et al., 2003). Fick's second law of diffusion describes species concentration change as a function of time and position. For unidirectional diffusion, it can be written as equation 5 (Crank, 1975).

$$\frac{\partial C_a}{\partial t} = D\frac{\partial^2 C_a}{\partial x^2} \tag{5}$$

where C_a is the concentration of the diffusing substance; D is diffusivity; x is the coordinate dimension in the direction of transport; and t is time.

Since the aim of this work was to assess the change in the thymol release kinetics due to DBD plasma treatment, a simple approach, such as reported by Mastromatteo et al. (2009), has been used, which assumes that both water diffusion and macromolecular matrix relaxation are much faster than the active compound diffusion through the swollen network, with a negligible change in film size due to swelling. Based on that, Fick's second law

intended for a plane sheet with a constant boundary condition and uniform initial concentration can be reported as Equation 6.

$$M(t) = M_{eq}\left[1 - \frac{8}{\pi^2}\sum_{n=0}^{\infty}\frac{1}{(2n+1)^2}.\exp\left\{\frac{-D.(2n+1)^2.\pi^2.t}{h^2}\right\}\right] \quad (6)$$

where M(t) is the amount of thymol released (ppm) at time t (h), M_{eq} is the amount of thymol released at equilibrium conditions (ppm), D is the thymol diffusion coefficient ($cm^2\ s^{-1}$) through the swollen polymeric matrix and h is the film thickness (cm).

A significant increase ($p < 0.05$) in the thymol diffusion coefficient after DBD plasma treatment was observed for both thymol concentration levels. The parameters after fitting experimental values to Fick's equation are presented in Table 32. It should be noted at this point that although different release rates after DBD plasma treatment were observed, the equilibrium thymol concentration in the solution remained at the same level of 160 ppm for antimicrobial zein film containing 10 % thymol and 341 ppm for film containing 20 % thymol. It is also evident from the data shown in Figure 42 that the proposed model satisfactorily described the experimental data and, in this specific case, thymol mass transport could be described through Fick's Second Law. The increase in the diffusion rate of thymol after DBD plasma treatment can be correlated with the etching effect leading to the increase in surface roughness and which in turn reduced the effective zein thickness and exposed thymol for an accelerated release from the zein film.

Table 32. Parameters obtained by fitting Eq (2) to experimental data (Mean±Standard deviation). Values with different superscript letters, are significantly different ($p \leq 0.05$).

Zein films	D	M_{eq}
10%-Control	$4.2X10^{-6a}$	160.6 ± 1.7^{a}
10%-Plasma treated	$1.9X10^{-5b}$	160.7 ± 0.1^{a}
20%-Control	$4.7X10^{-6a}$	341.1 ± 3.4^{b}
20%-Plasma treated	$1.6X10^{-5c}$	342.8 ± 0.1^{b}

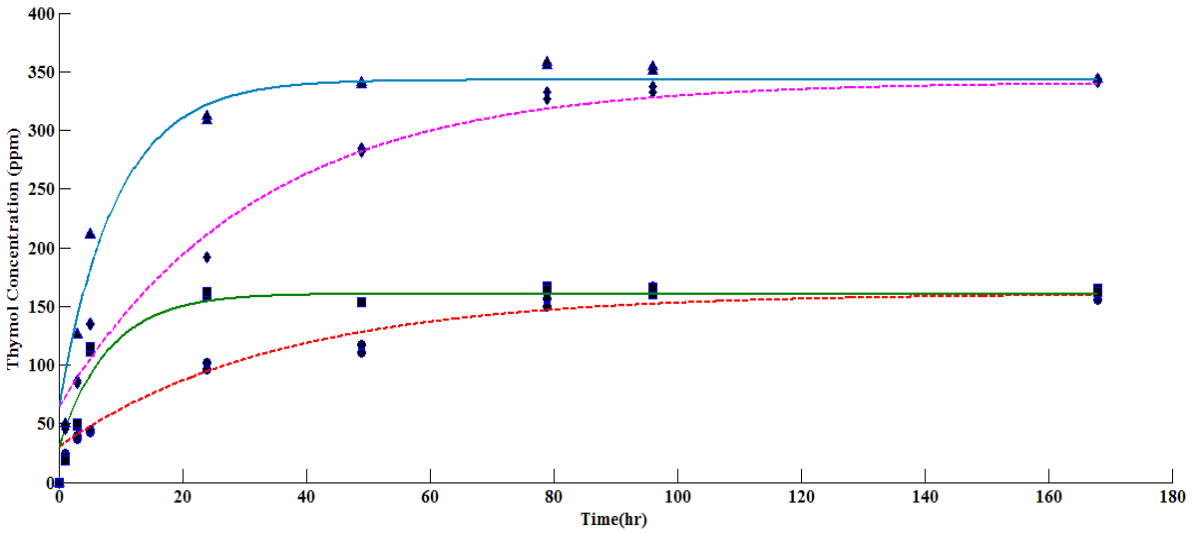

Figure 42. Release kinetics of thymol from zein films after plasma treatment. (•)10 %-Control, (■)10 %-Plasma treated, (⧫)20 %-Control, (▲)20 %-Plasma treated. The curves are the fitting experimental data to Fick's equation.

10.3. Conclusion

This study showed the effect of DBD plasma treatment on zein films containing thymol as an active ingredient. The significant increase ($p < 0.05$) in film roughness showed the etching effect of the DBD plasma which could also be correlated with the significant increase ($p < 0.05$) in the thymol diffusion rate in the food simulant. No significant changes ($p > 0.05$) in

the thermal properties of antimicrobial zein films were observed after plasma treatment, although increased thermal stability was seen for blank zein films. Control of kinetic release parameters by plasma treatment could be a useful practice at food industry to tailor certain food requirements and extend shelf life under controlled conditions.

Chapter 11 Antimicrobial chitosan film

11.1. Introduction

Traditionally, roles of packaging materials were limited to containment, protection, convenience and communication without any unwanted interaction with the contained food. However, in recent years, a wide variety of packages and approaches have been employed to interact with the food to provide desirable effects (Cha and Chinnan, 2004). Active Packaging is the approach in which the package, the product, and the environment interact to prolong shelf life or enhance safety or sensory properties, while maintaining the quality of the product (Suppakul et al., 2003). Antimicrobial packaging is a form of active packaging which reduces, inhibit or retard the growth of microorganisms that may be present in the packed food or packaging material itself (Appendini and Hotchkiss, 2002b). Chitosan has gained significant attention in this regard and has been evaluated for numerous applications in the medical, food, agricultural, and chemical industries (Zivanovic et al., 2005). Chitosan (poly β-(1→4) N-acetyl-d-glucosamine) is a collective name for the group of partially and fully deacetylated chitin, which is the major constituent of the exoskeleton of crustaceans. Antimicrobial chitosan films prepared by incorporating various organic acids and essential oils have shown the ability to inhibit the growth of various indigenous or inoculated microbes (Aider, 2010, Dutta et al., 2009). Essential oils are of great interest as they are naturally obtained from plants, often added to food products as ingredients, and can also serve as active ingredient for antimicrobial packaging systems. Thymol is one of the widely reported essential oils which is abundantly found in thyme (*Thymus vulgaris*) (10–64%) and oregano (*Origanum vulgare*) (traces-64%), formed via p-cymene from γ-terpinene and has a very

wide spectrum of antibacterial activity (Burt, 2004, Dorman and Deans, 2000, Kokkini et al., 1997, Marino et al., 1999).

11.2. Results and discussion

11.2.1. Surface Characteristics

The surface topographies of control and plasma treated active chitosan films by atomic force microscopy are shown in Figure 43. The roughness parameters for the control and plasma treated film surfaces are presented in Table 33. It is clear from these results that the DBD plasma treatment leads to an increase in the surface roughness of chitosan films. The surface topography of untreated active chitosan films were observed to be smooth and homogenous with root mean square roughness of 7.2 nm. The Rrms of DBD plasma treated films at 70 kV for 5 minutes was found to be significantly ($p<0.05$) higher than the untreated film. Although etching effect after plasma treatment have many applications in the packaging industry, it has also potential to be used for controlling the release kinetics of active compounds from an active packaging film (Pankaj et al., 2014c).

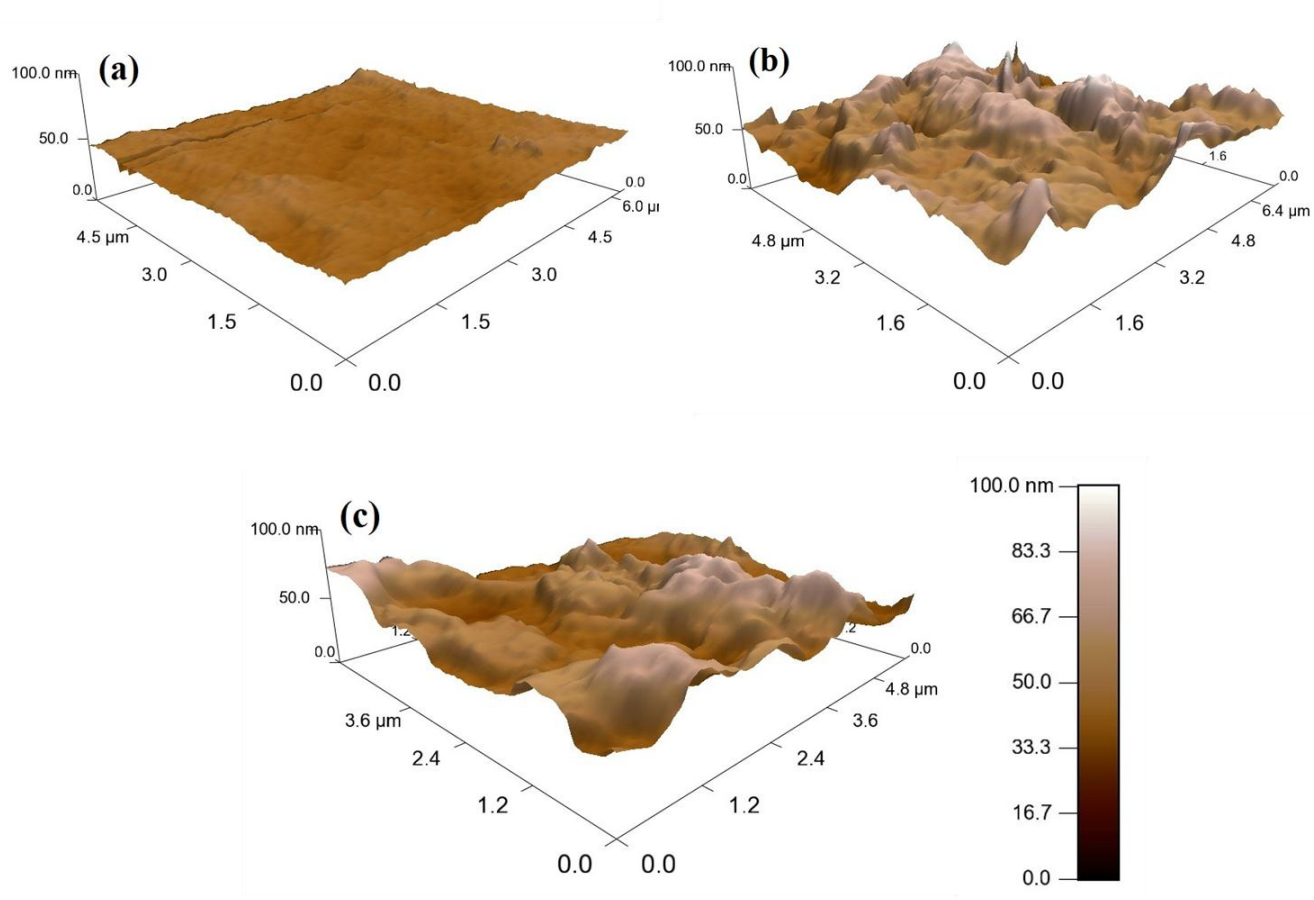

Figure 43. AFM images of the surface of (a) untreated and (b) plasma-treated active chitosan (2 %) (c) plasma-treated active chitosan (5 %) films.

Table 33. Roughness parameters for untreated and plasma treated active chitosan films (R_{rms}: root mean square roughness, R_{Peak}: Highest peak, R_{Groove}: lowest groove)

Characteristics	**Untreated active chitosan film**	**Plasma-treated active chitosan film (2 %)**	**Plasma-treated active chitosan film (5 %)**
R_{rms} (nm)	7.19	13.98	10.87
R_{Peak} (nm)	7.40	46.84	33.71
R_{GROOVE} (nm)	-20.13	-24.51	-20.33

Skew	0.342	0.115	0.784
Kurtosis	0.787	0.059	0.109

11.2.2. Thermal Properties

Thermogravimetric analysis was carried out in order to analyse the weight loss as a function of temperature for control and plasma treated active chitosan films and results are shown in Figure 44. Three different thermal behavior regions were observed in the TGA profile of all the active chitosan films. The slight weight loss below 100 °C was attributed to the moisture content of the samples. The weight loss observed at 220 °C was observed, which can be associated to glycerol evaporation (Leceta et al., 2015). No significant difference ($p>0.05$) was observed for the main stage weight loss due to the thermal and oxidative decomposition, vaporization and elimination of volatile products of chitosan at 285 °C (Neto et al., 2005).

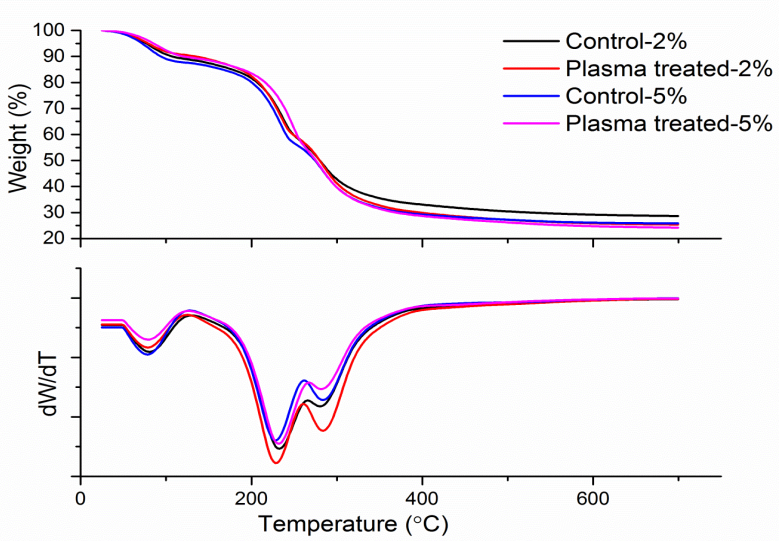

Figure 44. Thermogravimetric results for control and plasma treated active chitosan films

11.2.3. Release kinetics of thymol

The theory for the release kinetics has been discussed in detail in the previous chapter. In the present study also, it was assumed that the process occurred in a thin sheet of the active film, having a homogeneous thymol concentration distribution initially. Solvent absorption and solute diffusion occurred simultaneously and the thickness of the active film was considered to be very small in comparison with the width, so diffusivity was considered unidirectional and perpendicular to the surface of the sheet. When the film comes in contact with aqueous solution, firstly the water molecules penetrate into the matrix leading to its swelling and making the meshes of the polymeric network wider, allowing the active compound to diffuse through the matrix into the outer solution until a thermodynamic equilibrium between outer solution and polymer is reached. The parameters after fitting the experimental values to Equation 6 are reported in Table 34. As clearly seen, a significant increase ($p < 0.05$) in the thymol diffusion coefficient after DBD plasma treatment was observed for both active films with different thymol concentration levels (Figure 45). The equilibrium thymol concentration in the solution was reached within 60 h and was different after DBD plasma treatment. The equilibrium thymol concentrations for 2 % and 5 % thymol containing chitosan film were 5.9 ppm and 13.7 ppm respectively. The increase in the diffusion rate of thymol after DBD plasma treatment can be correlated with the etching effect leading to the increase in surface roughness, which in turn reduced the effective film thickness and exposed thymol for an accelerated release from the active film.

Table 34. Parameters obtained by fitting Eq (6) to experimental data. Values represented as Mean ± Standard deviation. Means, which are not followed by a common superscript letter, are significantly different ($p \leq 0.05$).

Active chitosan films	D ($cm^2.s^{-1}$)	M_{eq}(ppm)
2%-Control	$4.47X10^{-7a}$	5.91 ± 0.41^{a}
2%-Plasma treated	$7.70X10^{-7b}$	5.80 ± 0.20^{a}
5%-Control	$3.14X10^{-7c}$	13.70 ± 1.34^{b}
5%-Plasma treated	$6.18X10^{-7d}$	13.78 ± 0.85^{b}

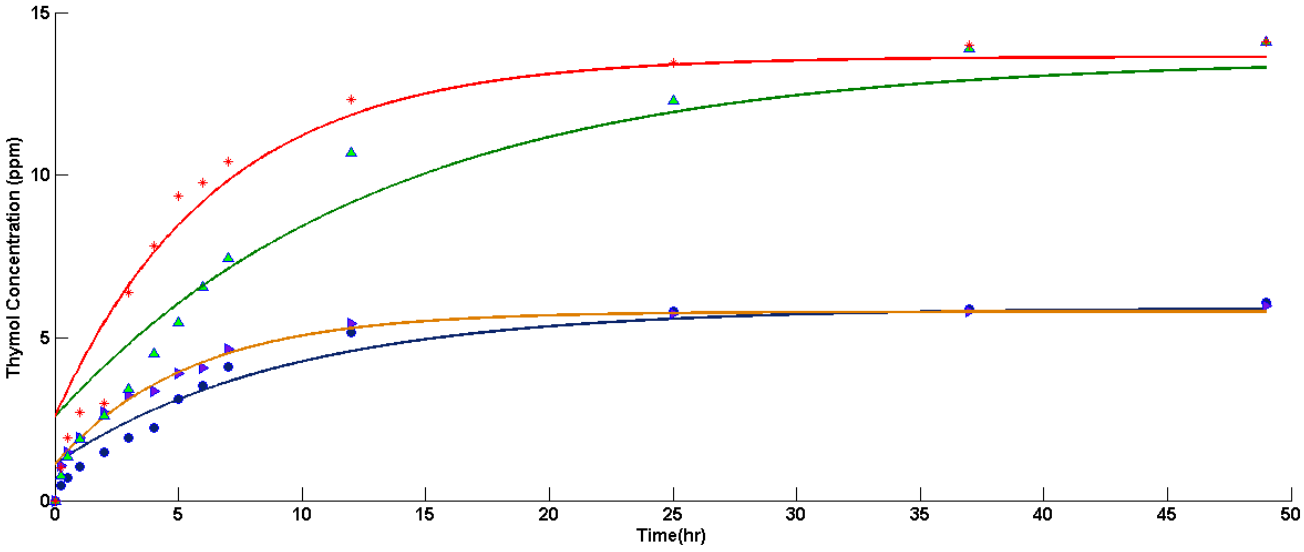

Figure 45. Release kinetics of thymol from chitosan films after plasma treatment in water. (●)2 %-Control, (►)2 %-Plasma treated, (▲)5 %-Control, (✦)5 %-Plasma treated. The curves are the fitting experimental data to equation 6.

11.3. Conclusion

This study showed the effect of DBD plasma treatment on antimicrobial chitosan films containing thymol as an active ingredient. A significant increase ($p < 0.05$) in the film surface roughness was observed. No significant changes ($p > 0.05$) in the thermal properties of antimicrobial chitosan films were observed after plasma treatment. A significant increase ($p < 0.05$) in the thymol diffusion rate in the food simulant was also observed. Control of release kinetics of an active ingredient from any antimicrobial film could serve as an important tool for tailoring certain food requirements and extend shelf life under controlled conditions.

Chapter 12 Oxygen sensors

12.1. Introduction

Non-thermal plasma has been used for decades in the packaging industry for surface modification and functionalisation of various polymers. However, in recent years non-thermal plasma has also drawn interest of various researchers as novel in-package food decontamination technology. This approach involves generation of NTP inside a sealed package by placing it between a high voltage and a ground electrode. Upon exposure to a sufficiently high voltage, the gas contained in the package is partly ionised, generating significant amounts of reactive species, which in turn leads to decontamination of the enclosed products. The effectiveness of this approach for microbial decontamination has been already reported by Connolly et al. (2013), Ziuzina et al. (2014) and Patil et al. (2014).

Since non-thermal plasma has also shown its potential application with various food products in which intelligent packaging systems are used, it became important to analyse the effectiveness of intelligent packaging systems in association with DBD plasma treatments. Intelligent packaging can be defined as a packaging system that is capable of carrying out intelligent functions (such as detecting, sensing, recording, tracing, communicating, and applying scientific logic) to facilitate decision making to extend shelf life, enhance safety, improve quality, provide information, and warn about possible problems (Yam et al., 2005). Package integrity is an essential requirement for the maintenance of quality and safety of food products in modified atmospheric packaging (MAP) and optical solid-state gas sensors offer an alternative, non-invasive approach to traditional destructive techniques to determine the package integrity (Vanderroost et al., 2014). The most important gases in MAP products

are oxygen and carbon dioxide and their headspace partial pressures serve as useful indicators of the quality status of food products (Kerry et al., 2006). Among these, oxygen indicators are the most common for food packaging applications, because oxygen in air can cause oxidative rancidity, color change, and microbial spoilage (Yam et al., 2005). In this study, two different types of phosphorescent solid-state oxygen sensors were used under atmospheric air and modified-air (30% CO_2 + 70% N_2) conditions for analysing the compatibility of these oxygen sensors with the in-package DBD plasma treatment.

12.2. Results and discussions

12.2.1. Initial screening of treated sensors

The two sensor types are based on the same reporter dye (PtBP), but different matrix polymer and fabrication process. The Optech sensor comprises a thin-film solid-state coating of a dye-polymer composition on light-scattering support. The second type comprises a microporous PP membrane impregnated with the dye by soaking/swelling in organic solvent. Both sensors are read by an Optech handheld reader.

Both the sensors were initially tested for changes in phosphorescence life time and intensity after DBD plasma treatments under air and nitrogen gas (Table 35). Sensor A has shown no significant ($p>0.05$) difference after DBD plasma treatment in modified atmospheric conditions while a significant ($p<0.05$) increase in the life time was observed when treated under air plasma. For sensor B, DBD plasma treatment showed insignificant changes under modified atmospheric condition, although no signals were observed when treated with air plasma.

The difference in the behavior of sensors under these two different gas conditions can be attributed to the difference in the reactive species generated and their reaction with the sensor components (the phosphorescent dye and matrix polymer) resulting in sensor degradation or altered behavior (calibration, intensity signals, etc.). In both gases, nitrogen was a common constituent, so the observed changes were primarily due to the difference in reactive species formed by oxygen and carbon dioxide gases. A detailed study on the reactive species generation and reaction mechanisms for air plasma has been described by Dorai and Kushner (2003) and for CO_2 plasma by Médard et al. (2002). Based on these studies, it can be concluded that the PtBP dye of the sensor B was more susceptible to the reactive species generated during the air plasma and was largely degraded. The difference in the gas mixture used for packaging of food products will be one of the deciding factors for the selection of right type oxygen sensor for plasma processing applications.

Table 35. Screening results of both oxygen sensors for sensor intensity (I) and lifetime (τ) signals in N_2 (0 kPa O_2) and air (21 kPa O_2). AC: Control sensor A, APA: sensor A plasma treated with atmospheric air, APM: sensor A plasma treated with modified air, BC: control sensor B, BPA: sensor B plasma treated with atmospheric air, BPM: sensor B plasma treated with modified air.

Sensors	**τ_0 (µs)**	**τ_{21} (µs)**	**I_0**	**I_{21}**
AC	49.37±0.55	19.88±0.27	34879±826	10751±736
APA	47.24±0.02	25.08±0.03	39462±335	20284±208
APM	50.11±0.12	19.79±0.16	26671±1020	8565±373

BC	47.54±0.06	15.72±0.37	4128±734	1713±329
BPA	ns	ns	ns	Ns
BPM	50.27±0.23	17.02±1.11	3701±1029	1548±116

*ns: no signal

12.2.2. Changes in sensor calibration

Phosphorescent oxygen sensors produce a reversible non-chemical (phosphorescence quenching) response to oxygen. Sensors in packaged foods are used on disposable basis, without any calibration (batch or factory calibration is provided by manufacturer). If DBD treatment alters sensor calibration/performance, this will result in compromised accuracy and reliability of oxygen measurements by those sensors.

Full O_2 calibrations (0–100 kPa) were performed for both sensors to cover the whole O_2 ranges in which food products are stored and in which oxygen sensors can be used. For sensor A at 20 °C going from 0 kPa to 21 kPa oxygen, the lifetime signals of AC sensors decreased from 48.27±0.02 to 20.42±0.07 µs. The signals for APM sensors also displayed a similar decrease while for APA sensors the lifetime signals were significantly higher than the other two, in the 2 kPa to 21 kPa oxygen range. The full O_2 calibration curve and corresponding Stern-Volmer plots for sensor A are shown in Figure 46. The Stern-Volmer plots can be related with sensor homogeneity and quenching. Lower Stern-Volmer constants reflect lower sensitivity of the sensor to oxygen (Kelly et al., 2014). The Stern-Volmer constant for AC, APA and APM sensors were found to be 0.068, 0.044 and 0.071 kPa^{-1} respectively. As evident for the data, DBD plasma treatment under air reduced the oxygen

sensitivity of APA sensors while DBD plasma treatment under modified atmosphere had an insignificant effect on the oxygen sensitivity of APM sensors.

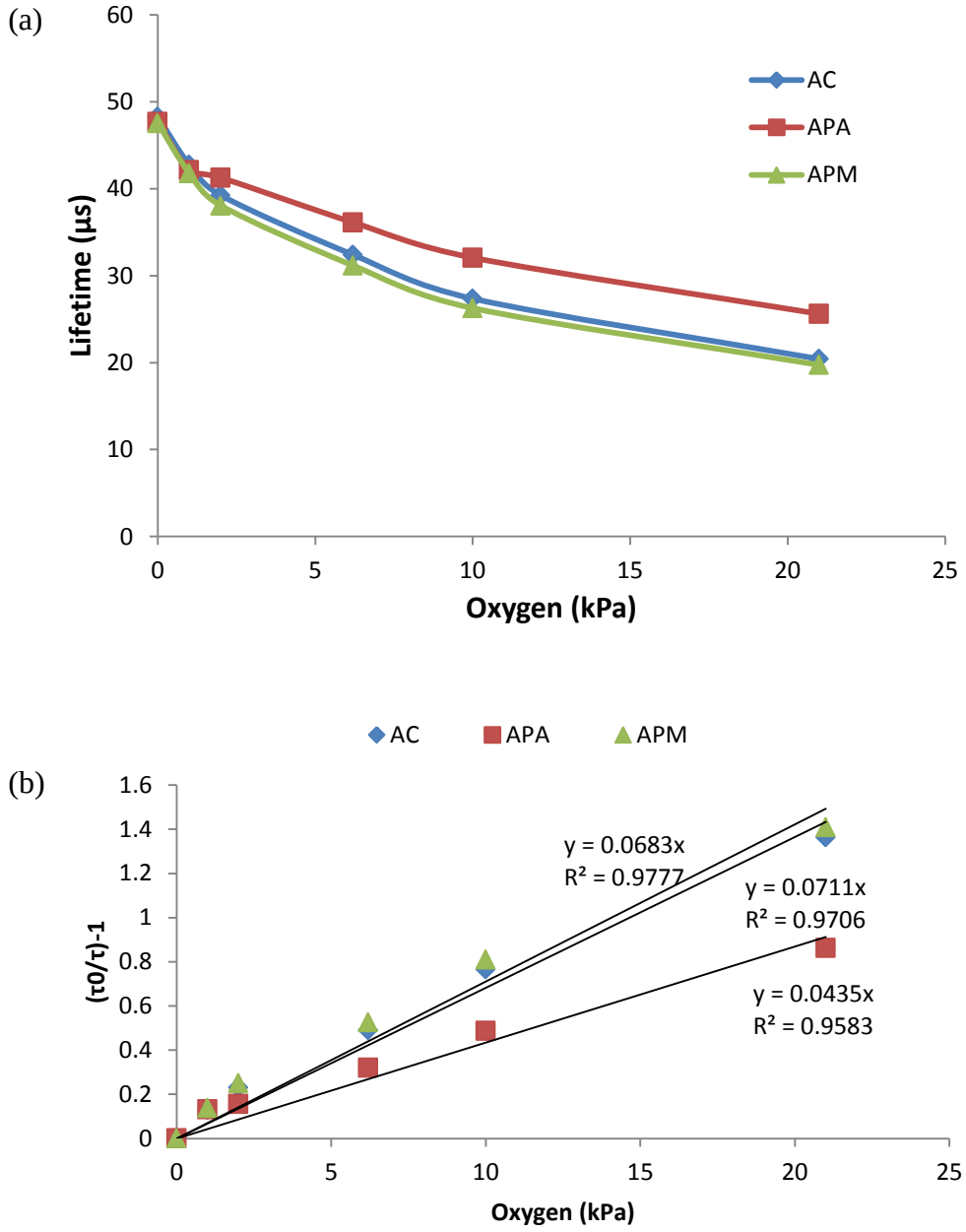

Figure 46. (a) Oxygen calibration curve of sensor A in dry gas presented in lifetime scale. (b) Corresponding Stern-Volmer plots. AC: Control sensor A, APA: sensor A plasma treated with atmospheric air, APM: sensor A plasma treated with modified air.

A full O_2 calibration curve (0 to 100 kPa) was also performed for sensor B. Since, there was no signal observed for sensor B treated by DBD plasma under air, results are only shown for BC and BPM sensors (Figure 47). The life time signal of BC sensors decreased from 46.27±0.01 to 7.63±0.01 µs from 0 to 100 kPa of oxygen. The DBD plasma treated BPM sensors also displayed a similar trend. Based on the Stern-Volmer constants, no significant change in the oxygen sensitivity was observed after DBD plasma treatment under modified atmospheric conditions.

(a)

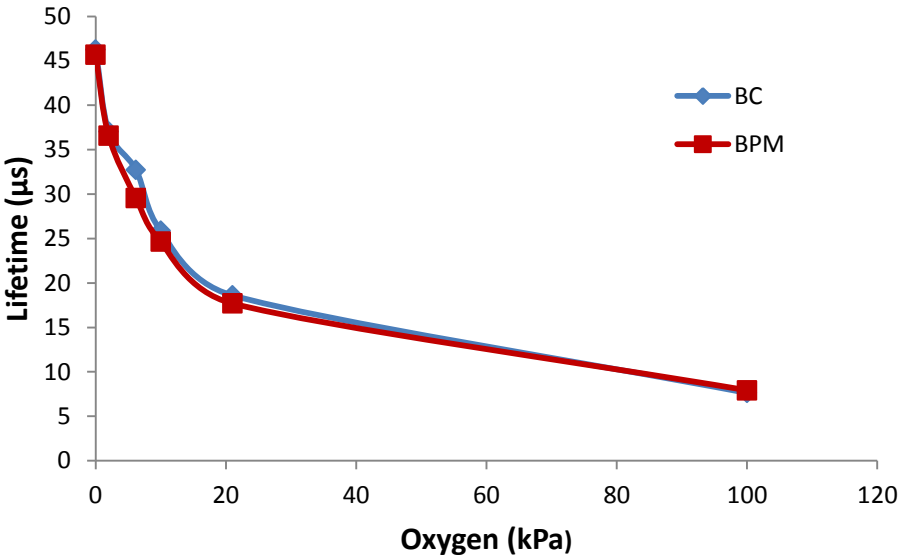

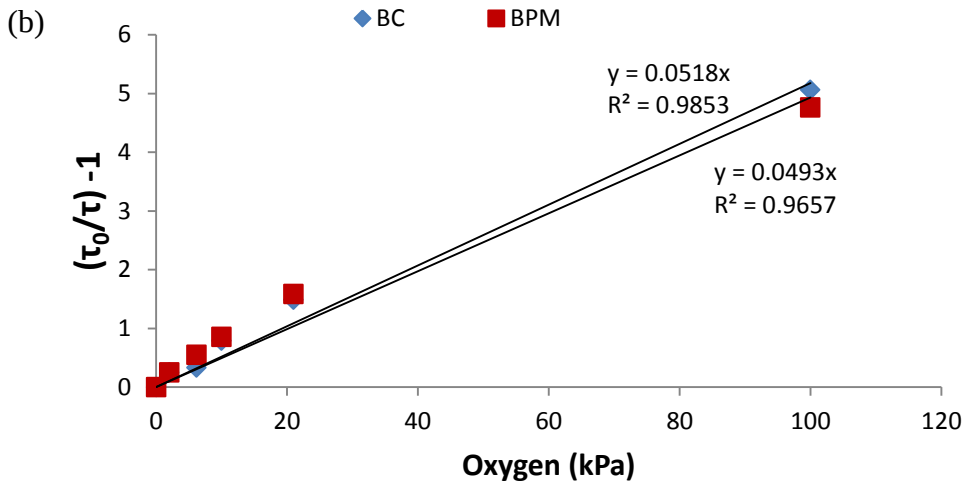

Figure 47. (a) Oxygen calibration curve of sensor B in dry gas presented in lifetime scale. (b) Corresponding Stern-Volmer plots. BC: control sensor B, BPM: sensor B plasma treated with modified air.

12.2.3. Effects of humidity and temperature

Oxygen calibrations of all the sensors were also performed under humid gas condition and at three different temperatures to analyse the effects of humidity and temperature after DBD plasma treatment. Under humid gas conditions, no significant difference was observed in the sensor signals after DBD plasma treatments. Also the temperature dependence of the sensors was also found not to be affected by the DBD plasma treatment (Figure 48). The negative slopes indicate that the phosphorescent lifetime decreases as the temperature increases (Kelly et al., 2014). For a narrow T-range, a linear dependence of lifetime is desirable which was not affected by the DBD plasma treatments.

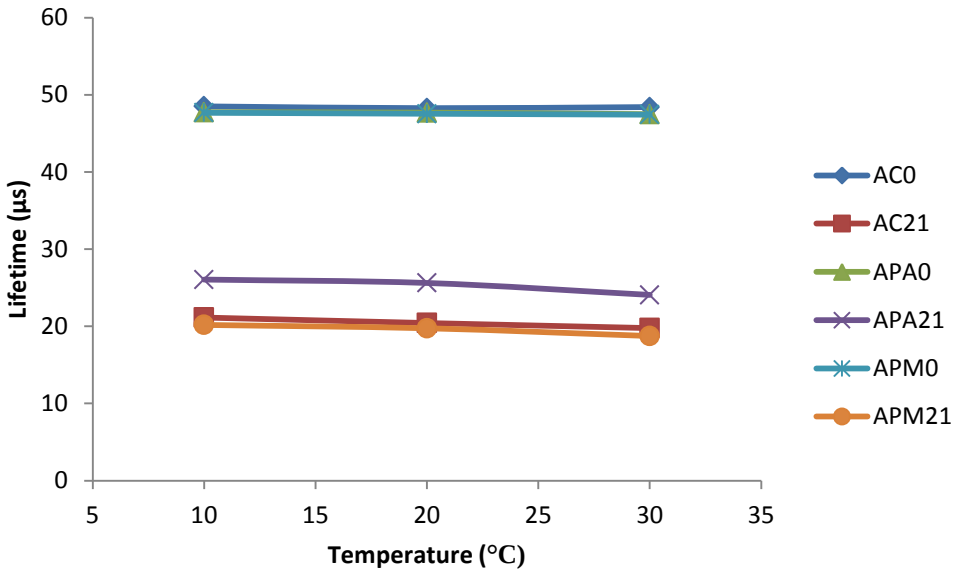

Figure 48. Temperature dependence of sensor A at 0 and 21 kPa in dry O_2 gas

12.2.4. Reversibility and photo-stability

Reversible operation, quick response time and high photo-stability are the essential criteria for practical applications of oxygen sensors (Banerjee et al., 2015). The response ($t_{90}\downarrow$) and recovery ($t_{90}\uparrow$) times of all the sensors are reported in Table 36. The response and recovery times of both the sensors A and B were not affected by the DBD plasma treatments.

The photo-stability studies of DBD plasma treated sensors under prolonged exposure also show no measurable photodegradation which is also a desirable criterion for sensors selection and applications.

Table 36. $t_{90}\downarrow$ and $t_{90}\uparrow$ times for control and plasma treated sensors A and B in dry gas at 20°C.

Sensors	$t_{90}\downarrow$(µs)	$t_{90}\uparrow$ (µs)
AC	16	22
APA	17	23
APM	17	23
BC	16	21
BPA	ns	ns
BPM	18	29

*ns: no signal

12.3. Conclusion

A detailed study of DBD plasma treatment of two different phosphorescent oxygen sensors under different gas conditions has been presented. For modified atmospheric gas packaging, both Optech™-O_2 platinum and PP PtBP sensors were found to be effective for oxygen sensing and there was no significant change in the sensors' characteristics after DBD plasma treatment. However, in the case of in-package air packaging, soaked PtBP sensors were largely degraded and were found to be incompatible with plasma processing. Although some changes in the lifetime signals were observed for Optech™-O_2 platinum sensors, they were still found to be effective for O_2 measurement. However, re-calibration will be needed post-plasma treatment as the original calibration obtained with the calibration card is no longer valid. This study also indicates that in-package gas composition of food products plays an

important role in selection of the right intelligent optochemical sensors for plasma processing. Further studies will be required for development of new sensors which can be used under a wide range of gas mixtures for plasma processed food products.

Chapter 13 Conclusions and future recommendations

13.1. General discussion and conclusions

This work focuses on the effects of cold plasma treatment on a wide range of bio-based polymers and smart packaging systems. The summary of observations on effects of cold plasma on bio-based films is presented in Table 37.

Table 37. Effects of cold plasma on bio-based films

	PLA	Zein	Caseinate	Starch	Gelatin	Chitosan
Surface roughness	↑(23 fold)	↑(8 fold)	↑(10 fold)	↑(4 fold)	↑(5 fold)	↑(3 fold)
Glass transition temperature	~	~	↓(24.2%)	Not observed	na	na
O/C ratio	↑*	na	↑(26.7 %)	↑(100 %)	↑(19.2 %)	↑(36.1 %)
Water contact angle	↓(27%)	↓(33.2%)	↓(28.6%)	↓(61.1%)	↓(54%)	↓(63.7%)
Total SFE	↑(21.9 %)	↑(22 %)	↑(28.6 %)	↑(30.8 %)	↑(9.7 %)	↑(161.5 %)
Polar SFE	↑(122.8 %)	↑(223.3 %)	↑(168.5 %)	↑(69.9 %)	↑(356 %)	↑(367.7 %)
OTR	~	na	~	~	~	~
WVTR	↑(52.1 %)	na	~	~	~	~
Structural change	No significant change	Re-organisation of inter-helical structure	Disruption of inter-helical structure	No significant change	Increase in triple helical structure	More structural compactness

*Based on FTIR results, ~Insignificant difference

Cold plasma treatment resulted in significant increase in surface roughness for all the films. However, the increase was observed less in case of polysaccharide films than the protein

films suggesting that polysaccharide films are more resistant to plasma etching effect. The XPS results indicated that atmospheric air cold plasma treatment increased the surface oxygen content of the films which in turn resulted in the increase in the film hydrophilicity. The increase in the total free surface energy after cold plasma treatment can be attributed to the increase in the polar component which can be explained by the increase in the polar groups on the film surface after plasma treatment. No significant change in the thermal profile was observed in all the treated films, which is desirable as it negates any required changes in the film preparation and processing. No significant change in the barrier properties of the films were observed after plasma treatment (except water vapour permeability of PLA, which was also found to be within acceptable limits) which further shows the compatibility of bio-based films for plasma processing. Overall, these observations suggests that although cold plasma modified the surface and structural conformity of some films, it does not adversely affect the film properties important for food packaging applications and so biodegradable polymers has a huge potential to be used as primary packaging for cold plasma processed products.

The results of cold plasma treatment on antimicrobial films show similar results for surface and thermal properties of the films. The major significant difference observed in these films was the accelerated diffusion rate of active compound from the films. This increase in the diffusion rate was observed to be dependent on the etching effect of the plasma i.e. film with more susceptibility for plasma etching has more accelerated diffusion due to decrease in the effective film thickness. This observation may be further exploited for development of tailored antimicrobial films where the active compound release can be controlled depending on the product quality and expected shelf-life.

The last section of this work was focussed on accessing the compatibility of intelligent sensors for the in-package plasma decontamination processing. The results clearly showed that in-package gaseous environment is an important parameter for selection, accuracy and reliability of the sensors. The presence of oxygen in the package headspace resulted in degradation of one of the sensors showing the need for development of more robust intelligent sensors specifically for plasma processing for future application.

The general conclusions derived from this work are listed as follows:

- ✓ DBD plasma increased the surface roughness of all the treated films. Among the evaluated polymers, the relative susceptibility for etching at same treatment level was observed in the order of: chitosan < corn starch < bovine hide gelatin < corn zein < sodium caseinate < PLA.
- ✓ DBD plasma increased the surface oxygen content of the treated polymers by increasing the amount of oxygen-containing polar groups such as C-O-H and C=O on the film surface.
- ✓ DBD atmospheric air plasma treatment also increased the film hydrophilicity. The increase in polar component of surface free energy was observed in all the evaluated polymers.
- ✓ Minimal or no changes were observed in the bulk structure and crystal structure of most of the polymers after DBD plasma treatment. However, reorganization of the protein conformational structure was observed for zein and gelatin films.
- ✓ No significant changes were observed after plasma treatment on the barrier properties (water vapor and oxygen permeability) of any of the evaluated polymers.

- ✓ In the case of active films, DBD plasma treatment increased the surface roughness and rate of diffusion of the active ingredient in the food simulants.
- ✓ Among the evaluated oxygen sensors, both Optech™-O_2 platinum and PP PtBP sensors were found to be suitable in the case of plasma treatment under modified atmospheric conditions. For air plasma treatment, only Optech™-O_2 platinum sensor was found to be suitable. However, re-calibration was deemed necessary post-plasma treatment as the original calibration obtained with the calibration card was no longer valid.

13.2. Future recommendations

DBD plasma treatment has been evaluated for food decontamination efficacy previously by various researchers and in this work its effects on the packaging films have been analysed. The effect of plasma treatment can be affected by the potential use of the polymers like as primary package, secondary package or edible coatings. The future work should include the evaluation of packaging films in actual food environments to determine if any effects from the food component interact with the packaging. In this work, barrier properties of all the films were measured at standard conditions. However, for commercial utilization of this technology, it will be important to measure the barrier properties of the films under realistic supply chain conditions as bio-based films are highly influenced by the environmental conditions.

DBD plasma creates different types of reactive species by various complex reactions. More works should be conducted in this area to fully understand the mechanisms behind the observed changes. Mathematical modeling of the structural changes in the plasma treated

polymers will also provide greater insights into the changes incurred by plasma at a molecular level.

In the case of active packaging systems, DBD plasma has shown potential to be used as a tool to control the release of active compounds. This area should also be considered for the development and application of innovative tailored active films where diffusion kinetics of entrapped active molecules can be externally controlled at any time during the shelf-life of product, providing a required dose response.

The present work on intelligent oxygen sensors warrants the need for further studies in the development of new sensors which can be used under wide range of gas mixtures for plasma processed food products. Further studies are also required to evaluate the compatibility of other sensors such as carbon dioxide sensors, freshness indicators and pathogen indicators with DBD plasma processing.

References

Achet, D. & He, X. W. 1995. Determination of the renaturation level in gelatin films. *Polymer,* 36, 787-791.

Adler, H. J., Fischer, P., Heller, A., Jansen, I., Kuckling, D., Komber, H., Lehmann, D., Piontek, J., Pleul, D. & Simon, F. 1999. Trends in polymer chemistry 1998. *Acta Polymerica,* 50, 232-239.

Aider, M. 2010. Chitosan application for active bio-based films production and potential in the food industry: Review. *LWT - Food Science and Technology,* 43, 837-842.

Akishev, Y., Grushin, M., Dyatko, N., Kochetov, I., Napartovich, A., Trushkin, N., Minh Duc, T. & Descours, S. 2008. Studies on cold plasma–polymer surface interaction by example of PP- and PET-films. *Journal of Physics D: Applied Physics,* 41, 235203.

Albert, S. & Mittal, G. S. 2002. Comparative evaluation of edible coatings to reduce fat uptake in a deep-fried cereal product. *Food Research International,* 35, 445-458.

Aliheidari, N., Fazaeli, M., Ahmadi, R., Ghasemlou, M. & Emam-Djomeh, Z. 2013. Comparative evaluation on fatty acid and Matricaria recutita essential oil incorporated into casein-based film. *International Journal of Biological Macromolecules,* 56, 69-75.

Almazan-Almazan, M. C., Paredes, J. I., Perez-Mendoza, M., Domingo-Garcia, M., Lopez-Garzon, F. J., Martinez-Alonso, A. & Tascon, J. M. 2005. Effects of oxygen and carbon dioxide plasmas on the surface of poly(ethylene terephthalate). *J Colloid Interface Sci,* 287, 57-66.

Almazan-Almazan, M. C., Paredes, J. I., Perez-Mendoza, M., Domingo-Garcia, M., Lopez-Garzon, F. J., Martinez-Alonso, A. & Tascon, J. M. 2006. Surface characterisation of plasma-modified poly(ethylene terephthalate). *J Colloid Interface Sci,* 293, 353-63.

Amaral, I. F., Granja, P. L. & Barbosa, M. A. 2005. Chemical modification of chitosan by phosphorylation: an XPS, FT-IR and SEM study. *Journal of Biomaterials Science, Polymer Edition,* 16, 1575-1593.

Andreuccetti, C., Carvalho, R. A. & Grosso, C. R. 2009. Effect of hydrophobic plasticizers on functional properties of gelatin-based films. *Food research international,* 42, 1113-1121.

Appendini, P. & Hotchkiss, J. H. 2002a. Review of antimicrobial food packaging. *Innovative Food Science & Emerging Technologies,* 3, 113-126.

Appendini, P. & Hotchkiss, J. H. 2002b. Review of antimicrobial food packaging. *Innovative Food Science and Emerging Technologies,* 3, 113-126.

Arrieta, M. P., Peltzer, M. A., Garrigós, M. D. C. & Jiménez, A. 2013. Structure and mechanical properties of sodium and calcium caseinate edible active films with carvacrol. *Journal of Food Engineering,* 114, 486-494.

Arvanitoyannis, I., Kalichevsky, M., Blanshard, J. M. V. & Psomiadou, E. 1994. Study of diffusion and permeation of gases in undrawn and uniaxially drawn films made from potato and rice starch conditioned at different relative humidities. *Carbohydrate Polymers,* 24, 1-15.

Arvanitoyannis, I., Psomiadou, E. & Nakayama, A. 1996. Edible films made from sodium casemate, starches, sugars or glycerol. Part 1. *Carbohydrate Polymers,* 31, 179-192.

Assis, O. B. G. & Hotchkiss, J. H. 2007. Surface hydrophobic modification of chitosan thin films by hexamethyldisilazane plasma deposition: effects on water vapour, CO2 and O2 permeabilities. *Packaging Technology and Science,* 20, 293-297.

Astm 2005. Standard Test Methods for Water Vapour Transmission of Materials. *American Society for Testing of Materials (ASTM)*.

Ataeefard, M., Moradian, S., Mirabedini, M., Ebrahimi, M. & Asiaban, S. 2009. Investigating the effect of power/time in the wettability of Ar and O_2 gas plasma-treated low-density polyethylene. *Progress in Organic Coatings,* 64, 482-488.

Audic, J. L., Poncin-Epaillard, F., Reyx, D. & Brosse, J. C. 2001. Cold plasma surface modification of conventionally and nonconventionally plasticized poly(vinyl chloride)-based flexible films: Global and specific migration of additives into isooctane. *Journal of Applied Polymer Science,* 79, 1384-1393.

Avena-Bustillos, R. J. & Krochta, J. M. 1993. Water Vapor Permeability of Caseinate-Based Edible Films as Affected by pH, Calcium Crosslinking and Lipid Content. *Journal of Food Science,* 58, 904-907.

Bai, J., Alleyne, V., Hagenmaier, R. D., Mattheis, J. P. & Baldwin, E. A. 2003. Formulation of zein coatings for apples (*Malus domestica* Borkh). *Postharvest Biology and Technology,* 28, 259-268.

Baldwin, E., Nisperos-Carriedo, M. & Baker, R. 1995. Edible coatings for lightly processed fruits and vegetables. *HortScience,* 30, 35-38.

Banerjee, S., Kuznetsova, R. T. & Papkovsky, D. B. 2015. Solid-state oxygen sensors based on phosphorescent diiodo-borondipyrromethene dye. *Sensors and Actuators B: Chemical,* 212, 229-234.

Banik, I., Kim, K. S., Yun, Y. I., Kim, D. H., Ryu, C. M. & Park, C. E. 2002. Inhibition of aging in plasma-treated high-density polyethylene. *Journal of Adhesion Science and Technology*, 16, 1155-1169.

Banu, M. S. 2012. Cold Plasma as a Novel Food Processing Technology. *International Journal of Emerging Trends in Engineering and Developments*, 4, 15.

Bárdos, L. & Baránková, H. 2010. Cold atmospheric plasma: Sources, processes, and applications. *Thin Solid Films,* 518, 6705-6713.

Bauer, S., Schmuki, P., Von Der Mark, K. & Park, J. 2013. Engineering biocompatible implant surfaces: Part I: Materials and surfaces. *Progress in Materials Science*.

Bertrand, P. & Poncin-Epaillard, F. 2003. Characterization of polypropylene surface treated in a CO_2 plasma. *Plasmas and polymers*, 8, 225-236.

Bertuzzi, M., Castro Vidaurre, E., Armada, M. & Gottifredi, J. 2007. Water vapor permeability of edible starch based films. *Journal of food engineering,* 80, 972-978.

Białopiotrowicz, T. & Jańczuk, B. 2001. The changes of the surface free energy of the adsorptive gelatin films. *European Polymer Journal*, 37, 1047-1051.

Bigi, A., Panzavolta, S. & Rubini, K. 2004. Relationship between triple-helix content and mechanical properties of gelatin films. *Biomaterials*, 25, 5675-5680.

Borcia, G., Anderson, C. A. & Brown, N. M. D. 2004. The surface oxidation of selected polymers using an atmospheric pressure air dielectric barrier discharge. Part I. *Applied Surface Science,* 221, 203-214.

Breen, A., Milosavljević, V. & Dowling, D. 2011. Influence of Gas Type on the Thermal Efficiency of Microwave Plasmas for the Sintering of Metal Powders. *Plasma Chemistry and Plasma Processing,* 31, 771-785.

Bronco, S., Bertoldo, M., Taburoni, E., Cepek, C. & Sancrotti, M. 2004. The Effects of Cold Plasma Treatments on LDPE Wettability and Curing Kinetic of a Polyurethane Adhesive. *Macromolecular Symposia,* 218, 71-80.

Brown, W. E. 1992. Plastics in food packaging: properties, design and fabrication. New York: Marcel Dekker Inc.

Buonocore, G. G., Del Nobile, M. A., Panizza, A., Bove, S., Battaglia, G. & Nicolais, L. 2003. Modeling the Lysozyme Release Kinetics from Antimicrobial Films Intended for Food Packaging Applications. *Journal of Food Science,* 68, 1365-1370.

Buonocore, G. G., Sinigaglia, M., Corbo, M. R., Bevilacqua, A., La Notte, E. & Del Nobile, M. A. 2004. Controlled Release of Antimicrobial Compounds from Highly Swellable Polymers. *Journal of Food Protection,* 67, 1190-1194.

Burgos, N., Martino, V. P. & Jiménez, A. 2013. Characterization and ageing study of poly (lactic acid) films plasticized with oligomeric lactic acid. *Polymer Degradation and Stability,* 98, 651-658.

Burt, S. 2004. Essential oils: their antibacterial properties and potential applications in foods—a review. *Int J Food Microbiol,* 94, 223-253.

Cao-Hoang, L., Chaine, A., Grégoire, L. & Waché, Y. 2010. Potential of nisin-incorporated sodium caseinate films to control Listeria in artificially contaminated cheese. *Food Microbiology,* 27, 940-944.

Cao, X., Mohamed, A., Gordon, S., Willett, J. & Sessa, D. 2003. DSC study of biodegradable poly (lactic acid) and poly (hydroxy ester ether) blends. *Thermochimica acta,* 406, 115-127.

Caprioli, I., O'sullivan, M. & Monahan, F. 2009. Use of sodium caseinate/glycerol edible films to reduce lipid oxidation in sliced turkey meat. *European Food Research and Technology,* 228, 433-440.

Carrino, L., Moroni, G. & Polini, W. 2002. Cold plasma treatment of polypropylene surface: a study on wettability and adhesion. *Journal of Materials Processing Technology,* 121, 373-382.

Carrino, L., Polini, W. & Sorrentino, L. 2004. Ageing time of wettability on polypropylene surfaces processed by cold plasma. *Journal of Materials Processing Technology,* 153-154, 519-525.

Cerrutti, P. & Alzamora, S. M. 1996. Inhibitory effects of vanillin on some food spoilage yeasts in laboratory media and fruit purees. *International Journal of Food Microbiology,* 29, 379-386.

Certel, M., Uslu, M. K. & Ozdemir, F. 2004. Effects of sodium caseinate- and milk protein concentrate-based edible coatings on the postharvest quality of Bing cherries. *Journal of the Science of Food and Agriculture,* 84, 1229-1234.

Cha, D. S. & Chinnan, M. S. 2004. Biopolymer-Based Antimicrobial Packaging: A Review. *Critical Reviews in Food Science and Nutrition,* 44, 223-237.

Chaiwong, C., Rachtanapun, P., Wongchaiya, P., Auras, R. & Boonyawan, D. 2010. Effect of plasma treatment on hydrophobicity and barrier property of polylactic acid. *Surface and Coatings Technology,* 204, 2933-2939.

Cheetham, N. W. H. & Tao, L. 1998. Variation in crystalline type with amylose content in maize starch granules: an X-ray powder diffraction study. *Carbohydrate Polymers*, 36, 277-284.

Chen, H. 1995. Functional Properties and Applications of Edible Films Made of Milk Proteins. *Journal of Dairy Science,* 78, 2563-2583.

Chen, H. 2002. Formation and Properties of Casein Films and Coatings. *In:* GENNADIOS, A. (ed.) *Protein-based films and coatings.* New York: CRC Press.

Chou, N. J. & Chang, C. A. 1994. Surface modification of polymers. *In:* TONG, H. M., KOWALCZYK, S. P., SARAF, R. & CHOU, N. J. (eds.) *Characterization of Polymers.* Boston: Butterworth-Heinemann Inc.

Cioffi, M. O. H., Voorwald, H. J. C. & Mota, R. P. 2003. Surface energy increase of oxygen-plasma-treated PET. *Materials Characterization,* 50, 209-215.

Conn, R. E., Kolstad, J. J., Borzelleca, J. F., Dixler, D. S., Filer Jr, L. J., Ladu Jr, B. N. & Pariza, M. W. 1995. Safety assessment of polylactide (PLA) for use as a food-contact polymer. *Food and Chemical Toxicology,* 33, 273-283.

Connolly, J., Valdramidis, V., Byrne, E., Karatzas, K.-A., Cullen, P., Keener, K. & Mosnier, J. 2013. Characterization and antimicrobial efficacy against E. coli of a helium/air plasma at atmospheric pressure created in a plastic package. *Journal of Physics D: Applied Physics,* 46, 035401.

Crank, J. 1975. *The mathematics of diffusion*, Oxford university press.

Cui, N. Y., Upadhyay, D. J., Anderson, C. A., Meenan, B. J. & Brown, N. 2007. Surface oxidation of a Melinex 800 PET polymer material modified by an atmospheric dielectric barrier discharge studied using X-ray photoelectron spectroscopy and contact angle measurement. *Applied Surface Science,* 253, 3865-3871.

Dangaran, K., Tomasula, P. M. & Qi, P. 2009. Structure and function of protein-based edible films and coatings. *Edible films and coatings for food applications.* Springer.

Das, D. K., Dutta, H. & Mahanta, C. L. 2013. Development of a rice starch-based coating with antioxidant and microbe-barrier properties and study of its effect on tomatoes stored at room temperature. *LWT - Food Science and Technology,* 50, 272-278.

Day, B. P. F. 2003. *Active packaging (in Food Packaging Technology)*, CRC Press.

Deilmann, M., Grabowski, M., Theiß, S., Bibinov, N. & Awakowicz, P. 2008a. Permeation mechanisms of pulsed microwave plasma deposited silicon oxide films for food packaging applications. *Journal of Physics D: Applied Physics,* 41.

Deilmann, M., Theiß, S. & Awakowicz, P. 2008b. Pulsed microwave plasma polymerization of silicon oxide films: Application of efficient permeation barriers on polyethylene terephthalate. *Surface and Coatings Technology,* 202, 1911-1917.

Del Nobile, M. A., Conte, A., Incoronato, A. L. & Panza, O. 2008. Antimicrobial efficacy and release kinetics of thymol from zein films. *Journal of Food Engineering,* 89, 57-63.

Dixon, D. & J. Meenan, B. 2012. Atmospheric Dielectric Barrier Discharge Treatments of Polyethylene, Polypropylene, Polystyrene and Poly(ethylene terephthalate) for Enhanced Adhesion. *Journal of Adhesion Science and Technology,* 26, 2325-2337.

Dobrucka, R. 2013. The future of active and intelligent packaging industry. *LogForum 9 (2), 103,* 110.

Donegan, M., Milosavljević, V., Dowling, D. P. 2013. Activation of PET using an RF Atmospheric Plasma System. *Plasma Chemistry and Plasma Processing,* in press.

Dong, A., Prestrelski, S. J., Allison, S. D. & Carpenter, J. F. 1995. Infrared spectroscopic studies of lyophilization-and temperature-induced protein aggregation. *Journal of Pharmaceutical Sciences,* 84, 415-424.

Dorai, R. & Kushner, M. J. 2003. A model for plasma modification of polypropylene using atmospheric pressure discharges. *Journal of Physics D: Applied Physics,* 36, 666.

Dorman, H. J. D. & Deans, S. G. 2000. Antimicrobial agents from plants: antibacterial activity of plant volatile oils. *J Appl Microbiol,* 88, 308-316.

Du, J. M., Gemma, H., Iwahori, S. 1997. Effects of Chitosan Coating on the Storage of Peach, Japanese Pear, and Kiwifruit. *Journal of the Japanese Society for Horticultural Science,* 66, 15-22.

Dutta, P. K., Tripathi, S., Mehrotra, G. K. & Dutta, J. 2009. Perspectives for chitosan based antimicrobial films in food applications. *Food Chemistry,* 114, 1173-1182.

El Ghaouth, A., Arul, J., Ponnampalam, R. & Boulet, M. 1991a. Chitosan coating effect on storability and quality of fresh strawberries. *Journal of Food Science,* 56, 1618-1620.

El Ghaouth, A., Arul, J., Ponnampalam, R. & Boulet, M. 1991b. Use of chitosan coating to reduce water loss and maintain quality of cucumber and bell pepper fruits. *Journal of Food Processing and Preservation,* 15, 359-368.

El Ghaouth, A., Ponnampalam, R., Castaigne, F. & Arul, J. 1992. Chitosan coating to extend the storage life of tomatoes. *HortScience,* 27, 1016-1018.

Esena, P., Zanini, S. & Riccardi, C. 2007. Plasma processing for surface optical modifications of PET films. *Vacuum,* 82, 232-235.

European Standard 2002. Materials and articles in contact with foodstuffs–Plastics–Part 1: Guide to the selection of conditions and test methods for overall migration. *EN 1186-1.*

Fabra, M. J., Talens, P. & Chiralt, A. 2010. Influence of calcium on tensile, optical and water vapour permeability properties of sodium caseinate edible films. *Journal of Food Engineering,* 96, 356-364.

Fan, M., Hu, Q. & Shen, K. 2009. Preparation and structure of chitosan soluble in wide pH range. *Carbohydrate Polymers,* 78, 66-71.

Fernandez-Gutierrez, S. A., Pedrow, P. D., Pitts, M. J. & Powers, J. 2010. Cold Atmospheric-Pressure Plasmas Applied to Active Packaging of Apples. *Plasma Science, IEEE Transactions on,* 38, 957-965.

Fernández-Gutierrez, S. A., Pedrow, P. D., Pitts, M. J. & Powers, J. 2010. Cold Atmospheric-Pressure Plasmas Applied to Active Packaging of Apples. *Plasma Science, IEEE Transactions on,* 38, 957-965.

Fitzgerald, D., Stratford, M., Gasson, M., Ueckert, J., Bos, A. & Narbad, A. 2004. Mode of antimicrobial action of vanillin against Escherichia coli, Lactobacillus plantarum and Listeria innocua. *Journal of applied microbiology,* 97, 104-113.

Fowkes, F. M. 1962. Determination of interfacial tensions, contact angles, and dispersion forces in surfaces by assuming additivity of intermolecular interactions in surfaces. *The Journal of Physical Chemistry,* 66, 382-382.

Gao, C., Stading, M., Wellner, N., Parker, M. L., Noel, T. R., Mills, E. N. C. & Belton, P. S. 2006. Plasticization of a Protein-Based Film by Glycerol: A Spectroscopic, Mechanical, and Thermal Study. *Journal of Agricultural and Food Chemistry,* 54, 4611-4616.

Garcia, D., Fenollar, O., Lopez, R., Sanchis, R. & Balart, R. 2008. Durability of the wettability properties of a polypropylene film with a low-pressure CH4–O2 plasma treatment. *Journal of Applied Polymer Science,* 110, 1201-1207.

García, M. A., Martino, M. N. & Zaritzky, N. E. 1998. Plasticized starch-based coatings to improve strawberry (Fragaria× ananassa) quality and stability. *Journal of Agricultural and Food Chemistry,* 46, 3758-3767.

García, M. A., Martino, M. N. & Zaritzky, N. E. 1999. Edible starch films and coatings characterization: scanning electron microscopy, water vapor, and gas permeabilities. *Scanning*, 21, 348-353.

Ghanem, A. & Ghaly, A. 2004. Immobilization of glucose oxidase in chitosan gel beads. *Journal of Applied Polymer Science*, 91, 861-866.

Gilliam, M. A. & Yu, Q. S. 2006. Surface characterization of low-temperature cascade arc plasma–treated low-density polyethylene using contact angle measurements. *Journal of Applied Polymer Science*, 99, 2528-2541.

Gnanasekharan, V., Floros, J. D. & Glacin, J. R. 1997. Migration and sorption phenomena in packaged foods. *Critical Reviews in Food Science and Nutrition*, 37, 519-559.

Goldsmith, B. B. 1909. Thermoplastic compound of proteids and amins. U.S. patent 922133.

Gomathi, N. & Neogi, S. 2009. Surface modification of polypropylene using argon plasma: Statistical optimization of the process variables. *Applied Surface Science*, 255, 7590-7600.

Gotoh, K., Yasukawa, A. & Taniguchi, K. 2011. Water Contact Angles on Poly(ethylene terephthalate) Film Exposed to Atmospheric Pressure Plasma. *Journal of Adhesion Science and Technology*, 25, 307-322.

Guillard, V., Mauricio-Iglesias, M. & Gontard, N. 2010. Effect of Novel Food Processing Methods on Packaging: Structure, Composition, and Migration Properties. *Critical Reviews in Food Science and Nutrition*, 50, 969-988.

Guimond, S., Radu, I., Czeremuszkin, G., Carlsson, D. J. & Wertheimer, M. R. 2002. Biaxially oriented polypropylene (BOPP) surface modification by nitrogen atmospheric pressure glow discharge (APGD) and by air corona. *Plasmas and polymers,* 7, 71-88.

Gupta, B., Revagade, N. & Hilborn, J. 2007. Poly(lactic acid) fiber: An overview. *Progress in Polymer Science,* 32, 455-482.

Han, F., Gao, C., Liu, M., Huang, F. & Zhang, B. 2013. Synthesis, optimization and characterization of acetylated corn starch with the high degree of substitution. *International Journal of Biological Macromolecules,* 59, 372-376.

Han, J. H. & Floros, J. D. 1998. Simulating diffusion model and determining diffusivity of potassium sorbate through plastics to develop antimicrobial packaging films. *Journal of Food Processing and Preservation,* 22, 107-122.

Hong, S.-I. & Krochta, J. M. 2006. Oxygen barrier performance of whey-protein-coated plastic films as affected by temperature, relative humidity, base film and protein type. *Journal of Food Engineering,* 77, 739-745.

Inagaki, N., Narushim, K., Tuchida, N. & Miyazaki, K. 2004. Surface characterization of plasma-modified poly(ethylene terephthalate) film surfaces. *Journal of Polymer Science Part B: Polymer Physics,* 42, 3727-3740.

Isobe, S. 2003. Production technology of biodegradable materials using agricultural wastes. *Farming Japan,* 37, 21-25.

Jacobs, T., De Geyter, N., Morent, R., Van Vlierberghe, S., Dubruel, P. & Leys, C. 2011. Plasma modification of PET foils with different crystallinity. *Surface and Coatings Technology,* 205, Supplement 2, S511-S515.

Jamshidian, M., Tehrany, E. A., Imran, M., Jacquot, M. & Desobry, S. 2010. Poly-Lactic Acid: Production, Applications, Nanocomposites, and Release Studies. *Comprehensive Reviews in Food Science and Food Safety,* 9, 552-571.

Jayakody, L., Hoover, R., Liu, Q. & Weber, E. 2005. Studies on tuber and root starches. I. Structure and physicochemical properties of innala (*Solenostemon rotundifolius*) starches grown in Sri Lanka. *Food Research International,* 38, 615-629.

Jiang, Y. & Li, Y. 2001. Effects of chitosan coating on postharvest life and quality of longan fruit. *Food Chemistry,* 73, 139-143.

Joerger, R. D., Sabesan, S., Visioli, D., Urian, D. & Joerger, M. C. 2009. Antimicrobial activity of chitosan attached to ethylene copolymer films. *Packaging Technology and Science,* 22, 125-138.

Kamińska, A., Kaczmarek, H. & Kowalonek, J. 2002. The influence of side groups and polarity of polymers on the kind and effectiveness of their surface modification by air plasma action. *European Polymer Journal,* 38, 1915-1919.

Keener, K. M., Jensen, J., Valdramidis, V., Byrne, E., Connolly, J., Mosnier, J. & Cullen, P. Decontamination of Bacillus subtilis spores in a sealed package using a non-thermal plasma system. *In:* HENSEL, K. & MACHALA, Z., eds. NATO Advanced Research Workshop:

Plasma for Bio-Decontamination, Medicine and Food Security, 2012 Jasná, Slovakia. 445-455.

Kelly, C. A., Toncelli, C., Kerry, J. P. & Papkovsky, D. B. 2014. Phosphorescent O2 sensors based on polyolefin fabric materials. *Journal of Materials Chemistry C,* 2, 2169-2174.

Kenawy, E.-R., Worley, S. D. & Broughton, R. 2007. The Chemistry and Applications of Antimicrobial Polymers: A State-of-the-Art Review. *Biomacromolecules,* 8, 1359-1384.

Kerry, J., O'grady, M. & Hogan, S. 2006. Past, current and potential utilisation of active and intelligent packaging systems for meat and muscle-based products: A review. *Meat science,* 74, 113-130.

Kokkini, S., Karousou, R., Dardioti, A., Krigas, N. & Lanaras, T. 1997. Autumn essential oils of Greek oregano. *Phytochemistry,* 44, 883-886.

Kowalonek, J., Kaczmarek, H. & Dąbrowska, A. 2010. Air plasma or UV-irradiation applied to surface modification of pectin/poly(vinyl alcohol) blends. *Applied Surface Science,* 257, 325-331.

Kozlov, P. & Burdygina, G. 1983. The structure and properties of solid gelatin and the principles of their modification. *Polymer,* 24, 651-666.

Kristo, E., Koutsoumanis, K. P. & Biliaderis, C. G. 2008. Thermal, mechanical and water vapor barrier properties of sodium caseinate films containing antimicrobials and their inhibitory action on Listeria monocytogenes. *Food Hydrocolloids,* 22, 373-386.

Kulinski, Z. & Piorkowska, E. 2005. Crystallization, structure and properties of plasticized poly(l-lactide). *Polymer,* 46, 10290-10300.

Kun, W., Jian, L., Chunsheng, R., Dezhen, W. & Younian, W. 2008. Surface modification of polyethylene (PE) films using dielectric barrier discharge plasma at atmospheric pressure. *Plasma Science and Technology*, 10, 433.

Lacroix, M., Le, T. C., Ouattara, B., Yu, H., Letendre, M., Sabato, S. F., Mateescu, M. A. & Patterson, G. 2002. Use of γ-irradiation to produce films from whey, casein and soya proteins: structure and functionals characteristics. *Radiation Physics and Chemistry*, 63, 827-832.

Lai, H. M., Geil, P. H. & Padua, G. W. 1999. X-ray diffraction characterization of the structure of zein–Oleic acid films. *Journal of Applied Polymer Science*, 71, 1267-1281.

Law, V. J., O'neill F. T. , Twomey, B., Milosavljević, V., Kong,M. G., Anghel, S. D., Dowling, D. P. 2012. Electrical power dissipation within a helium APPJ flowing afterglow and its impact on spatial-temporal properties. *IEEE Transitions on plasma science*, 40, 2994-3002

Lawton, J. W. 2002. Zein: A History of Processing and Use. *Cereal Chemistry Journal*, 79, 1-18.

Lawton, J. W. 2004. Plasticizers for Zein: Their Effect on Tensile Properties and Water Absorption of Zein Films. *Cereal Chemistry Journal*, 81, 1-5.

Leceta, I., Guerrero, P., Ibarburu, I., Dueñas, M. T. & De La Caba, K. 2013. Characterization and antimicrobial analysis of chitosan-based films. *Journal of Food Engineering*, 116, 889-899.

Leceta, I., Peñalba, M., Arana, P., Guerrero, P. & De La Caba, K. 2015. Ageing of chitosan films: Effect of storage time on structure and optical, barrier and mechanical properties. *European Polymer Journal,* 66, 170-179.

Lee, K. T. 2010. Quality and safety aspects of meat products as affected by various physical manipulations of packaging materials. *Meat Science,* 86, 138-150.

Lerouge, S., Wertheimer, M. R. & Yahia, L. H. 2001. Plasma Sterilization: A Review of Parameters, Mechanisms, and Limitations. *Plasmas and Polymers,* 6, 175-188.

Leroux, F., Campagne, C., Perwuelz, A. & Gengembre, L. 2008. Polypropylene film chemical and physical modifications by dielectric barrier discharge plasma treatment at atmospheric pressure. *Journal of Colloid and Interface Science,* 328, 412-420.

Li, M., Liu, P., Zou, W., Yu, L., Xie, F., Pu, H., Liu, H. & Chen, L. 2011. Extrusion processing and characterization of edible starch films with different amylose contents. *Journal of food engineering,* 106, 95-101.

Liang, Y., Jensen, R. E., Pappas, D. D. & Palmese, G. R. 2011. Toughening vinyl ester networks with polypropylene meso-fibers: Interface modification and composite properties. *Polymer,* 52, 510-518.

Liu, C., Cui, N., Brown, N. M. D. & Meenan, B. J. 2004. Effects of DBD plasma operating parameters on the polymer surface modification. *Surface and Coatings Technology,* 185, 311-320.

Liu, H., Xie, F., Yu, L., Chen, L. & Li, L. 2009a. Thermal processing of starch-based polymers. *Progress in Polymer Science,* 34, 1348-1368.

Liu, P., Yu, L., Liu, H., Chen, L. & Li, L. 2009b. Glass transition temperature of starch studied by a high-speed DSC. *Carbohydrate Polymers,* 77, 250-253.

López, R., Sanchis, R., García, D., Fenollar, O. & Balart, R. 2009. Surface characterization of hydrophilic coating obtained by low-pressure CH4-O2 plasma treatment on a polypropylene film. *Journal of Applied Polymer Science*, 111, 2992-2997.

Marino, M., Bersani, C. & Comi, G. 1999. Antimicrobial activity of the essential oils of Thymus vulgaris L. measured using a bioimpedometric method. *Journal of Food Protection®,* 62, 1017-1023.

Martel, A.-C. & Zeggane, S. 2002. Determination of acaricides in honey by high-performance liquid chromatography with photodiode array detection. *Journal of Chromatography A*, 954, 173-180.

Mastromatteo, M., Barbuzzi, G., Conte, A. & Del Nobile, M. A. 2009. Controlled release of thymol from zein based film. *Innovative Food Science & Emerging Technologies,* 10, 222-227.

Mastromatteo, M., Lecce, L., De Vietro, N., Favia, P. & Del Nobile, M. A. 2011. Plasma deposition processes from acrylic/methane on natural fibres to control the kinetic release of lysozyme from PVOH monolayer film. *Journal of Food Engineering,* 104, 373-379.

Médard, N., Soutif, J.-C. & Poncin-Epaillard, F. 2002. CO2, H2O, and CO2/H2O Plasma Chemistry for Polyethylene Surface Modification. *Langmuir*, 18, 2246-2253.

Medard, N., Soutif, J. C. & Poncin-Epaillard, F. 2002. Characterization of CO_2 plasma-treated polyethylene surface bearing carboxylic groups. *Surface and Coatings Technology,* 160, 197-205.

Mendes De Souza, P., Fernández, A., López-Carballo, G., Gavara, R. & Hernández-Muñoz, P. 2010. Modified sodium caseinate films as releasing carriers of lysozyme. *Food Hydrocolloids,* 24, 300-306.

Milosavljević, V., Ellingboe, A. R. & Daniels, S. 2011. Influence of plasma chemistry on oxygen triplets. *The European Physical Journal D,* 64, 437-445.

Milosavljevic, V., Ellingboe, A. R., Gaman, C. & Ringwood, J. V. 2008. Real-time plasma control in a dual-frequency, confined plasma etcher. *Journal of Applied Physics,* 103, 083302-083302-10.

Milosavljevic, V., Faulkner, R. & Hopkins, M. B. 2007. Real time sensor for monitoring oxygen in radio?frequency plasmaapplications. *Opt. Express,* 15, 13913-13923.

Milosavljević, V., Karkari, S. K. & Ellingboe, A. R. 2007. Characterization of the pulse plasma source. *Plasma Sources Science and Technology,* 16, 304.

Milosavljević, V., Macgearailt, N., Daniels, S., Turner, M. M. 2013. Phase Resolved Optical Emission Spectroscopy for an Electron Cyclotron Resonance etcher. *Journal of Applied Physics*, in press

Mirabedini, S., Arabi, H., Salem, A. & Asiaban, S. 2007. Effect of low-pressure O_2 and Ar plasma treatments on the wettability and morphology of biaxial-oriented polypropylene (BOPP) film. *Progress in Organic Coatings,* 60, 105-111.

Misra, N. N., Tiwari, B. K., Raghavarao, K. S. M. S. & Cullen, P. J. 2011. Nonthermal Plasma Inactivation of Food-Borne Pathogens. *Food Engineering Reviews,* 3, 159-170.

Mittendorfer, J., Bierbaumer, H., Gratzl, F. & Kellauer, E. 2002. Decontamination of food packaging using electron beam—status and prospects. *Radiation Physics and Chemistry,* 63, 833-836.

Morent, R., De Geyter, N., Leys, C., Gengembre, L. & Payen, E. 2008. Comparison between XPS-and FTIR-analysis of plasma-treated polypropylene film surfaces. *Surface and Interface Analysis,* 40, 597-600.

Muranyi, P., Wunderlich, J. & Heise, M. 2007. Sterilization efficiency of a cascaded dielectric barrier discharge. *Journal of applied microbiology,* 103, 1535-44.

Muranyi, P., Wunderlich, J. & Heise, M. 2008. Influence of relative gas humidity on the inactivation efficiency of a low temperature gas plasma. *Journal of applied microbiology,* 104, 1659-1666.

Muranyi, P., Wunderlich, J. & Langowski, H. C. 2010. Modification of bacterial structures by a low-temperature gas plasma and influence on packaging material. *Journal of Applied Microbiology,* 109, 1875-1885.

Navaneetha Pandiyaraj, K., Selvarajan, V., Deshmukh, R. R. & Gao, C. 2008. Adhesive properties of polypropylene (PP) and polyethylene terephthalate (PET) film surfaces treated by DC glow discharge plasma. *Vacuum,* 83, 332-339.

Neto, C. G. T., Giacometti, J. A., Job, A. E., Ferreira, F. C., Fonseca, J. L. C. & Pereira, M. R. 2005. Thermal Analysis of Chitosan Based Networks. *Carbohydrate Polymers,* 62, 97-103.

Nobile, M. a. D., Cannarsi, M., Altieri, C., Sinigaglia, M., Favia, P., Iacoviello, G. & D'agostino, R. 2004. Effect of Ag-containing Nano-composite Active Packaging System on Survival of Alicyclobacillus acidoterrestris. *Journal of Food Science,* 69, E379-E383.

Novák, I., Števiar, M., Chodák, I., Krupa, I., Nedelčev, T., Špírková, M., Chehimi, M. M., Mosnáček, J. & Kleinová, A. 2007. Study of adhesion and surface properties of low-density poly(ethylene) pre-treated by cold discharge plasma. *Polymers for Advanced Technologies,* 18, 97-105.

O'connor, N., Milosavljevic, V. & Daniels, S. 2011. Development of a real time monitor and multivariate method for long term diagnostics of atmospheric pressure dielectric barrier discharges: Application to He, He/N[sub 2], and He/O[sub 2] discharges. *Review of Scientific Instruments,* 82, 083501-10.

O'hare, L. A., Smith, J. A., Leadley, S. R., Parbhoo, B., Goodwin, A. J. & Watts, J. F. 2002. Surface physico-chemistry of corona-discharge-treated poly (ethylene terephthalate) film. *Surface and Interface Analysis,* 33, 617-625.

Ogawa, K., Yui, T. & Okuyama, K. 2004. Three D structures of chitosan. *International Journal of Biological Macromolecules,* 34, 1-8.

Owens, D. K. & Wendt, R. C. 1969. Estimation of the surface free energy of polymers. *Journal of Applied Polymer Science,* 13, 1741-1747.

Ozdemir, M. & Sadikoglu, H. 1998. A new and emerging technology: Laser-induced surface modification of polymers. *Trends in Food Science & Technology,* 9, 159-167.

Ozdemir, M., Yurteri, C. U. & Sadikoglu, H. 1999a. Physical polymer surface modification methods and applications in food packaging polymers. *Critical Reviews in Food Science and Nutrition,* 39, 457-77.

Ozdemir, M., Yurteri, C. U. & Sadikoglu, H. 1999b. Surface treatment of food packaging polymers by plasmas. *Food Technology,* 53, 54-58.

Pandiyaraj, K. N., Selvarajan, V., Deshmukh, R. R. & Bousmina, M. 2008. The effect of glow discharge plasma on the surface properties of Poly (ethylene terephthalate) (PET) film. *Surface and Coatings Technology,* 202, 4218-4226.

Pankaj, S. K., Bueno-Ferrer, C., Misra, N. N., Milosavljević, V., O'donnell, C. P., Bourke, P., Keener, K. M. & Cullen, P. J. 2014a. Applications of cold plasma technology in food packaging. *Trends in Food Science & Technology,* 35, 5-17.

Pankaj, S. K., Bueno-Ferrer, C., Misra, N. N., O'neill, L., Jiménez, A., Bourke, P. & Cullen, P. J. 2014b. Characterization of polylactic acid films for food packaging as affected by dielectric barrier discharge atmospheric plasma. *Innovative Food Science & Emerging Technologies,* 21, 107-113.

Pankaj, S. K., Bueno-Ferrer, C., Misra, N. N., O'neill, L., Jiménez, A., Bourke, P. & Cullen, P. J. 2014c. Surface, Thermal and Antimicrobial Release Properties of Plasma-Treated Zein Films. *Journal of Renewable Materials,* 2, 77-84.

Pankaj, S. K., Kadam, S. U. & Misra, N. N. 2011. *Trends in food packaging,* Germany, VDM Publishing House.

Pascual, M., Balart, R., Sánchez, L., Fenollar, O. & Calvo, O. 2008. Study of the aging process of corona discharge plasma effects on low density polyethylene film surface. *Journal of Materials Science,* 43, 4901-4909.

Patil, S., Moiseev, T., Misra, N. N., Cullen, P. J., Mosnier, J. P., Keener, K. M. & Bourke, P. 2014. Influence of high voltage atmospheric cold plasma process parameters and role of relative humidity on inactivation of Bacillus atrophaeus spores inside a sealed package. *Journal of Hospital Infection,* 88, 162-169.

Pereda, M., Aranguren, M. I. & Marcovich, N. E. 2009. Water vapor absorption and permeability of films based on chitosan and sodium caseinate. *Journal of Applied Polymer Science,* 111, 2777-2784.

Péroval, C., Debeaufort, F., Seuvre, A. M., Chevet, B., Déspre, D. & Voilley, A. 2003. Modified Arabinoxylan-Based Films. Part B. Grafting of Omega-3 Fatty Acids by Oxygen Plasma and Electron Beam Irradiation. *Journal of Agricultural and Food Chemistry,* 51, 3120-3126.

Plastics-the-Facts 2012. *European Association of Plastics Manufacturers,* **http://www.plasticseurope.org/cust/documentrequest.aspx?DocID=54693**, (accesed 15/04/2013).

Plog, S., Schneider, J., Walker, M., Schulz, A. & Stroth, U. 2011. Investigations of plasma polymerized SiOx barrier films for polymer food packaging. *Surface and Coatings Technology,* 205, S165-S170.

Poncin-Epaillard, F., Brosse, J.-C. & Falher, T. 1999. Reactivity of surface groups formed onto a plasma treated poly(propylene) film. *Macromolecular Chemistry and Physics,* 200, 989-996.

Popelka, A., Novák, I., Lehocký, M., Chodák, I., Sedliačik, J., Gajtanska, M., Sedliačiková, M., Vesel, A., Junkar, I., Kleinová, A., Špírková, M. & Bílek, F. 2012. Anti-bacterial Treatment of Polyethylene by Cold Plasma for Medical Purposes. *Molecules,* 17, 762-785.

Prasertsung, I., Mongkolnavin, R., Kanokpanont, S. & Damrongsakkul, S. 2010. The effects of pulsed inductively coupled plasma (PICP) on physical properties and biocompatibility of crosslinked gelatin films. *International Journal of Biological Macromolecules,* 46, 72-78.

Prysiazhnyi, V., Zaporojchenko, V., Kersten, H. & Černák, M. 2012. Influence of humidity on atmospheric pressure air plasma treatment of aluminium surfaces. *Applied Surface Science,* 258, 5467-5471.

Qun, G., Ajun, W. & Yong, Z. 2007. Effect of reacetylation and degradation on the chemical and crystal structures of chitosan. *Journal of Applied Polymer Science,* 104, 2720-2728.

Rakotonirainy, A. M., Wang, Q. & Padua, G. W. 2001. Evaluation of Zein Films as Modified Atmosphere Packaging for Fresh Broccoli. *J Food Sci,* 66, 1108-1111.

Rasal, R. M., Janorkar, A. V. & Hirt, D. E. 2010. Poly(lactic acid) modifications. *Progress in Polymer Science,* 35, 338-356.

Ren, C.-S., Wang, K., Nie, Q.-Y., Wang, D.-Z. & Guo, S.-H. 2008. Surface modification of PE film by DBD plasma in air. *Applied Surface Science,* 255, 3421-3425.

Rivero, S., García, M. & Pinotti, A. 2010. Correlations between structural, barrier, thermal and mechanical properties of plasticized gelatin films. *Innovative food science & emerging technologies,* 11, 369-375.

Ryan, K., O'farrell, D. & Ellingboe, A. R. 2011. Spatial structure of plasma potential oscillation and ion saturation current in VHF multi-tile electrode plasma source. *Current Applied Physics,* 11, S114-S116.

Schneider, J., Akbar, M. I., Dutroncy, J., Kiesler, D., Leins, M., Schulz, A., Walker, M., Schumacher, U. & Stroth, U. 2009. Silicon Oxide Barrier Coatings Deposited on Polymer Materials for Applications in Food Packaging Industry. *Plasma Processes and Polymers,* 6, S700-S704.

Schneider, J., Baumgärtner, K. M., Feichtinger, J., Krüger, J., Muranyi, P., Schulz, A., Walker, M., Wunderlich, J. & Schumacher, U. 2005. Investigation of the practicability of low-pressure microwave plasmas in the sterilisation of food packaging materials at industrial level. *Surface and Coatings Technology,* 200, 962-966.

Shi, K., Huang, Y., Yu, H., Lee, T.-C. & Huang, Q. 2010. Reducing the Brittleness of Zein Films through Chemical Modification. *Journal of Agricultural and Food Chemistry,* 59, 56-61.

Shi, K., Kokini, J. L. & Huang, Q. 2009. Engineering Zein Films with Controlled Surface Morphology and Hydrophilicity. *Journal of Agricultural and Food Chemistry,* 57, 2186-2192.

Shukla, R. & Cheryan, M. 2001. Zein: the industrial protein from corn. *Industrial Crops and Products,* 13, 171-192.

Simpson, B. K., Gagné, N., Ashie, I. N. A. & Noroozi, E. 1997. Utilization of chitosan for preservation of raw shrimp (Pandalus borealis). *Food Biotechnology,* 11, 25-44.

Singh, N., Georget, D. M. R., Belton, P. S. & Barker, S. A. 2009. Zein−Iodine Complex Studied by FTIR Spectroscopy and Dielectric and Dynamic Rheometry in Films and Precipitates. *Journal of Agricultural and Food Chemistry,* 57, 4334-4341.

Siracusa, V., Rocculi, P., Romani, S. & Rosa, M. D. 2008. Biodegradable polymers for food packaging: a review. *Trends in Food Science & Technology,* 19, 634-643.

Slepička, P., Vasina, A., Kolská, Z., Luxbacher, T., Malinský, P., Macková, A. & Švorčík, V. 2010. Argon plasma irradiation of polypropylene. *Nuclear Instruments and Methods in Physics Research Section B: Beam Interactions with Materials and Atoms,* 268, 2111-2114.

Soares, R., Scremin, F. F. & Soldi, V. Thermal stability of biodegradable films based on soy protein and corn starch. Macromolecular symposia, 2005. Wiley Online Library, 258-265.

Soliman, E. A. & Furuta, M. 2009. Influence of γ-irradiation on mechanical and water barrier properties of corn protein-based films. *Radiation Physics and Chemistry,* 78, 651-654.

Sorrentino, L., Carrino, L. & Napolitano, G. 2007. Oxygen cold plasma treatment on polypropylene: influence of process parameters on surface wettability. *Surface Engineering,* 23, 247-252.

Stefanakis, M. K., Touloupakis, E., Anastasopoulos, E., Ghanotakis, D., Katerinopoulos, H. E. & Makridis, P. 2013. Antibacterial activity of essential oils from plants of the genus Origanum. *Food Control,* 34, 539-546.

Strobel, J. M., Strobel, M., Lyons, C. S., Dunatov, C. & Perron, S. J. 1991. Aging of air-corona-treated polypropylene film. *Journal of Adhesion Science and Technology,* 5, 119-130.

Suppakul, P., Miltz, J., Sonneveld, K. & Bigger, S. W. 2003. Active Packaging Technologies with an Emphasis on Antimicrobial Packaging and its Applications. *J Food Sci,* 68, 408-420.

Tanioka, A., Miyasaka, K. & Ishikawa, K. 1976. Reconstitution of collagen-fold structure with stretching of gelatin film. *Biopolymers,* 15, 1505-1511.

Tenn, N., Follain, N., Fatyeyeva, K., Valleton, J. M., Poncin-Epaillard, F., Delpouve, N. & Marais, S. 2012. Improvement of water barrier properties of Poly(ethylene-co-vinyl alcohol) films by hydrophobic plasma surface treatments. *Journal of Physical Chemistry C,* 116, 12599-12612.

Teraoka, F., Nakagawa, M. & Hara, M. 2006. Surface modification of poly (L-lactide) by atmospheric pressure plasma treatment and cell response. *Dental materials journal,* 25, 560-565.

Uemura, Y., Maetsuru, Y.-S., Fujita, T., Yoshida, M., Hatate, Y. & Yamada, K. 2006. The effect of coatings formed by low temperature tetramethoxysilane plasma treatment on water-

vapor permeability of poly(L-lactic acid) film. *Korean Journal of Chemical Engineering*, 23, 144-147.

Upadhyay, D. J., Cui, N.-Y., Anderson, C. A. & Brown, N. M. D. 2004. Surface oxygenation of polypropylene using an air dielectric barrier discharge: the effect of different electrode–platen combinations. *Applied Surface Science*, 229, 352-364.

Van Den Broek, L. a. M., Knoop, R. J. I., Kappen, F. H. J. & Boeriu, C. G. 2015. Chitosan films and blends for packaging material. *Carbohydrate Polymers,* 116, 237-242.

Van Oss, C. J., Chaudhury, M. K. & Good, R. J. 1988. Interfacial Lifshitz-van der Waals and polar interactions in macroscopic systems. *Chemical Reviews*, 88, 927-941.

Vanderroost, M., Ragaert, P., Devlieghere, F. & De Meulenaer, B. 2014. Intelligent food packaging: The next generation. *Trends in Food Science & Technology,* 39, 47-62.

Vartiainen, J., Rättö, M. & Paulussen, S. 2005. Antimicrobial activity of glucose oxidase-immobilized plasma-activated polypropylene films. *Packaging Technology and Science*, 18, 243-251.

Vesel, A. & Mozetic, M. 2012. Surface modification and ageing of PMMA polymer by oxygen plasma treatment. *Vacuum,* 86, 634-637.

Vieira, M. G. A., Da Silva, M. A., Dos Santos, L. O. & Beppu, M. M. 2011. Natural-based plasticizers and biopolymer films: A review. *European Polymer Journal,* 47, 254-263.

Viña, S. Z., Mugridge, A., García, M. A., Ferreyra, R. M., Martino, M. N., Chaves, A. R. & Zaritzky, N. E. 2007. Effects of polyvinylchloride films and edible starch coatings on quality aspects of refrigerated Brussels sprouts. *Food Chemistry*, 103, 701-709.

Wagner, C. & Muilenberg, G. 1979. *Handbook of X-ray photoelectron spectroscopy*, Perkin-Elmer.

Wang, C. & He, X. 2006. Polypropylene surface modification model in atmospheric pressure dielectric barrier discharge. *Surface and Coatings Technology*, 201, 3377-3384.

Wang, T. L., Bogracheva, T. Y. & Hedley, C. L. 1998. Starch: as simple as A, B, C? *Journal of Experimental Botany*, 49, 481-502.

Wang, Y., Geil, P. & Padua, G. W. 2005. Effects of processing on the structure of zein/oleic acid films investigated by X-ray diffraction. *Macromolecular bioscience,* 5, 1200-1208.

Wang, Y., Rakotonirainy, A. M. & Padua, G. W. 2003. Thermal Behavior of Zein-based Biodegradable Films. *Starch - Stärke,* 55, 25-29.

Wei, W. & Baianu, I. Physicochemical properties of plasticized corn zein films: NMR and adsorptivity studies. Macromolecular Symposia, 1999. Wiley Online Library, 197-209.

Xia, Y., Gao, W., Wang, H., Jiang, Q., Li, X., Huang, L. & Xiao, P. 2013. Characterization of tradition Chinese medicine (TCM) starch for potential cosmetics industry application. *Starch-Stärke,* 65, 367-373.

Xiong, H., Tang, S., Tang, H. & Zou, P. 2008. The structure and properties of a starch-based biodegradable film. *Carbohydrate Polymers,* 71, 263-268.

Xu, Y., Kim, K. M., Hanna, M. A. & Nag, D. 2005. Chitosan–starch composite film: preparation and characterization. *Industrial Crops and Products,* 21, 185-192.

Yam, K. L., Takhistov, P. T. & Miltz, J. 2005. Intelligent packaging: concepts and applications. *Journal of Food Science,* 70, R1-R10.

Yang, L., Chen, J., Gao, J. & Guo, Y. 2009a. Plasma sterilization using the RF glow discharge. *Applied Surface Science,* 255, 8960-8964.

Yang, L., Chen, J., Guo, Y. & Zhang, Z. 2009b. Surface modification of a biomedical polyethylene terephthalate (PET) by air plasma. *Applied Surface Science,* 255, 4446-4451.

Yannas, I. 1972. Collagen and gelatin in the solid state. *Journal of Macromolecular Science—Reviews in Macromolecular Chemistry,* 7, 49-106.

Yoshino, T., Isobe, S. & Maekawa, T. 2000. Physical evaluation of pure zein films by atomic force microscopy and thermal mechanical analysis. *Journal of the American Oil Chemists' Society,* 77, 699-704.

Young, T. 1805. An Essay on the Cohesion of Fluids. *Philosophical Transactions of the Royal Society of London,* 95, 65-87.

Zapata, P. J., Guillén, F., Martínez-Romero, D., Castillo, S., Valero, D. & Serrano, M. 2008. Use of alginate or zein as edible coatings to delay postharvest ripening process and to maintain tomato (Solanum lycopersicon Mill) quality. *Journal of the Science of Food and Agriculture,* 88, 1287-1293.

Zhang, H. & Mittal, G. 2010. Biodegradable protein-based films from plant resources: A review. *Environmental Progress & Sustainable Energy,* 29, 203-220.

Zhang, W., Chu, P. K., Ji, J., Zhang, Y., Ng, S. C. & Yan, Q. 2006. Surface antibacterial characteristics of plasma-modified polyethylene. *Biopolymers,* 83, 62-68.

Ziuzina, D., Patil, S., Cullen, P. J., Keener, K. M. & Bourke, P. 2014. Atmospheric cold plasma inactivation of Escherichia coli, Salmonella enterica serovar Typhimurium and Listeria monocytogenes inoculated on fresh produce. *Food Microbiology,* 42, 109-116.

Zivanovic, S., Chi, S. & Draughon, A. F. 2005. Antimicrobial Activity of Chitosan Films Enriched with Essential Oils. *J Food Sci,* 70, M45-M51.

List of publications

Peer-Reviewed Articles

1. Pankaj, S. K., Bueno-Ferrer, C., Misra, N. N., Milosavljević, V., O'Donnell, C. P., Bourke, P., Keener, K. M., & Cullen, P. J. (2014). Applications of cold plasma technology in food packaging. *Trends in Food Science & Technology, 35*(1), 5-17.

2. Pankaj, S. K., Bueno-Ferrer, C., Misra, N. N., O'Neill, L., Jiménez, A., Bourke, P., & Cullen, P. J. (2014). Characterization of polylactic acid films for food packaging as affected by dielectric barrier discharge atmospheric plasma. *Innovative Food Science & Emerging Technologies, 21*, 107-113.

3. Pankaj, S. K., Bueno-Ferrer, C., Misra, N. N., Bourke, P., & Cullen, P. J. (2014). Zein film: Effects of dielectric barrier discharge atmospheric cold plasma. *Journal of Applied Polymer Science, 131*(18).

4. Pankaj, S. K., Bueno-Ferrer, C., Misra, N. N., O'Neill, L., Jiménez, A., Bourke, P., & Cullen, P. J. (2014). Surface, Thermal and Antimicrobial Release Properties of Plasma-Treated Zein Films. *Journal of Renewable Materials, 2*(1), 77-84.

5. Pankaj, S. K., Bueno-Ferrer, C., Misra, N. N., O'Neill, L., Tiwari, B.K., Bourke, P., & Cullen, P. J. (2014). Physicochemical characterization of plasma-treated sodium caseinate film. *Food Research International*, 66, 438-444.

6. Pankaj, S. K., Bueno-Ferrer, C., Misra, N. N., O'Neill, L., Tiwari, B.K., Bourke, P., & Cullen, P. J. (2015). Dielectric barrier discharge atmospheric air plasma treatment of high amylose corn starch films. *LWT-Food Science and Technology*. Accepted.

7. Pankaj, S. K., Bueno-Ferrer, C., Misra, N. N., O'Neill, L., Tiwari, B.K., Bourke, P., & Cullen, P. J. Characterization of dielectric barrier discharge atmospheric air cold plasma treated gelatin films. *Food packaging and shelf-life*. Accepted.

8. Pankaj, S. K., Bueno-Ferrer, C., O'Neill, L., Tiwari, B.K., Bourke, P., & Cullen, P. J. Characterization of dielectric barrier discharge atmospheric air cold plasma treated chitosan films. *Journal of food processing and preservation*. In Review.

9. Pankaj, S. K., Bueno-Ferrer, C., Misra, N. N., O'Neill, L., Bourke, P., & Cullen, P. J. Surface, thermal and antimicrobial release properties of plasma-treated chitosan films. *Journal of Renewable Materials,* In Review.

10. Pankaj, S. K., Kelly, Caroline A., Bueno-Ferrer, C., Kerry, Joe P., Papkovsky, Dmitri B., Bourke, P., & Cullen, P. J. Application of phosphorescent oxygen sensors in in-package dielectric barrier discharge plasma environment. *Innovative Food Science & Emerging Technologies*, Accepted.

Book Chapters

1. Pankaj, S. K., Bueno-Ferrer, C., & Cullen, P. J. Plasma technology in Food packaging, *Encyclopedia of Plasma Technology*, Taylor & Francis, Accepted.

2. Pankaj, S. K. & Thomas, Sabu. Nonthermal plasma applications for food packaging polymers, *Nonthermal Plasma in Food Processing*, Elsevier, In Review.

Oral presentations

1. Effects of In-Package Dielectric Barrier Discharge atmospheric plasma on Polylactic Acid, *4th International Conference on Biodegradable and Biobased Polymers (BIOPOL)*, Rome, Oct. 2013.

2. Characterization of dielectric barrier discharge atmospheric plasma treated sodium caseinate films, *22nd Annual meeting of the Bio-Environmental Polymer Society (BEPS)*, Kansas city, Oct. 2014

Poster presentations

1. Investigation of changes in cold plasma treated strawberries using spectroscopic and chemometric approaches, International Food Convention (IFCON), CSIR-CFTRI, India, Dec 2013.

2. A computational model of the nonthermal plasma discharge inside a sealed package, International Food Convention (IFCON), CSIR-CFTRI, India, Dec 2013.

3. In-package nonthermal plasma degrades contemporary pesticides on strawberries, International Conference on Plasma Science and Applications (ICPSA), Nanyang Technological University, Singapore, Dec. 2013.

4. Effects of dielectric barrier discharge atmospheric plasma on antimicrobial zein film, 4th International Conference on Biodegradable and Biobased Polymers (BIOPOL), Rome, Oct. 2013.

5. Kinetics of Tomato Peroxidase Activity Following Atmospheric Cold Plasma Treatments, 42nd Annual Food Research Conference, Teagasc Food Research Centre, Ashtown, June 2013.